The Effects of *MYC* and *BCL6* Rearrangements on The Molecular Profile of Diffuse Large B-cell Lymphomas, Not Otherwise Specified

Research dissertation submitted to the Faculty of Health Sciences, University of the Witwatersrand, Johannesburg, in fulfilment of the requirements for the degree:

Masters of Science in Medicine (Anatomical Pathology).

Johannesburg, 2024

Sibusiso Zinhle Radebe

BHSc. Hons (University of the Witwatersrand)

66988

Supervisor:

Dr Pumza Magangane

PhD (University of Cape Town)

Keywords

Diffuse Large B-cell Lymphoma; Not otherwise specified; Immunohistochemistry; MALDI; MicroRNA; *MYC*/*BCL6* rearrangements; Proteomics; RT-qPCR.

Abstract

Background: Diffuse large B-cell lymphomas (DLBCL) are genetically heterogeneous and the most common subtype of Non-Hodgkin Lymphomas in adults. They account for approximately 40% of all B-cell lymphomas and more than 80% of all aggressive lymphomas worldwide. DLBCL harbouring *MYC* and/or *BCL6* translocations were reported by studies using fluorescence in situ hybridisation to account for approximately 10% of DLBCL. We conducted a study investigating the proteomic and microRNA expression profiles of single- (MYC^R or $BCL6^R$) and dual-rearrangement (DR) (MYC^RBCL6^R) lymphomas.

Methods: We employed Matrix-Assisted Laser Desorption Ionisation Imaging Mass Spectrometry and Liquid Chromatography-Tandem Mass Spectrometry for proteomic analysis and RT-qPCR for microRNA analysis. The study cohort consisted of three experimental groups including $BCL6^R$ (n=2), MYC^R (n=4), and $BCL6^RMYC^R$ (n=2). The study also included a control group which was the group with no translocation for both genes (n=8). To validate our findings, we utilised immunohistochemistry on the proteomics data and RT-qPCR for Let-7d and *KRAS* on the microRNA-related data.

Results: Ten proteins belonging to the cytoskeletal family were differentially expressed between the experimental and control groups. These proteins differentiated between two groups with at least an area under the curve of 0,8. MiR-155-5p, miR-21-5p, miR-29a-3p, miR-34a-5p, and the miR-17-92 cluster were dysregulated in the experimental groups.

Conclusion: DLBCL, NOS with *MYC* and/or *BCL6* translocations are associated with dysregulated miRNAs and proteins. These proteins are associated with NF-kB and BCR pathways, and developments of poor response or resistance to treatment. Decreased patient overall survival rate and increased poor prognosis can be attributed to rearrangements of *MYC* and *BCL6*.

Table of Contents

List of Figures

List of Tables

List of Abbreviations

ABC:	Activated B-cell
cSL:	cBF1-suppressor of hairless-LAG1
AID:	Activation-induced cytidine deaminase
AEG-1:	Astrocyte elevated gene 1
BCL2:	B-cell leukaemia/lymphoma-2
BCL6:	B-cell leukaemia/lymphoma-6
BCR:	B-cell receptor
BL:	Burkitt lymphoma
ETS:	C-ets-1
COO:	Cell of origin
CNS:	Central nervous system
DA-EPOCH-R:	Dose-adjusted etoposide, cyclophosphamide, doxorubicin, vincristine, prednisone, and rituximab
DHL:	Double hit lymphoma
DLBCL:	Diffuse large B-cell lymphoma
EBV:	Epstein-Barr virus
FFPE:	Formalin fixed paraffin embedded
FISH:	Fluorescence in situ hybridisation
FL:	Follicular lymphoma
FOXP:	Forkhead box P
GC:	Germinal centre
GCB:	Germinal centre B-cell
HCCA:	α-cyano-4-hydroxycinnamic acid
HGBCL:	High-grade B-cell lymphoma
IHC:	Immunohistochemistry
IMS:	Imaging mass spectrometry
IG:	Immunoglobulin
IGF1R:	insulin-like growth factor 1
IPI:	International prognostic index
JNK:	JUN N-terminal kinase
LDH:	Lactate dehydrogenase
LC:	Liquid chromatography
MALDI:	Matrix-assisted laser desorption/ionisation
MAML:	Mastermind-like protein
MS:	Mass spectrometry
m/z:	Mass-to-charge ratio
NECD:	Notch extracellular domain
NHL:	Non-Hodgkin lymphoma
NHLS:	National Health Laboratory service
NICD:	Notch intramembrane domain
NK:	Natural killer
NTMD:	Notch transmembrane domain
OS:	Overall survival
PS:	Performance status
PDK1:	pyruvate dehydrogenase kinase isoenzyme 1

R-CHOP:	Rituximab, cyclophosphamide, doxorubicin, vincristine, and prednisone
SCT:	Stem cell transplant
SEC:	Super elongated complex
SHIP-1:	SH2-domain-containing inositol-5-phosphatase-1
SHM:	Somatic hyper-mutation
THL:	Triple hit lymphoma
UBE2A:	Ubiquitin-conjugation enzyme E2A
WHO:	World Health Organisation
YAP1:	Yes-associated protein 1

Statement of Original Authorship

Candidate's Declaration

I, Sibusiso Zinhle Radebe declare that this Dissertation is my own, unaided work. It is being submitted for the Degree of Masters of Science in Medicine (Anatomical Pathology) at the University of the Witwatersrand, Johannesburg. It has not been submitted before for any degree or examination at any other University.

Candidates Signature: _____

Date: _17th____day____of____September____2025___in____Johannesburg_

Dedication

I dedicate this dissertation to my beloved son, Nqabayezizwe Radebe. May it kindle a flame of immense potential within you. Moreover, I also pay tribute to the departed soul of my dear grandmother, Sibongile Dlamini, who forever serves an inspiration in my life.

Acknowledgements

I am grateful to express my heartfelt gratitude towards Dr. Pumza Magangane, who served as my sole supervisor during the entirety of my MSc career. Her unwavering support and guidance have been invaluable on this remarkable journey. Despite numerous challenges that made it feel like reaching the end was impossible, she consistently inspired and encouraged me throughout. I truly acknowledge her immense dedication to ensuring the achievement of this significant academic milestone.

I would like to express my gratitude to The Hair and Skin Research Lab, Department of Medicine at the University of Cape Town for permitting me to utilise their instruments in addition to their invaluable assistance with MALDI IMS. I extend a special acknowledgement towards Ms. Nandi Mehlala for her guidance on the analysis of MALDI IMS data, as well as Ms. Nokuphila Shezi for providing me with valuable guidance and support regarding Immunohistochemistry procedures. I also express my gratitude to Dr Zama Mtshali for screening the IHC slides and Mr Eric Liebenberg for assistance in the taking of photomicrographs. Furthermore, I appreciate the help offered by Dr. Sugeshnee Pather and Dr. Tracey Wiggill in assisting me with case selection.

I would like to express my heartfelt gratitude to two remarkable individuals in my life, Mr Mandla Radebe and Mrs Thuli Radebe -my parents- for their unwavering support and endless motivation throughout the journey. I am especially grateful to my loving mother whose wise words of encouragement have been a constant source of strength.

Chapter 1: General Introduction

BACKGROUND

B-cell non-Hodgkin lymphomas (NHLs) are lymphoproliferative neoplasms derived from mature B-cells, with vastly unknown pathogenesis, which are estimated to account for approximately 70-90% of all lymphoid malignancies worldwide and approximately 4% of newly diagnosed cancers yearly (Xei et al., 2015). The most common NHLs include Diffuse Large B-cell Lymphoma (DLBCL) and follicular lymphoma, accounting for more than 60% of all NHL cases when combined (Perry et al., 2016). DLBCL is a major public health concern both locally and internationally as studies have shown that these malignancies account for 30-58% in Europe (France, Italy, Germany, United Kingdom, and Spain) and between 25-35% in the United States of America, of all NHLs (Joy et al., 2013).

DLBCL is a heterogeneous disease characterised by very distinct pathogenic subtypes, gene expression profiles, and morphological variants (Swerdlow et al., 2008). Chemo-immunotherapy for DLBCL is a regimen proven to yield an average cure rate of 70% and includes the use of rituximab, an anti-CD20 monoclonal antibody, with cyclophosphamide, doxorubicin, vincristine, and prednisone (R-CHOP) (Leonard et al., 2017). There are, however, factors that influence DLBCL curability which are the molecular cell of origin (COO), age, presence of chromosomal rearrangements or protein expression, and the International Prognostic Index (IPI) (Lenz et al., 2008; Lenz and Staudt, 2010).

Numerous chromosomal rearrangements are known to indicate a poor prognosis in DLBCL. *MYC* and *BCL6* gene translocations with the immunoglobulin gene are examples of this. A single translocation indicates a poor prognosis for the patient, but the presence of more than one rearrangement indicates an extremely poor outcome. Individuals diagnosed with B-cell lymphoma and have rearrangement on their *MYC* and *BCL6* genes were previously classified as a high-grade B-cell lymphoma (HGBCL) with the said rearrangement commonly referred to as double-hit lymphoma (DHL) (Swerdlow et al., 2016). This has since been reviewed in the World Health Organisation's 5th edition of haematolymphoid tumour classification and reclassified to be DLBCL not otherwise specified (NOS) (Alaggio et al., 2022).

CONTEXT

DLBCL, NOS with rearrangements in the *MYC* and/or *BCL6* are not yet fully understood, as they recently have been reclassified by the World Health Organisation (WHO). For better clinical management of the disease, there is need for more research on this class of DLBCL focusing on the identification of diagnostics and prognostic indicators or markers be continuously carried out as this will aid in developing treatment plans that will improve patient prognosis.

PURPOSES

This study aims at characterising the proteomic and microRNA profiles of DLBCL, NOS. This will enable us to better understand this sub-group of DLBCL with a dire outcome and ultimately add to the already existing knowledge on the identification of possible treatment options for patients diagnosed with the disease.

STUDY SIGNIFICANCE

This study is significant because it aims to profile both diagnostic and prognostic indicators of DLBCL, NOS through molecular techniques, including microRNA identification and proteomics, and by extension attempt to identify associated pathways that might potentially be dysregulated.

The microRNA profile was established by use of polymerase chain reaction (PCR). Through this technique, microRNAs that were upregulated or downregulated were identified and analysed. The proteomic profile was established by use of Matrix-assisted laser desorption ionisation imaging mass spectrometry (MALDI IMS). This technique identifies proteins that are differentially expressed, these proteins are then analysed further.

The investigative approaches taken in this study are not popular compared to the most commonly seen approach in studies that investigate diagnostic and prognostic biomarkers as they are relatively new. Most studies report their findings where they use immunohistochemistry (IHC) and cytogenetics. Identification of microRNAs and proteins associated with DLBCL, NOS will provide a new perspective on how the disease has been viewed previously and identify more areas to be investigated going forward.

Chapter 2: General Literature Review

2.1 B LYMPHOCYTES

B lymphocytes (B-cells) are cells of the immune system that arise and mature in the bone marrow. They are one of the major cells of the second line of defence also known as the adaptive immune response (Abbas and Lichtman, 2012). A receptor molecule that detects antigens called B-cell antigen receptor (BCR) is secreted by the B-cell and its main function is to trigger the adaptive immune response (Braun et al., 2020).

2.1.1 B-cell Development, differentiation and maturity

The process of B cell development involves a sequence of cellular changes during which haematopoietic stem cells transform into immunocompetent B-cells. These transformations occur in different organs, such as the bone marrow, lymph nodes, and spleen. Similar to other blood cell types, B-cells have their origins in haematopoietic stem cells. Haematopoietic stem cells give rise to common lymphoid progenitor cells that can differentiate into either B-cells or T cells (Abbas and Lichtman, 2012).

The progression of B-cell development occurs through various stages which are illustrated below in Figure 1: starting with common lymphoid progenitor cells transitioning into early pro-B cells, followed by late pro-B cells until they transform into large pre-B cells before eventually becoming small pre-B cells before full maturation as immature B-cells. Following this, immature B-cells migrate from the bone marrow to the lymph nodes and spleen to complete subsequent maturation processes (Abbas and Lichtman, 2012; Sylvie, 2023).

B-cells have unique antigen receptors that cause a specific differentiation post-activation as a result of antigen recognition. B-cells either differentiate into effector B-cells or memory B-cells (Abbas and Lichtman, 2012). Effector B-cells function as secretors of the differentiated Ig molecules called antibodies and the memory B-cells, upon stimulation, activate the secondary immune response (Abbas and Lichtman, 2012).

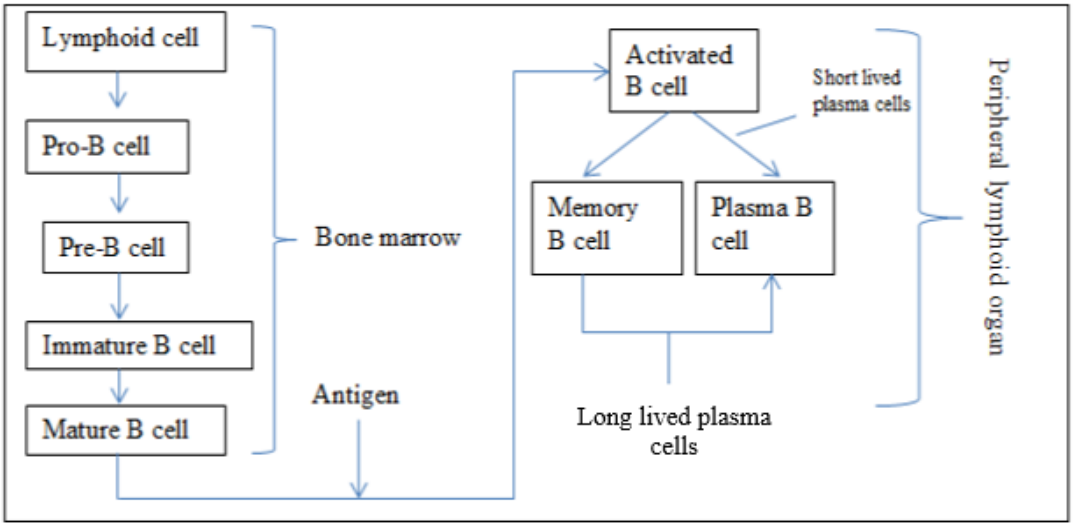

Figure 1: The development and differentiation of B-cells. (Adopted from Sylvie, 2023).

The role of the IG gene in B-cell development:

During early B-cell differentiation in the bone marrow, immunoglobulin (*Ig*) genes undergo a well-coordinated rearrangement process to create their primary repertoire. This involves bringing together different gene segments such as variable (V), diversity (D), and joining (J). The development of these B-cells is marked by the organised recombination of *Ig* H and L chain loci (Alt et al., 1986). Additionally, the Ig proteins themselves actively contribute to regulating the progression of B-cell development (Alt et al., 1986).

2.1.2 Abnormalities

Disruption of the normal control of homeostasis in B-cells results in the formation of tumours. Even though tumours have vast characteristics owing to the cell type they develop from, in B-cells they share a common rearranging of the *Ig* gene (Cook, 2000). This rearrangement, known as gene translocation, occurs in the *Ig* loci and might result in the alteration of gene expression and disruption of cell growth regulation (Cook, 2000).

2.2 B-CELL LYMPHOMA

There are two main types of lymphomas, Hodgkin lymphoma (HL) accounting for 10%, and non-Hodgkin lymphoma (NHL) making up the remaining 90% (Swerdlow et al., 2008). HL can be further categorised into classical and non-classical, while NHL

is classified as a B-cell, T cell, or natural killer (NK) cell type (Swerdlow et al., 2008). When considering clinical implications, it is important to differentiate between aggressive (high-grade) lymphomas and indolent (low-grade) ones. Most low-grade lymphomas fall under the category of NHL except for nodular lymphocyte-predominant Hodgkin lymphoma, which is a HL (Swerdlow et al., 2008).

2.2.1 Non-Hodgkin lymphoma

NHLs are clinically divided into low- and high-grade malignant tumours. The distinguishing characteristic between the two groups is that indolent/low-grade lymphomas such as follicular lymphoma (FL) are not as aggressive as high-grade tumours. However, paradoxically, FLs are more challenging to treat due to their slower growth rate making them resistant to chemotherapy (Tun and Ansell, 2020; Shipp et al., 1993). High-grade tumours have cells that proliferate rapidly translating to fast tumour growth and the disease can be cured (Tun and Ansell, 2020). Examples of high-grade include DLBCL and Burkitt lymphoma (BL).

2.3 DIFFUSE LARGE B-CELL LYMPHOMA

The most common subtype of NHL in the adult population is the genetically heterogeneous and aggressive DLBCL. The global incidence of DLBCL ranges from 2.3 to 13.8 cases per 100,000 person-years (Garg et al., 2022). In Germany, the estimated incidence is approximately 7 cases per 100,000 person-years (Garg et al., 2022). It is roughly estimated that the prevalence over a 10-year period in Western Europe is 45 cases per 100,000 patients (Skalt et al., 2022). DLBCL accounts for approximately 40% of all B-cell lymphomas and more than 80% of all aggressive lymphomas worldwide (Rosenthal and Younes, 2017; Campo et al., 2011). In Southern Africa, DLBCL are reported to have a prevalence of 37% of all NHLs (Perry et al., 2016).

DLBCL originates in the B lymphocytes that produce immunoglobulin within the lymphatic system (De Felice et al., 2018). Clinically patients with DLBCL present with lymphadenitis as a result of the rapidly proliferating tumour cells, accompanied by weight loss, fever and excessive night sweats. In less common cases, organ involvement also presents.

2.3.1 Morphological variants of DLBCL

The morphology of DLBCL consists of large and diffusely organised lymphoma cells that completely or partially destroy normal nodal or extra nodal architecture (Swerdlow et al., 2016). Groups of lymphoma cells may be compartmentalised by fine fibrosis, or the neoplasm may be linked to sclerosis (Korkolopoulou et al., 2016). The rate of mitosis may be high and single-cell apoptosis may be noticeable. Approximately 10% of DLBCL cases exhibit a starry sky pattern (Swerdlow et al., 2016). A high rate of proliferation is usually always linked to this pattern. In every incidence of DLBCL, there are varying amounts of background reactive small T cells and histiocytes. Although other DLBCL variants have been described, the most prevalent are the centroblastic, immunoblastic, and anaplastic types (Swerdlow et al., 2016).

Centroblastic:

The most commonly found morphological variant accounts for over 80% of DLBCL cases, making it the most prevalent (Swerdlow et al., 2016). Centroblasts are large cells that comprise 2-3 tiny nucleoli that are frequently peripherally positioned next to the nuclear membrane. These cells have round to oval vesicular nuclei, vesicular chromatin, and a considerable amount of cytoplasm (Swerdlow et al., 2016).

Immunoblastic:

This variant accounts for approximately 8-10% of DLBCL cases (Swerdlow et al., 2016). The immunoblastic subtype has typically been identified by the presence of at least 90% immunoblastic cells. These are large lymphoid cells with moderate to abundant basophilic cytoplasm, a centrally positioned, conspicuous trapezoid-shaped nucleolus, and thin chromatin strands adhering to the nuclear membrane (Swerdlow et al., 2016).

Anaplastic:

This variant makes up just approximately 3% of all DLBCL cases and is substantially less prevalent than the immunoblastic and centroblastic variants (Swerdlow et al., 2016). Large lymphoma cells with pleomorphic or strange nuclei are characteristics of the anaplastic subtype (Swerdlow et al., 2016).

2.4 DLBCL CLASSIFICATION

Currently, DLBCL can be classified into three subtypes based on the cell of origin (COO): activated B-cell-like (ABC), germinal centre B-cell-like (GCB), and Unclassified. ABC and GCB subgroups jointly account for 75% - 80% of all DLBCL (Rosenwald et al., 2022). However, these subtypes have limited prognostic and clinical value due to the common use of standard treatment regimens for all three types (Schmitz et al., 2018).

The determination of subtypes primarily relies on the resemblance of the malignant cells to specific stages of B-cell development, both morphologically and genetically (ABC/GCB), or the absence of identifying characteristics (Unclassified) (Campo et al., 2011; Rosenquist et al., 2016; Rosenquist et al., 2017).

While these subtypes do exhibit high occurrences of similar genetic mutations within their respective groups (e.g., B-cell receptor or *NOTCH* abnormalities), they are not sufficient for precise treatment and prognosis prediction, especially in cases where traditional R-CHOP therapy is ineffective. The heterogeneity among DLBCL within the ABC/GCB/Unclassified groups poses a significant challenge in implementing a standardised regimen like R-CHOP, underscoring the necessity for narrower and more well-defined subgroups with targeted treatment options.

2.4.1 Subgrouping based on cell of origin (COO)

ABC, GCB, and unclassified DLBCL are categorized based on the stage of development they most closely resemble after genetic mutation disrupts typical progression and causes malignant transformation. The cells of these subtypes acquire their morphologic and clinical characteristics during the stage of development in which they accumulate sufficient genetic variation to become malignant. At this point, differentiation either ceases or continues along a path that is not observed in healthy and functional B-cells (Schmitz et al., 2018).

The ABC subtype is believed to have progressed through the germinal centre and is committed to plasmablastic differentiation, while GCB cells are thought to originate from the light zones in the germinal centre (Pfreundschuh et al., 2008). Although the clinical outcomes of GCB lymphomas are generally considered superior to ABC malignancies when traditional R-CHOP therapy is used, risk stratification has not resulted in improved treatment outcomes. Approximately 30% to 50% of DLBCL

patients do not respond to this therapy, and only 10% of those with treatment-refractory disease are cured with second-line salvage treatment or bone marrow transplants (Pfreundschuh et al., 2008; Gisselbrecht et al., 2010; Friedberg, 2011; Coiffier and Sarkozy, 2016).

The heterogeneity of treatment outcomes, even among ABC, GCB, and Unclassified subtypes, is likely the result of specific pathways with altered regulation, expression, or end products that are not defined by classical subtyping.

2.4.1.1 Activated B-cell-like subtype (ABC)

Cells falling into the ABC classification commonly exhibit specific mutations and translocations, such as *PRDM1* truncations or homozygous deletions, which are unique to the ABC subtype. These genetic alterations provide valuable insights into the behaviour patterns of these cells (Mandelbaum et al., 2010; Schmitz et al., 2018). Furthermore, the identification of these defining pathways and their association with a specific disease course, even in mouse models, reinforces the concept of grouping diseases for prognostic and treatment purposes (Mandelbaum et al., 2010; Miao et al., 2019).

ABC cells are characterized by a higher incidence of "chronic active" BCR signalling, which is distinguished by BCR clustering and autoreactive self-antigens. This is in contrast to tonic signalling, which is antigen-independent and lacks BCR clustering, as observed in GCB cells. Importantly, *MYD88* mutations leading to extranodal involvement, *TNFAIP3* inactivation resulting in uncontrolled NF-κB expression, and *NOTCH1* mutations are predominantly found in the ABC subtype. While these mutations are not exclusive to cells expressing the ABC phenotype, they are significantly more strongly associated with this subtype compared to the GCB or Unclassified types.

2.4.1.2 Germinal centre B-like subtype (GCB)

GCB cells are influenced by the master regulator *BCL6*, similar to ABC cells. However, they also have distinctive mutations. These mutations include *REL* amplifications, which facilitate lymphomagenesis, almost exclusive presentation of t(14;18)(q32;q21) translocations resulting in *BCL2* activation and overexpression, and *CREBBP* mutation affecting the histone acetyltransferase domain, leading to epigenetic dysregulation (Ennishi et al., 2017; Miao et al., 2019).

The incidence of these mutations among all patients diagnosed with GCB DLBCL is relatively low and cannot be considered definitive for the disease type. However, the presence of these mutations in GCB DLBCL and the correlation between GCB type and a favourable response to first-line R-CHOP therapy support the clear notion that dysregulated pathways respond differently, or not at all, to a given treatment.

One of the major issues with the accepted stratification of DLBCL is the variation in treatment response even when seemingly identical focal mutations are present in both ABC and GCB, such as *TP53* deletion or *MYC* mutations (Cao et al., 2016; Xu-Monette et al., 2016). This observation, combined with the substantial number of possible mutations, suggests that we should not group based on individual pathway alterations, but rather based on sets of mutations that can be found together and targeted therapeutically (Mansouri et al., 2022).

2.4.2 Subgrouping based genetic alterations and signalling pathways

The current ABC and GCB subgroups have limited utility due to their failure to account for the diverse genomic alterations that cannot be detected via immunohistochemical staining techniques. To establish efficacious targeted therapies and reliably forecast disease progression, it is imperative to thoroughly investigate the precise pathways underlying the aberrant proliferation of these cells, pinpoint the specific dysregulations within these pathways, and ascertain their overall contribution to the progression of malignancy.

Genetic alterations:

Understanding which genetic anomalies tend to co-occur and their associated prognosis is a crucial initial step in establishing a new categorization system for DLBCL. However, this is not the ultimate objective. To develop effective treatments, it is imperative to thoroughly comprehend the pathways that have been modified and determine their impact on disease progression. Equally important is the identification of the precise location of disruption within a pathway, as mutations downstream of drug targets may render the drug ineffective, even if it targets the correct pathway. By closely examining the pathways that undergo alteration and the specific locations of these alterations, we can not only grasp the complexity of DLBCL but also identify potential drug targets for further discussion on therapeutic applications.

Disrupted signalling pathway:

The most commonly mutated pathways in DLBCL encompass BCR signalling, PI3K-AKT-mTOR signalling, BCR dependent NF-κB activation, NF-κB signalling, TLR signalling, and the BCL2 anti-apoptotic family. These pathways are intricately interconnected as they facilitate the evasion of apoptotic pathways, promote cell proliferation and gene expression, and play a role in lymphoma development. By focusing on both the general aberrant pathways and specific mutations within them, we can make progress in targeted DLBCL treatment. Identifying significant mutations is the first stride in this endeavour.

2.4.2.1 B-cell receptor (BCR) signalling pathway

BCR signalling plays a crucial role in the regulation of B-cell survival, development, and differentiation. In DLBCL, BCR signalling can manifest as either chronic active or tonic. Both the overexpression and overactivation of BCR signalling have been implicated in the development of lymphoma (Rawlings et al., 2017).

Upon binding of the BCR to its appropriate ligand, a heterodimer is formed by CD79A and CD79B. Following the dual phosphorylation of the intracellular immunotyrosine-based activation motifs (ITAMs) of CD79A/CD79B, SYK kinase is recruited and activated. This, in turn, leads to the activation of Bruton's tyrosine kinase (BTK), resulting in downstream activation of BCR signalling pathways, including mTOR and NF-κB (Miao et al., 2019). Any mutations occurring along this pathway can potentially lead to its overactivation.

Positive regulation of B-cell receptors may occur through the mutation or amplification of CD79B and CD79A. Conversely, some inhibitors negatively regulate BCR signalling, such as LAPTM5, LYN, PTPN6, GRB2, PRKCD, DGKZ, SLA, and MAP4K1 (Anders et al., 2015; Seshan, 2017). The loss of function of these negative regulators of BCR signalling can lead to uncontrolled activation or the loss of negative feedback from the BCR. This has been observed in 38.5% of DLBCL cases (Schmitz et al., 2018).

The loss of function of negative regulators is more prevalent in cases with *MYD88* and *CD79A*/*CD79B* activating mutations compared to cases without these alterations (56% vs. 36.4%) (Schmitz et al., 2018). This may have clinical significance because aggressive lymphomas with $MYD88^{L265P}$ and *CD79B* mutations have shown a response to ibrutinib, which targets Bruton's tyrosine kinase downstream of BCR

signalling (Chapuy et al., 2016; Schmitz et al., 2018). These lymphomas are presumed to have chronic active BCR signalling (Chapuy et al., 2016; Schmitz et al., 2018). The most common mutation affecting both BCR and TLR signalling is *MYD88*, observed in 18% to 27% of cases. *MYD88* directly affects TLR signalling and indirectly influences BCR signalling since MYD88, TLR9, and BCR form a multiprotein supercomplex that promotes downstream NF-κB and mTOR activation (Phelan et al., 2018).

2.4.2.2 NF-κB signalling (IκB kinase-dependent NF-κB activation)

NF-κB signalling can also be stimulated by the activation of the IKBKG/IKBKB complex. This activation is partially dependent on the BCR pathway and can occur through various mechanisms (Schmitz et al., 2018). Mutations in the positive regulators TLR2 and MYD88, or the inactivation of the negative regulators TNIP1/TNFAIP3, enable IκB kinase (IKBKG/IKBKB) to inhibit the NFKBIA/NFKBIE complex (Schmitz et al., 2018; Miao et al., 2019; Ma and Malynn, 2020).

Inhibition of this complex leads to the release of p65/p50 and REL pathways, which can also undergo activating mutations, resulting in the overexpression of NF-κB (Schmitz et al., 2018; Miao et al., 2019). Genetic alterations of NF-κB negative regulators were a prominent feature in subtype BN2, with 55% of cases showing mutations in negative regulators TNFAIP3 or TNIP1 (Schmitz et al., 2018). Mutations in the positive regulator MYD88 are also a defining characteristic of the MCD subtype and make a significant contribution to gene overexpression (Schmitz et al., 2018).

2.4.2.3 Toll-like receptor (TLR) signalling

The Toll-like receptor 2 (TLR2) signalling pathway is typically mediated by *MYD88*, an adapter protein that facilitates signalling when complexed with IRAK1/4 (Ngo et al., 2011). However, mutation of *MYD88* leads to the formation of a complex composed of IRAK1 and IRAK4, which augments IRAK4 kinase activity and IRAK1 phosphorylation. Subsequently, hyperphosphorylated IRAK1 then activates TRAF6, which then activates TAK1. Through the IκB kinase pathway, TAK1 can initiate downstream NF-κB and JAK/STAT signalling (Ngo et al., 2011; Schmitz et al., 2018; Miao et al., 2019).

It is important to note that activating mutations of *TLR2*, *MYD88*, and *TRAF6* have been observed, which can stimulate this pathway even in the absence of the appropriate TLR ligand (Schmitz et al., 2018). Moreover, activating mutations of *MYD88* lead to increased activity in both the NF-κB and JAK/STAT pathways (Rosenquist et al., 2017). Conversely, inactivating mutations of negative regulators UBE2O and TNFAIP3, which normally inhibit TRAF6, have also been identified. These mutations result in overstimulation of the downstream NF-κB pathway (Miao et al., 2019).

2.4.2.4 B-cell lymphoma 6 (BCL6) signalling

BCL6 fusions are commonly associated with *NOTCH2* mutations, which are key characteristics of the BN2 subtype (Schmitz et al., 2018). Normally, BCL6 recruits histone deacetylase 3 (HDAC3) to deacetylate the transcriptional enhancers it binds to, preventing them from being transcribed (Hatzi et al., 2013; Miao et al., 2019). Changes in the first noncoding exon of BCL6 also disrupt negative autoregulation, leading to increased gene activity (Miao et al., 2019).

BCL6 controls various processes such as plasma cell differentiation (IRF4, PRDM1), cell migration (S1PR1), DNA damage response (ATR, CHEK1), cell cycle (CDKN1A, CDKN1B), and cell death (TP53) (Miao et al., 2019). Activating mutations in *BCL6* (or its activators like MEF2B), or inactivating mutations in BCL6 inhibitors (*EP300*, *CREBBP*, *FBXO11*), suppress the aforementioned processes, promote germinal centre formation, and disrupt plasma cell formation (Pasqualucci et al., 2011; Miao et al., 2019).

2.4.2.5 Myelocytomatosis (MYC) signalling

MYC is a proto-oncogene that plays a central role in multiple second messenger pathways. It regulates the transcription of genes involved in various cellular processes, such as cell growth and proliferation, apoptosis, metabolism, DNA replication, and protein biosynthesis (Dang, 2012; Karube and Campo, 2022). Cells exhibiting gene expression characteristic of MYC, along with proliferation, are highly associated with the MCD and BN2 subtypes (Schmitz et al., 2018). Interestingly, *MYC* rearrangements do not predict a poorer prognosis in patients receiving the DA-EPOCH-R regimen (etoposide, prednisone, vincristine, cyclophosphamide, doxorubicin, rituximab). This suggests the possibility of targeting this pathway (Lai et al., 2018).

Another study found that the partner of MYC is prognostically significant. *IGH-MYC* translocations, in particular, have the worst prognosis among all *MYC* translocations. This is likely because *IGH-MYC* translocations place MYC adjacent to immunoglobulin enhancers, leading to constitutive MYC expression (Copie-Bergman et al., 2015; Karube and Campo, 2015).

Activation-induced cytidine deaminase (AID) is thought to mediate MYC translocations with *IGH* or *BCL6*. AID is responsible for somatic hypermutation and class switch recombination but can also target and create breaks in *BCL6* and *MYC* (Miao et al., 2019). More than half of DLBCL patients have reported mutations resulting from incorrect AID-related hypermutation, especially in regions not coding for immunoglobulin genes (Deutsch et al., 2007; Miao et al., 2019).

In addition to activating *MYC* translocations, which lead to the upregulation of downstream genes, inactivating mutations of the negative regulator MAX-gene associated protein (MGA) are also implicated in improper MYC expression (Miao et al., 2019). The clinical relevance of MYC aberrations is evident from trials using the DA-EPOCH-R protocol. Furthermore, further subtyping based on MYC partner or mutation location may provide additional prognostic significance (Copie-Bergman et al., 2015; Karube and Campo, 2015; Xu-Monette et al., 2016).

2.4.2.6 NOTCH signalling

BCL6 translocation frequently co-occurs with the aberrantly triggered Notch pathway, which encourages NF-kB signalling and cell proliferation (Schmitz et al., 2018). Notch-targeted genes are up-regulated, promoting their differentiation into marginal zone cells (Wright et al., 2020).

2.4.2.7 Cell migration

Under normal circumstances, GCB cells should only be present within appropriate germinal centres. However, in DLBCL, they can also be found circulating and in extranodal sites (Cao et al., 2017; Franco et al., 2017; Zheng et al., 2017; Zhou et al., 2018; Miao et al., 2019). The migration of these cells is likely due to the inactivation or under-activation of the sphingosine 1-phosphate receptor-2 (S1PR2) (Green et al., 2011; Muppidi et al., 2014; Miao et al., 2019). In malignant conditions, S1PR2 is inactivated, preventing downstream activation of GNA13. Consequently, ARGHEF1 and RHOA cannot be activated, leading to a lack of inhibition of cell migration

(Muppidi et al., 2014; Rosenquist et al., 2017; Miao et al., 2019). Normally, *GNA13* and *ARHGEF1* encode mediators that control the growth of GCB cells and confine them to germinal centres. The absence of these mediators results in the systemic distribution and uncontrolled migration of GCB cells (Morin et al., 2011; Muppidi et al., 2014). The disruption of the homing pathway encoded by *GNA13* and *ARHGEF1* is observed in 38% of EZB subtype cases, underscoring the significance of this specific pathway (Schmitz et al., 2018).

Epigenetic regulation alterations leading to lymphomagenesis:

A correlation has been observed between an unfavourable clinical outcome and increased epigenetic heterogeneity (De et al., 2013; Jiang and Melnick, 2015). Therapeutic interventions for DLBCL may involve the application of inhibitors targeting mechanisms such as DNA methyltransferase and histone methyltransferase (Jiang and Melnick, 2015). Distinctive forms of epigenetic dysregulation can be found in each DLBCL subtype. For instance, the EZB subtype commonly exhibits mutations in *EZH2* or inactivation of *KMT2D* (Schmitz et al., 2018).

2.4.2.8 Enhancer of zeste homolog 2 (EZH2)

EZH2 plays a vital role in the inhibition of gene transcription by adding three methyl groups to a specific amino acid, Lys27, on the histone H3 subunit. This modification is commonly referred to as H3K27 (Velichutina et al., 2010; Beguelin et al., 2013; Caganova et al., 2013). Overactivation of EZH2 leads to the excessive activation of regulators and promoters involved in cell cycle control and plasma cell differentiation. Notable examples include CDKN1A, CDKN1B, CDKN2A, PRDM1, IRF4, and XBP1 (Miao et al., 2019). Consequently, defective formation of germinal centers in GCB cells occurs, as these cells can proliferate without regulation by cell cycle regulators. Furthermore, they are protected from apoptosis induced by genotoxic damage and exhibit limited differentiation ability (Velichutina et al., 2010; Beguelin et al., 2013; Caganova et al., 2013).

2.4.2.9 EP300 and CREBBP

H3K27 acetylation, among multiple histone lysine acetylation sites, is associated with active transcription, while deacetylation inhibits transcription. EP300 and CREBBP are involved in H3K27 acetylation, promoting the transcription of tumour suppressor genes such as *PRDM1*, *IRF4*, *CIITA*, *CD74*, and *HLADR*. Additionally, acetylation of

BCL6 and p53 leads to the inhibition and activation of transcription, respectively (Miao et al., 2019).

A mutation in *CREBBP* reduces the expression of these genes, which are crucial for plasma cell differentiation and immune responses against lymphomagenesis. This mutation can be found in approximately 20% of patients with DLBCL, more commonly in the GCB subtype than the ABC subtype (Pasqualucci et al., 2011; Lohr et al., 2012). In mice, *CREBBP* mutations have been observed to significantly increase the number of germinal center B-cells, promoting the development of MYC-driven lymphoma (Hashwah et al., 2017). Deficiencies in CREBBP also lead to reduced expression of genes responsible for the germinal center exit, antigen presentation, and immune response, thus promoting lymphomagenesis (Jiang et al., 2017). *EP300* is mutated in approximately 10% of both ABC and GCB types of DLBCL, and its effects are phenotypically similar to *CREBBP* mutations (Pasqualucci et al., 2011).

2.4.3 Historical WHO Classification

The World Health Organisation (WHO), in the year 2017, revised the classification of high-grade B-cell lymphomas. The term was repurposed to refer to high-grade B-cell lymphomas with chromosomal rearrangements on three different genes which included the *MYC*, *BCL2*, and/or *BCL6* (Swerdlow et al., 2017). High-grade B-cell lymphomas harbouring two gene translocations were classified as ‘double-hits’ and those with three gene translocations as ‘triple-hits’.

2.4.4 Current WHO Classification

The 5th edition of the WHO classification of haematolymphoid tumours (WHO-HAEM5) delineates 17 distinct entities of DLBCL, which can be further categorised based on morphology, genetic features, viral association, site of origin, and other overlapping criteria (Alaggio et al., 2022). Within WHO-HAEM5, three morphological subtypes are recognized: centroblastic, immunoblastic, and anaplastic. Gene expression profiling (GEP) studies have identified two major profiles that can further subclassify DLBCL, NOS into molecular subtypes: germinal centre B-cell-like (GCB-like) and activated B-cell-like (ABC-like). The GCB-like subtype predominantly expresses genes observed in cells within the reactive germinal centre (GC), whereas the ABC-like subtype exhibits a gene expression profile resembling

activated B-cells. This classification system is incorporated in the International Consensus Classification (ICC) proposal (see Campo et al., 2022).

DLBCL or high-grade B-cell lymphoma (HGBCL) with co-occurring *MYC* and *BCL6* rearrangements encompass a wider spectrum of cases, characterized by diverse gene expression profiles and mutations that distinguish them from DLBCL/HGBCL with both *MYC* and *BCL2* rearrangements (Cucco et al., 2020). As a result, these cases were excluded from the category of double-hit lymphoma (DHL) within DLBCL/HGBCL and are now classified as either a subtype of DLBCL, NOS or HGBCL, NOS based on their cytological features (Alaggio et al., 2022).

2.5 DLBCL, NOS

The aetiology of DLBCL is multifaceted with genetic predisposition, immunodeficiency, and viral infection all believed to play a role in its development (Cerhan et al., 2014). While most cases of DLBCL, not otherwise specified (DLBCL, NOS), originate from lymph nodes and do not meet the criteria for more specific classifications, DLBCL can also occur in extranodal lymphatic tissues like the tonsil or Peyer patches in the gastrointestinal tract, as well as in other tissues throughout the body (Cerhan et al., 2014).

Recently, more advanced methods have been employed to investigate the mutational landscape of DLBCL, NOS through exome or targeted sequencing. These methods have revealed a highly heterogeneous range of molecular changes in DLBCL, NOS, with recurrent mutations identified in approximately 150 coding genes or targets of copy number changes. On average, in each case of DLBCL, NOS exhibits approximately 8% of mutated genes (Reddy et al., 2017). Three separate research groups have identified molecular subtypes of DLBCL that either refine the COO classification or exist independently of COO (Lacy et al., 2020; Chapuy et al., 2018; Schmitz et al., 2018). Interestingly, despite using different platforms and algorithms, these studies have produced classification trees that overlap, although they are not identical. However, due to the lack of a unified concept for these proposed clusters and their significant genetic drivers, both WHO-HAEM5 and ICC currently do not recommend molecular subclassification of DLBCL.

2.6 DIAGNOSIS AND STAGING

DLBCL, NOS is an aggressive neoplasm characterised by the presence of large B lymphoid cells with a diffuse growth pattern, which can be observed in tissue samples through microscopy. A proper diagnosis of DLBCL, NOS requires obtaining a biopsy of sufficient size (Liu and Barta, 2019). Syrykh et al. (2022) found that core needle biopsy (CNB) can definitively diagnose suspected lymphoma in 92% of patients, while surgical excision achieves a definitive diagnosis in 98% of cases. Therefore, unless strictly contraindicated, surgical lymph node biopsy is considered essential for diagnosis when compared to CNB or fine needle aspiration (FNA).

Microscopy is used to examine the size and diffuse growth pattern of the B-cells and confirm the diagnosis. Additionally, immunohistochemistry (IHC) staining, flow cytometry, and cytogenetics (including fluorescence in situ hybridisation (FISH) and karyotyping) tests are conducted to further characterise the lymphomas.

Once a diagnosis is confirmed, various laboratory tests are performed as part of the clinical prognostic systems, which assist in informing treatment selection. The disease is staged using imaging techniques such as computerised tomography (CT) or positron emission tomography (PET) scans, with a preference for PET/CT when available. PET-CT is regarded as essential for staging patients with DLBCL for two primary reasons: (i) CT scans alone frequently fail to detect extranodal disease, which can result in under-staging, and (ii) a staging scan is crucial for identifying initial disease sites, facilitating accurate reporting of end-of-treatment scans (Barrington et al., 2014).

Subsequently, different clinical scoring systems, including the International Prognostic Index (IPI), are used to risk-stratify newly diagnosed DLBCL, NOS patients before selecting a treatment plan (Ruppert et al., 2020). These systems consider factors such as disease stage, presence of extranodal disease, lactate dehydrogenase (LDH) level, age, and performance status of the patient to determine the most appropriate treatment regimen based on the patient's risk group.

2.6.1 Diagnosis

2.6.1.1 Histology

Haematoxylin and Eosin:

The haematoxylin and eosin (H&E) stained tissue section plays a crucial role in diagnosing anatomical pathology. This procedure uses haematoxylin and eosin dyes

to stain the nucleus and cytoplasm, respectively, allowing easy identification of cellular components. However, successful staining relies on proper specimen processing which includes tissue preservation, dehydration, clearing, and paraffin infiltration. The characteristic pathological features of the tumour are identified through microscopic analysis of tissue sections stained with H&E. These include widespread growth patterns where large neoplastic B-cells have either completely or partially eliminated the normal structure (Quintanilla-Martinez, 2015).

Immunohistochemistry:

Immunohistochemistry (IHC) is a highly effective method that utilises the specific interaction between an antibody and antigen to identify particular antigens in cells and tissues. This technique is primarily employed with light microscopy for detection purposes. IHC has become imperative in clinical diagnostics within anatomical pathology due to advancements like antigen retrieval methods (Lin and Chen, 2014). These approaches enable convenient testing on formalin-fixed paraffin-embedded (FFPE) tissue samples. Furthermore, automated techniques have been developed to handle large volumes of specimens while ensuring reproducible results throughout the process (Lin and Chen, 2014; Shi et al., 1991).

2.6.1.2 Genetics

DLBCL is caused by mutations in proto-oncogenes and genes responsible for tumour suppression (Reddy et al., 2017). The conditions within lymph nodes can further contribute to the development of lymphomagenesis. Through exome sequencing, more than 150 genetic drivers associated with DLBCL have been identified (Reddy et al., 2017).

Molecular genetic research demonstrates that there are alterations in the genes responsible for immunoglobulin heavy and light chains. Within the immunoglobulin heavy-chain variable region gene, hypermutation takes place. Rearrangements of the *BCL6* gene occur in approximately 30% of cases (Reddy et al., 2017). In contrast to Burkitt lymphoma, around 10% of cases involve *MYC* (8q24) translocation fused with a non-immunoglobulin gene (Reddy et al., 2017)

2.6.1.3 Cytogenetics

DLBCL can be classified by cytogenetic or fluorescence in situ hybridization (FISH). These techniques reveal characteristic chromosomal translocations, including t(3q27)

(associated with *BCL6* rearrangement), which is present in 35% of cases and t(8;14)(q24;q32)(which indicates *MYC* rearrangement), found in less than 5% of cases (Ghandi, 2015).

2.6.1.4 Biomarkers

MYC:

MYC (also known as c-*MYC*), *NMYC*, and *LMYC*, are three members of a transcription factor family that have historically been among the most investigated proteins in the biology of B-cells and cancer. *MYC* is a crucial transcription factor that controls up to 15% of all human genes, allowing it to control hundreds of target genes involved in different cellular pathways (Calado et al., 2012).

The *MYC* transcription factor regulates the expression of various target genes involved in cell cycle control, DNA damage repair, metabolism, protein synthesis, and stress response (Dang et al.2006). In humans, *MYC* is located on chromosome 8 (8q24) and can be activated through mutations affecting regulatory or promoter regions, chromosomal translocation events, or an increase in copy number (Meyer and Penn, 2008).

Normally functioning cells activate the *TP53* pathway upon *MYC* activation leading to apoptosis, however, cells with *MYC* translocations often possess inhibitory *TP53* mutations that allow them to evade programmed cell death (Tzankov et al., 2014). DLBCL cases featuring *MYC* translocations may also exhibit *BCL6* translocations which contribute to aggressive clinical behaviour.

It has been that approximately 10% of DLBCL cases (ranging from 4% to 14%) show evidence of a *MYC* mutation primarily detected within the GCB subtype (Copie-Bergmant et al., 2014). The *MYC* transcriptional network is cellular context-dependent, and due to its broad function in cell activation and proliferation, it has the potential to function as a potent proto-oncogene (Calado et al., 2012).

BCL6:

BCL6 is an oncogene found on chromosome 3q27 (Basso and Dalla-Favera, 2012), contributes to the regulation of several cellular processes, including activation, differentiation, and apoptosis, by acting as a transcriptional repressor (Phan and Dalla-Favera, 2004). As a transcription factor, *BCL6* is controlled by CREBBP/EP300, which binds to conserved sequence in the target gene's promoter region, this

interaction regulates the expression of the target genes by interacting with the target gene's co-repressor complexes (Basso and Dalla-Favera, 2012).

TP53:

The tumour suppressor gene *TP53*, found on chromosome 17, encodes a nuclear phosphoprotein called p53. This protein plays a crucial role in the regulation of DNA transcription, cellular proliferation, and apoptosis (Gouveia et al., 2012). Approximately 30% of B-cell lymphomas are associated with mutations in *TP53* specifically occurring on exons 5 and 9 (Ahmadi et al., 2021; Gouveia et al., 2012). These particular exons have an important function in repairing damaged DNA.

Additionally, when there are mutations present in the *BCL6* gene it may lead to the deactivation or inhibition of p53's normal activity within cells. Further promoting the development of lymphoma (Ahmadi et al., 2021). Notably, the presence of these *TP53* mutations or the nonexistence of the gene corresponds to an especially aggressive progression and dismal prognosis for patients (Ahmadi et al., 2021; Lossos, 2005).

2.6.2 Staging

The stage of lymphoma is critical in determining a patient's treatment options; however, its significance varies among different types of lymphoma. For many common types of NHL, treatment decisions depend on whether the lymphoma is classified as "limited" (stage I or stage II non-bulky) or "advanced" (stage III or IV) (Armitage, 2005). In the case of stage II bulky lymphomas, additional factors, known as prognostic factors, are considered to assist in determining whether to treat the lymphoma as limited or advanced (Armitage, 2005).

The Ann Arbor staging system, first introduced for Hodgkin's lymphoma in 1974 and modified in 1988, serves as the foundation for the current staging system. The Lugano classification, which is based on the Ann Arbor system, is now employed for both Hodgkin's lymphoma and NHL (Armitage, 2005).

Stage I NHL involves either a single lymph node region or an extra-lymphatic site. Stage IE indicates involvement of a single extra-lymphatic site, with the "E" denoting limited extranodal involvement. Stage II refers to the involvement of two or more lymph nodes on the same side of the diaphragm. Stage III involves lymph nodes on both sides of the diaphragm. Finally, Stage IV indicates the spread to one or more extra-lymphatic organs (such as the bone marrow, liver, or lungs), with or without lymph node involvement.

2.7 TREATMENT

Generally, the GCB subtype of DLBCL has positive treatment outcome when the patient is put on immunochemotherapy with standard R-CHOP (rituximab, cyclophosphamide, doxorubicin, vincristine, and prednisone) regimen regardless of how they are defined (Scott et al., 2015).

The ABC subtype, characterised by activated NF-kB signalling has been reported to have a poor clinical prognosis with aggressive features of DLBCL (Wright et al., 2003). A large number of DLBCL patients develop refractory disease which is quite unfortunate as the mechanism underlying drug resistance in DLBCL is yet to be determined (Bai et al., 2013).

The patient's overall survival (OS) rate has been improved through combination therapy, however, treatment outcome remains variable. Furthermore, additional complexities in treatment exist as a result of the heterogeneous nature of DLBCL (Sehn et al., 2005). Consequentially, a substantial amount of patients with DLBCL remain uncured as it is very difficult to identify second-line therapy for them. Additional treatment approaches to the standard R-CHOP have been reported and an example of such a treatment is autologous stem cell transplant (SCT) for 'advanced stage' disease patients, DA-EPOCH-R (dose-adjusted etoposide, cyclophosphamide, doxorubicin, vincristine, prednisone, and rituximab) for DLBCL patients with positive *BCL6* protein expression (Kim et al., 2014; Wilson et al., 2008).

2.8 PROGNOSIS AND OVERALL SURVIVAL RATE

International prognostic index:

The International Prognostic Index (IPI), which was first introduced in 1993 and used to determine the prognosis of DLBCL, considers factors such as Ann Arbor stage, patients age, performance status (PS), serum lactate dehydrogenase (LDH), and extranodal involvement (Sehn et al., 2005). The IPI reflects the biology of the tumour and host, however, it is not able to reliably predict the patient's response to treatment (Xei et al., 2014). Thus, to identify high-risk individuals who can benefit from targeted or focused therapy there is a need for additional techniques or markers (Banham et al., 2005).

2.9 GENERAL OVERVIEW AND SUMMARY

DLBCL, NOS has been designated as a distinct category in the 5th edition WHO classification of lymphoid neoplasms (Alaggio et al., 2022). This category encompasses DLBCL, previously also known as double-hit lymphomas with *MYC* and *BCL6* rearrangements. Diagnosing these entities is quite challenging, requiring meticulous morphologic descriptions and various additional analyses such as FISH. However, determining which patients should undergo these analyses remains challenging.

DLBCL, NOS exhibit an extremely aggressive clinical course with a tendency towards resistance to chemotherapy and early relapses. There is currently no standard treatment approach established for this condition, even the commonly used R-CHOP chemoimmunotherapy regimen proves largely dissatisfactory.

Intensified chemoimmunotherapy approaches that resemble Burkitt-like regimens have been explored but are still not yielding completely satisfactory outcomes. Consolidation therapy involving ASCT does not provide significant survival benefits except under limited circumstances like when patients achieve less than complete remission after induction therapy. Improving the grim prognosis associated with DLBCL, NOS continues to be an urgent unmet need in clinical practice. Novel drugs hold promise for playing a critical role in enhancing current therapeutic strategies.

With the knowledge that DLBCL, NOS remain a complex condition to diagnose, it is crucial to conduct additional research to establish precise guidelines for identifying cases that require thorough investigation through molecular test methods.

This study analysed and described the microRNA and proteomic profiles of DLBCL, NOS to obtain a more comprehensive understanding of this specific subset within DLBCL which displays an unfavourable prognosis. Through this investigation, we strive to uncover potential therapeutic options for individuals belonging to this particular group.

2.10 STUDY AIM

The study aimed to profile the miRNA and proteomics associated with DLBCL, NOS single-hits, MYC^R or $BCL6^R$, and dual-rearrangements, MYC^RBCL6^R.

Chapter 3: The MicroRNA profile of DLBCL, NOS with rearrangements in *MYC* and *BCL6*

3.1 OVERVIEW

The primary emphasis of this chapter is the microRNA profile of the study. Section 3.2 will delve into the existing literature regarding DLBCL, NOS with genetic rearrangements on specific genes, namely *MYC* and *BCL6*. Section 3.3 discusses the research design and methodology for processing specimens to obtain results which were subsequently analysed and reported in section 3.4. For a comprehensive understanding of the findings, sections 3.5 and 3.6 serve as platforms to thoroughly examine and deliberate upon the obtained results before drawing an encompassing conclusion from them.

3.2 LITERATURE REVIEW

3.2.1 MicroRNA biogenesis

Micro Ribonucleic Acids (miRNAs) are naturally occurring, small (22 nucleotides), non-protein-coding regulatory RNA molecules (Denli et al., 2004). They are made in the nucleus from lengthy primary miRNA (pri-miRNA) transcripts, which are subsequently cut into precursor (pre-miRNA) transcripts by the ribonucleases Drosha and DGCR8/Pasha (Chendrimada et al., 2005). The pre-miRNA is then exported by Exportin 5 to the cytoplasm, where it is further cleaved by the ribonuclease dicer in association with TRBP and PACT proteins to form a duplex of 22-nucleotide long miRNAs (Chendrimada et al., 2005; Lee et al., 2006). One strand of the duplex is then loaded onto the Argonaute proteins to create the ribonucleoprotein inhibitory complex (miRISC), which acts as a fully developed and functional miRNA (Robb and Rana, 2007).

Previously, it was thought that the other strand of the duplex was a degrading carrier strand, but Newman and Hammond (2010) reported that it is expressed and plays a role in gene regulation. The miRISC assembly interacts with particular messenger RNAs (mRNAs) based on the complementation of its sequence in the mRNA's 3'-untranslated region (UTR), coding sequences, or 5'-UTR (Fabian et al., 2010). To decrease mRNA translation, stability, or both, the interaction of miRNA with mRNA controls gene expression at the post-transcriptional level (Bartel, 2009).

3.2.2 MicroRNA gene regulation mechanism

MicroRNAs have various functions such as contributing to the formation of heterochromatin, modifying histones, methylation of DNA, and silencing gene expression. All of this ultimately influences the level at which the target gene is expressed (Hawkins and Morris, 2008). Typically, they attach themselves to a particular mRNA that possesses a complementary sequence to facilitate cleavage or degradation through a feedback mechanism. Additionally, miRNAs can accelerate the deadenylation process resulting in the rapid degradation of mRNAs (Williams, 2008).

MicroRNAs play a pivotal role in regulating a wide range of processes, including cell cycle regulation, developmental patterns, cell proliferation and apoptosis rates, differentiation mechanisms, organ development, and morphogenesis procedures (Kloosterman and Plasterk, 2006). Furthermore, miRNAs have a significant impact on

haematopoiesis as well as the progression of diseases, including cancer-related manifestations.

MicroRNAs have a significant impact on tumour development due to their often fragile position within chromosomes, which are associated with cancer (Zhao et al., 2016). As a result of their role in target mRNA expression, miRNAs can regulate tumour growth, metastasis, angiogenesis and immune evasion.

In the pathogenesis of B-cell malignancies, miRNAs participate in essential pathways for cell development such as the BCR signalling pathway. MicroRNAs affect different types of matured B-cells, including pre-, marginal zone, follicular, B1, plasma and memory B-cells. Thereby, having control over various stages during proliferation inhibition through regulatory mechanisms involving certain proteins (Musilova and Mraz, 2014).

3.2.3 miRNAs associated with the normal and inhibition of B-cell development.

The two prominent miRNAs in the B-cell development pathway are miR-181a, whose expression has been reported to increase in B-cell lineage, and miR-155, which regulates germinal center (GC) development by targeting activated-induced cytidine deaminase (AID) (Chen et al., 2004; de Yebenes et al., 2008; Basso et al., 2012). Members of the miR-17-92 family control the transition from pro-B cell to pre-B cell by targeting BIM (Ventura et al., 2008). However, the increased expression of miR-34a, through FOXP1 inhibition, and miR-150, through MYB downregulation, inhibits the conversion of pro-B cells to pre-B cells (Rao et al., 2010; Zhou et al., 2007; Xiao et al., 2007). Several genes, including *BCL6*, *HGAL*, *CD10*, and *LMO2*, are upregulated during GC reaction, while others (MUM1/IRF4, BLIMP1, and XBP1) are downregulated due to their involvement in lymphocyte terminal differentiation (Dagan et al., 2012; Lin et al., 2011). These genes are regulated by the miR-30 family of miRNAs, miR-155, let-7a, miR-125b, and miR-9 (Dagan et al., 2012; Lin et al., 2011; Gururajan et al., 2010).

3.2.4 MicroRNA associated DLBCL, NOS pathogenesis

One of the most dysregulated mechanisms in DLBCL pathogenesis is the nuclear factor kappa light-chain-enhancer of activated B-cells (NF-kB) pathway, which miR-125a and miR-125b constitutively activate (Li et al., 2010). Tumour necrosis factor alpha-induced protein 3 (TNFAIP3), a negative regulator of NF-kB, is typically

increased or overexpressed by DLBCL, and as a result, miR-125a and miR-125b target this protein and boost NF-kB signalling (Li et al., 2010). These two miRNAs were shown to play an oncogenic function in lymphomagenesis by ectopic expression and inhibition in cell lines (Compagno et al., 2009; Li et al., 2010). At chromosome 13q31-q32, a region typically amplified in the GCB subtype, lies the miR-17-92 cluster, which codes for six different miRNAs. By suppressing anti-apoptotic genes, this group of microRNAs aids in the survival of early B-cell progenitors and leads to lymphomagenesis(Compagno et al., 2009).

3.2.5 Detection of miRNAs

Polymerase Chain Reaction:

Polymerase chain reaction (PCR), the basis of many specialised molecular biology procedures, transforms minimal amounts of DNA into very large amounts. In vitro, mitotic cell division components are used in PCR because they react consistently to user inputs (Ramesh et al., 1992). Components used in PCR include template DNA, deoxynucleotide triphosphate (dNTPs), Taq DNA polymerase, and oligonucleotide primers. PCR follows three core steps. The first step is called denaturation, a PCR tube which contains the PCR components is heated to 94–96 °C. Tearing the two complementary strands apart denatures the DNA (Ramesh et al., 1992). The second step is known as Annealing, the DNA primers anneal with their target sequence by base pairing after the tube is cooled (Ramesh et al., 1992). The third and final step is extension, DNA polymerase connects to the DNA primers and extends them one nucleotide at a time (Ramesh et al., 1992).

Real-time polymerase chain reaction (RT-PCR):

Conventional PCR calls for the analysis of the result after the reaction has ended, this procedure is frequently referred to as "endpoint" analysis (Mackay et al., 2002). A separation approach is typically needed for end-point analysis. For instance, PCR products stained with ethidium bromide may be separated using gels. The end-point analysis makes quantification possible. PCR quantification and analysis are possible in real-time while amplification is taking place. Additionally, endpoint melting analysis is frequently carried out in the same tube as the PCR, a "closed-tube" analytical technique (Mackay et al., 2002).

Quantitative polymerase chain reaction (qPCR):

Simultaneous amplification and product measurement of a target DNA can be accomplished using the quantitative real-time polymerase chain reaction method in a "closed-tube" system in real-time (Dymond, 2013). Although this method can quantify the first template copy number in absolute terms, it is usually sufficient to quantify the quantity in relation to a control sample or second sequence. The amplification and genotyping steps of the quantification procedure can be completed quickly thanks to the use of melting curve analysis and/or fluorescence detection technologies (Dymond, 2013).

3.2.6 Diagnostic and prognostic miRNA biomarkers

There are numerous DLBCL diagnostic biomarkers however the eight most commonly dysregulated ones include miR-15a, miR-21, miR-29, miR-34a, miR-145, miR-155, miR-210, and miR-375 (Khare et al., 2017). MiR-145 and miR-375 are considered tumour suppressors with miR-145 specifically targeting an oncogene called *MYC* together with protein C-ets-1 (ETS) and miR-375 targeting astrocyte elevated gene 1 (AEG-1), insulin-like growth factor 1 (IGF1R), yes-associated protein 1 (YAP1), and pyruvate dehydrogenase kinase isoenzyme 1(PDK1) (Yan et al., 2014).

MicroRNA-21:

This miRNA is most prevalent in solid tumours and has been shown to have an oncogenic function, as evidenced by the fact that it is highly expressed in most tumour types, including B-cell cancers (Medina et al., 2010). In DLBCL it has been reported that it is mostly expressed in the ABC subtype than in the GC subtype (Lawrie et al., 2007). Research supports the idea that miR-21 is crucial for DLBCL drug resistance by showing that miR-21's downregulation might greatly boost DLBCL cell sensitivity to the CHOP chemotherapy regimen (Bai et al., 2013).

MicroR-21 is thought to target *BCL2* and *PTEN* in apoptotic and cell proliferation pathways in DLBCL patients, increasing cellular viability and allowing tumour cells to resist apoptosis (Song et al., 2014). According to reports, miR-21 suppression makes DLBCL cell lines more sensitive to the R-CHOP regimen, which reduces tumour cell proliferation and invasion (Yuan et al., 2016).

MicroRNA-34:

The miR-34 family includes miR-34a, whose change has been linked to a variety of cancers. Numerous studies showed that the tumour suppressor p53 controls the transcription of the miR-34a gene (Hermeking, 2010). MicroRNA-34a has been

identified as a potent tumour suppressor and has been demonstrated to be repressed in DLBCL cells, in contrast to the miR-155 and miR-21 (Craig et al., 2012). While its silencing raised the number of mature B-cells, constitutive overexpression of miR-34a partially inhibits the growth of B-cells (Rao et al., 2010). MicroRNA-34a plays a similar role in B-cell proliferation and development to the miR-17-92 cluster. In a xenograft mouse model of DLBCL, the therapeutic advantage of miR-34a modification was shown in vivo, where systemic treatment of miR-34a inhibited the growth of DLBCL by its pro-apoptotic features (Craig et al., 2012). Further research into the mechanisms underlying miR-34a's tumour-suppressor activity revealed that miR-34a predominantly inhibits the transcription factor FoxP1 that drives the formation of DLBCL (Craig et al., 2011; Craig et al., 2012).

The overexpression of miR-34a in patients with DLBCL is associated with a negative prognosis and the presence of a positive feedback loop (He et al., 2014). On the other hand, the downregulation of miR-34a and the upregulation of miR-21 have been linked to improved relapse-free survival (He et al., 2014). MicroRNA-21 is an oncogene that directly targets PTEN, PDCD4, and FOXO1 tumour suppressors, thereby activating the PI3K/AKT/mTOR oncogenic pathway (He et al., 2014). A research study that involved inhibiting miR-21 demonstrated a significant decrease in DLBCL cell lines' growth rate while increasing their sensitivity to RCHOP treatments (He et al., 2014). Additionally, it led to reduced invasion and proliferation capabilities for tumour cells (He et al., 2014).

MicroRNA-155:

As an oncogenic miRNA (oncomiR) in various malignancies, particularly B-cell lymphoproliferative diseases, miR-155 has been shown to operate in haematopoiesis and the immune response (Rodriguez et al., 2007; Li et al., 2013). On a physiological level, it has been demonstrated that miR-155 is essential for B-cell development and lymphocyte activation (Li et al., 2013). Numerous lymphomas, including DLBCL, have been reported to overexpress miR-155 (Zhong et al., 2013; Roehle et al., 2008). Studies have demonstrated that the upregulation of miR-155 causes the overexpression of SH2-domain-containing inositol-5-phosphatase-1 (SHIP-1), which then activates the AKT pathway and promotes the proliferation of B-cells (Constinean et al., 2009; Huang et al., 2012). Additionally, activation-induced cytidine deaminase (AID), a key

DNA mutator in GCB cells, was discovered to be regulated by miR-155 (Dorsette et al., 2008).

Recent research shows that *BCL6* modulates miR-155 transcriptionally, which affects the expression of AID and other genes important for the GC phenotype (Basso et al., 2012). Moreover, miR-155 upregulation and NF-kB activation show a positive correlation in DLBCL cell lines and primary samples (Ma et al., 2011). In contrast to GCB-type DLBCL, larger amounts of miR-155 were seen in ABC phenotypes (Zhong et al., 2012). Therefore, differential miR-155 expression in DLBCL subtypes can be a useful marker for the diagnosis and prognosis of DLBCL.

MicroRNA-214 and miR-144:

MicroRNA-214 has been documented to play a role in enhancing the stability of *BCL6* expression, thereby regulating germinal centre formation (Jablonska et al., 2017)). In contrast, a separate study revealed that miR-144 functions as a tumour suppressor by inhibiting the activity of *BCL6* in DLBCL xenografted mice (Wang et al, 2016).

MicroRNA-10a and miR-187:

Numerous studies have confirmed that both miR-10a and miR-187 can suppress tumour growth by controlling *BCL6* expression, which triggers cell apoptosis (Huang et al., 2016; Fn et al., 2016). These findings have been validated through extensive research on both cell cultures and tumour microarrays. The outcomes of these examinations imply that targeting these particular miRNAs could offer an advantageous therapeutic intervention strategy in addressing DLBCL treatment.

MicroRNA-181a:

A recent study has revealed miR-181a's role as a repressor of NF-kB signalling (Kozloski et al., 2016). The excessive presence of miR-181a resulted in a notable reduction in the expression and function of important components involved in the NF-kB signalling pathway within DLBCL, consequently causing diminished proliferation and survival rates among tumour cells. This effect was achieved by directly targeting key regulators such as CARD11, NFKB1A, NFKB1, RELA and REL (Kozloski et al., 2016).

Let-7d:

The miRNA Let-7d belongs to a family of 13 Let-7 members, it is a tumour suppressor that inhibits oral squamous cell carcinoma cell invasion and epithelial-mesenchymal transition (Chang et al., 2011). Furthermore, Let-7d is well-known for treating triple-

negative breast cancer by making cancer cells more responsive to radiotherapy by concentrating on cancer stem cells and blocking the cyclin D1/Aktl/Wntl pathway (Sun et al., 2016). Downregulation or the complete loss of Let-7d potentially might result in the overexpression of *RAS* thereby enhancing apoptosis of cancer cells (Nuovo et al., 2012).

3.2.7 Overview and summary

Through controlling the expression of target mRNA, miRNAs play a crucial role in promoting tumour growth, invasion, angiogenesis and immune evasion within DLBCL biology. MicroRNAs hold great significance for pathogenesis understanding as well as diagnostic and prognostic determination due to their detectability and stability during sample handling. It is for this reason that miRNAs stand out among other diagnostic tools currently available as the most important biomarker with both diagnostic potentials alongside prognostic capabilities.

This portion of the overall study aims to profile miRNAs in DLBCL, NOS with rearrangements in the two specific genes including *MYC* and *BCL6*.

3.3 AIM AND OBJECTIVES

3.3.1 Aim

The study aimed to profile the miRNAs associated with DLBCL, NOS single-hits, MYC^R or $BCL6^R$, and dual-rearrangements, MYC^RBCL6^R.

3.3.2 Objectives

- Determine the miRNA expression profile of DLBCL, NOS single- and dual-rearrangements.
- Evaluate the miRNA expression profile of DLBCL, NOS single-hits and dual-rearrangements and link the miRNA expression to those previously found to have diagnostic and prognostic marker potential.

3.4 METHODOLOGY AND RESEARCH DESIGN

3.4.1 Study design

This study was a descriptive cross-sectional retrospective analysis of 16 archived FFPE tissue samples from 116 cases diagnosed with DLBCL, NOS with rearrangements on the *MYC* and/or *BCL6* genes at the Department of Anatomical Pathology, University of the Witwatersrand.

3.4.1.1 Ethical considerations

The study was approved by the Human Research Ethics Committee (HREC, Medical) with certificate number M200434, Appendix A.

3.4.1.2 Study site

This study was conducted at the University of Witwatersrand, Department of Anatomical Pathology at Charlotte Maxeke Johannesburg Academic Hospital.

3.4.1.3 Study population

The study population consisted of DLBCL, NOS cases with known translocation status for *MYC* and *BCL6*. Based on the translocation status, they were either classified as dual-rearrangement (MYC^R and $BCL6^R$), single-hit (containing single MYC^R or $BCL6^R$ translocation), or null-hit (without *MYC* or *BCL6* translocations), Appendix B.

3.4.1.4 Sample collection

A search on the National Health Laboratory Service (NHLS) database was conducted through SNOMED codes (M-96803, M-96873, M-80003, M-95903) to identify and retrieve DLBCL case records from Charlotte Maxeke Johannesburg Academic Hospital from 2017 to 2019. The corresponding FISH results were retrieved at the Department of Cytogenetics. With data collection sheet (appendix C), information was sourced from the records. Based on the FISH results for *MYC* and *BCL6*, the cases were classified as dual-rearrangement DLBCL, NOS (MYC^R and $BCL6^R$), single-hit DLBCL, NOS (MYC^R or $BCL6^R$) or null-hit DLBCL, NOS (no *MYC* and *BCL6* rearrangement) according to specific criteria that provided cut-off values, Appendix D, Figure 2.

All the Formalin-fixed Paraffin-Embedded (FFPE) tissue blocks that were collected after identification from pathology and cytogenetic reports were evaluated and only those with adequate tissue were selected for the study.

Description of the control group

The control group included 8 cases of DLBCL, NOS, confirmed to have no genetic rearrangements in the MYC and BCL6 genes.

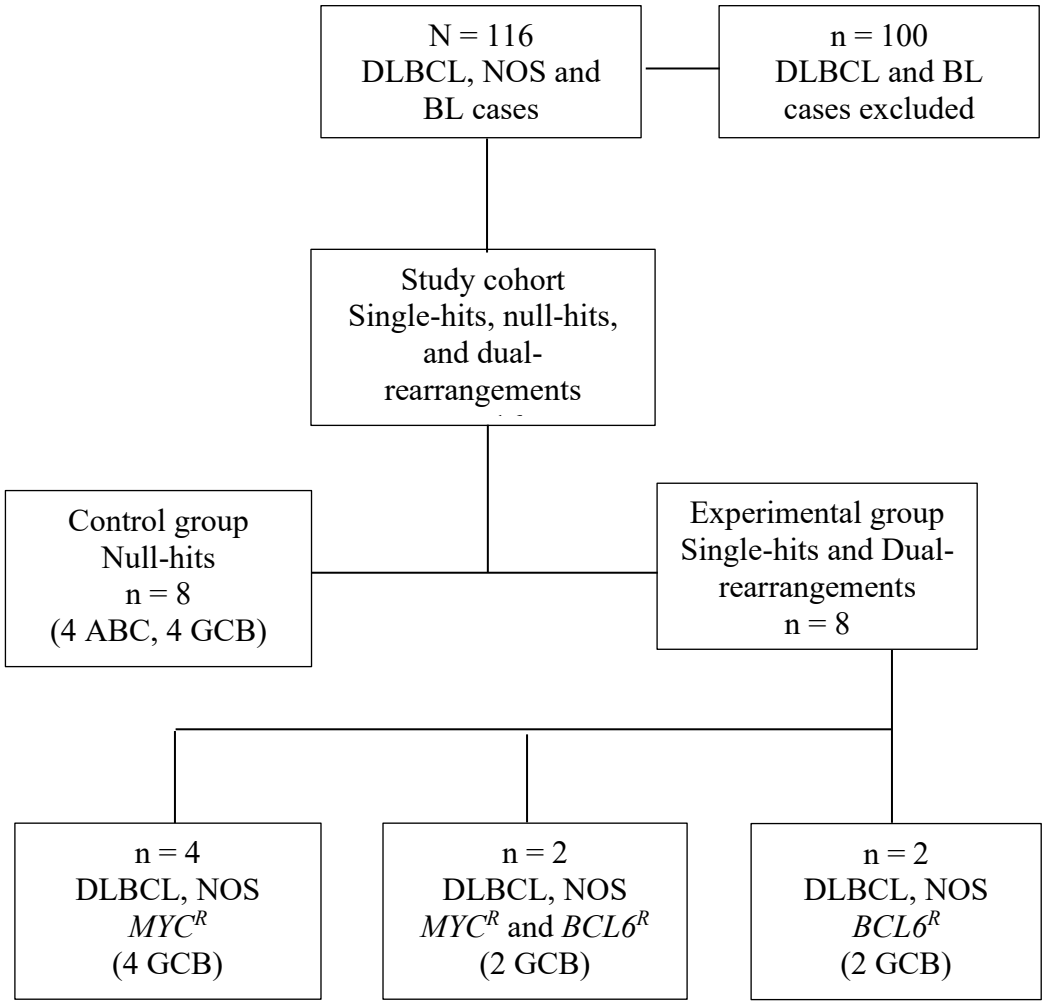

Figure 2: A summary of how the study group was collected. The study consisted of two DLBCL, NOS groups, the experimental groups (Single- and dual-rearrangement) and the control group (null-hits).

3.4.2 Methodology

3.4.2.1 RNA extraction from FFPE tissue

The FFPE tissue was sectioned at 10 µm and 6 pieces of sections were collected into a 1.5ml Eppendorf tube. To isolate the nucleic acid from the formalin-fixed paraffinised samples, they were deparrafinised. To achieve this, sections were submerged into 1ml of xylene in a tube and vortexed for 10 seconds on a vortex (BioSan, Latvia). The submerged tissue was centrifuged at 13 000 rpm for 1 minute on a centrifuge (Labotec, South Africa) at room temperature (RT). The supernatant was expelled carefully to prevent loss of the pellet. Then, 1ml of 100% ethanol was added to remove the Xylene. This was also vortexed and centrifuged at 13 000 rpm for 1 minute at RT. The sections then underwent nucleic acid extraction.

The nucleic acid was isolated from the deparaffinised tissue using the Invitrogen PureLink FFPE Total RNA isolation kit (Thermo Fisher Scientific, United States). To extract RNA from the tissue, 300 µl of the melting buffer was added to the tube. Then the tube with the tissue was centrifuged at 13000 rpm for 15 seconds and then allowed to incubate for 10 minutes at 72ºC for digestion of the wax. Twenty microliters of Proteinase-K was added to the tube and allowed to incubate at 60ºC for an hour with occasional mixing. Then the tube with the mixture was centrifuged for a minute at full speed (13000 rpm) for the separation of the tissue lysate from paraffin. With an RNase-free pipette, the solution containing the tissue lysate was aspirated and transferred to a clean RNase-free tube.

Four hundred microliters of binding buffer and 800 µl 100% ethanol were added to the tube with the tissue lysate and mixed well by the vortex. Following this, 700 µl was transferred to a spin cartridge in a collection tube. The tube was then centrifuged at 300 rpms for a minute. The flow-through was discarded and the collection tube was replaced with a clean wash tube. To the cartridge, 500 µl of the wash buffer with ethanol was added then centrifuged at full speed for a minute and the wash tube was discarded.

The spin cartridge was then placed into a clean 1.5 ml RNA recovery tube. 50 µl of RNase-free water heated to 65ºC was then added into the centre of the cartridge and allowed to incubate for a minute then immediately centrifuged at maximum speed for a minute to recover all the RNA.

The purity and amount of the isolated RNA (A260/280 ratio and A260/230 ratio) were measured using the NanoDrop One Spectrophotometer (Thermo Fischer Scientific, United States), see Appendix E.

3.4.2.2 cDNA synthesis

The Qiagen miScript® II RT Kit (Qiagen, Germany), which is commercially available, was utilised to carry out the reverse transcription and convert RNA into cDNA. Briefly, the master mix for a 20 µl reaction was prepared by adding 4 µl of 5x miScript HiSpec buffer, 2 µl of 10x miScript nucleic mix, 2 µl of miScript reverse-transcription mix, and 7 µl of RNase-free water. For each cDNA synthesis reaction, 15 µl of the master mix was used.

In a sterile nuclease-free tube placed in ice, 15 µl of the master mix and 5 µl of the template RNA (125 ng) were added. The mixture was centrifuged briefly and then incubated at 37ºC for an hour. The reaction was then stopped by increasing the temperature to 95ºC for 5 minutes. The reaction was then diluted with 200 µl of RNase-free water.

3.4.2.3 Quantitative Real time PCR

The miScript® SYBR® Green PCR kit (Qiagen, Germany) was used with miScript miRNA PCR Arrays. The reaction mix for Pathway-Focused miScript PCR Array was prepared for each sample by adding 1375 µl of 2x QuantiTect SYBR Green PCR master mix, 275 µl of 10x miScript universal primer, 1000 µl of RNase-free water, and 100 µl of the template cDNA into a reaction container. In a 96-well miScript miRNA PCR Array, 25 µl of the reaction was added to each well, the plate was then tightly sealed with optical thin-wall 8-cap strips. The plate was centrifuged for 1 minute at 1000x g at RT.

Quantitative real-time PCR was subsequently carried out using the LightCycler® 480 System (Roche, Switzerland). Cycling conditions for the PCR (Table 1).

Table 1: Real time quantitative polymerase chain reaction cycling conditions

Step	Duration	Temperature (ºC)	Cycle
Initial activation	15 minutes	95	1
Three step cycling			45
Denaturation	15 seconds	94	
Annealing	30 seconds	55	
Extension	35 seconds	70	

3.4.2.4 Validation of microRNA data

The microRNA expression data was validated by determining Let-7d and *KRAS* expression through RT-qPCR. The primary reason for our choice in selecting the let-7d is that it is an interesting microRNA and not much research has been done on it in lymphoma cases. The *KRAS* is a target gene for let-7d (De Santis and Götte, 2021). Post RNA extraction and quantification, cDNA was synthesised from the RNA using the iScript cDNA Synthesis Kits (Bio-Rad, South Africa). For quantification the iTaq™ Universal SYBR® Green One-Step Kit, (Bio-Rad, South Africa). Master-mix for Let-7d and *KRAS* containing cDNA, Sybergreen, dH2O, and primers were prepared in several Eppendorf tubes. In a 96-well plate, quantitative RT-qPCR was subsequently carried out using the LightCycler® 480 System (Roche, Switzerland). Amplification for 45 cycles was carried out under the cycling conditions as stipulated in Table 1.

3.4.3 Data analysis

3.4.3.1 MicroRNA selection:

The selection of miRNA was conducted based on a comprehensive review of microRNAs in diffuse large B-cell lymphoma performed by Huiyun et al. (2015). Where miRNAs that were detected in a minimum of 80% of the samples examined, Table 2. Twenty common aberrantly expressed miRNAs were selected for further analysis and further investigated in the experimental and control group.

Table 2: Aberrantly expressed, diagnostic, and prognostic microRNAs commonly found in diffuse large B-cell lymphoma, NOS.

Aberrantly expressed	***Diagnostic***		***Prognostic***	
miRNA	***miRNA***	***Regulation***	***miRNA***	***Regulation and function***
miR-9-5p	***miR-15a-5p***	↑	***miR-19a-3p***	↓***- Poor EFS time***
miR-15a-5p	***miR-16-5p***	↑	***miR-21-5p***	↑***- Poor prognosis,*** ↓***- Poor OS time***
miR-16-5p	***miR-21-5p***	↑	***miR-23b-3p***	↓***- Poor OS time***
miR-17-5p	***miR-29a-3p***	↑	***miR-27a-3p***	↓***- Poor OS time***
miR-18a-5p	***miR-34a-5p***	↓	***miR-34a-5p***	↓***- Poor OS time***
miR-19a-3p	***miR-155-5p***	↑	***miR-92a-3p***	↓***- High relapse rate***
miR-20a-5p			***miR-127-5p***	↓***- Poor OS time,*** ↓***- Poor EFS time***
miR-21-5p				
miR-23b-3p				
miR-27a-3p				
miR-29a-3p				
miR-34a-5p				
miR-92a-3p				
miR-127-5p				
miR-144-3p				
miR-150-5p				
miR-155-5p				
miR-181a-5p				
miR-222-3p				
let-7d-5p				

Overall Survival (OS), Event-free Survival (EFS).

3.4.3.2 MicroRNA data analysis:

The microRNA profiling data was analysed on GeneGlobe Qiagen online software (http://geneglobe.qiagen.com/za/analyze). The data obtained from quantifying microRNA using RT-qPCR was organised in an Excel spreadsheet and subsequently exported to Geneglobe for analysis. SNORD48 (hsa) was used to normalise the data, based on the NormFinder algorithm on the Geneglobe software. The lower limit detection Ct cut-off value was set to 45. An unpaired two-tailed t-test was done to compare the levels of miRNA expression between the test group and the control group. P-values could not be calculated in this study due to an insufficient number of cases per subtype. Specifically, the minimum threshold of three cases per subtype, required for meaningful statistical analysis, was not met. This limitation arose from the small number of subtypes identified within the study cohort. All miRNAs with a fold change value greater than one were considered up-regulated and those with a fold change value less than one were considered downregulated.

3.4.3.3 GraphPad Prism Statistical analysis for Validation:

GraphPad Prism was used because of its comprehensive library of statistical functions, including nonparametric procedures, linear and nonlinear regression, contingency tables, and specialised routines for clinical research. Additionally, GraphPad Prism provides guidance throughout the analysis process, aiding in the selection of appropriate statistical tests and assisting with result interpretation.

To compare miRNA expression levels between each group (single-hits, dual-rearrangements, and null-hits), One-way ANOVA was done with the Kruskal-Wallis test as a non-parametric statistical test to compare the four independent groups for statistically significant differences. The assumptions for a one-way analysis of variance were not met, therefore, the Kruskal-Wallis test was a more suitable option. Furthermore, as a non-parametric test, the Kruskal-Wallis test does not require the data to adhere to a normal distribution. The Dunns post-test was used to perform multiple comparisons of the means across single-hits, dual-rearrangements, and null-hits because the Dunn's test maintains the ranks utilised by the Kruskal-Wallis test and employs a pooled variance estimate to create post hoc approximate z-test statistics.

3.4.3.4 Microsoft Excel analysis:

Descriptive statistical analysis was performed on Excel where variables including age, gender, race, and tumour-occurring sites were analysed. We used graphs and pie charts to display the distribution of the study cohort.

3.5 RESULTS

A total of 116 cases were initially identified; however, only 16 met the inclusion criteria. The study encompassed three experimental groups: single-hits with $BCL6^R$ translocation (n=2), MYC^R translocation (n=4), and dual-rearrangement with concurrent $BCL6^R$ and MYC^R translocations (n=2). The control group consisted of null hits without translocation for both genes (n=8). This section reports on the microRNA expression and comparisons among the miRNAs detected by RT-qPCR in the 16 patients from whom the tissue was collected, Appendix F.

3.5.1 Cohort description

The study cohort consisted of patients aged between 23 and 53 years, with a mean age of 37±6 years. There was a balanced distribution of gender, with 50% (n=8) each for females and males, Figure 3. In the DLBCL, NOS single-hit MYC^R subgroup accounting for 25% of the study sample, we observed a presence of females (n=4) only. In the DLBCL, NOS single-hit $BL6^R$ subgroup accounting for 12.5% of the study sample, we observed an equal distribution of both genders (n=1 male and n=1 female). In the DLBCL, NOS dual-rearrangements (DR) MYC^RBCL6^R subgroup accounting for 12.5% of the study sample, we found males exclusively (n=2). Lastly, in the null-hit subgroup accounting for 50% of the study sample, we found n=3 females and n=5 males.

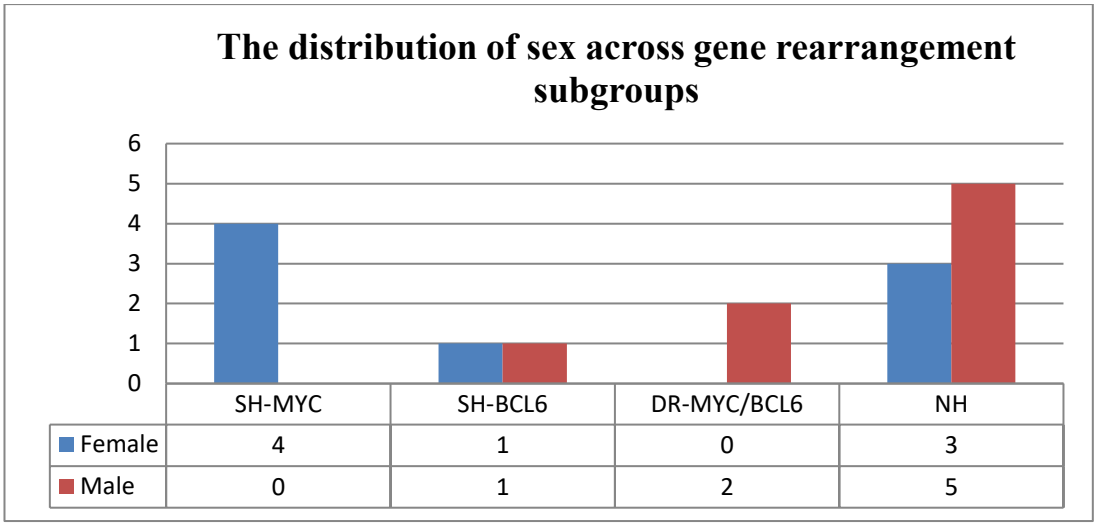

Figure 3: The distribution of the gender, including male and female, across both the DLBCL, NOS experimental and control groups. SH refers to single-hit, DR refers to dual-rearrangement, and NH refers to null-hit.

The study cohort consisted of two races, namely Blacks and Whites, with a specific population distribution, Figure 4. The majority of patients were Blacks, representing 94% of the total DLBCL, NOS population, while the remaining 6% were White patients. When examining the distribution of Black patients across the gene rearrangement subgroups, we found that null-hits DLBCL, NOS accounted for the highest proportion at 47%, followed by single-hit DLBCL, NOS MYC^R at 27%. Lastly, single-hit DLBCL, NOS $BCL6^R$ and dual-rearrangement DLBCL, NOS MYC^RBCL6^R each accounted for 13% of the population. All White patients were found to fall into the null-hit subgroup.

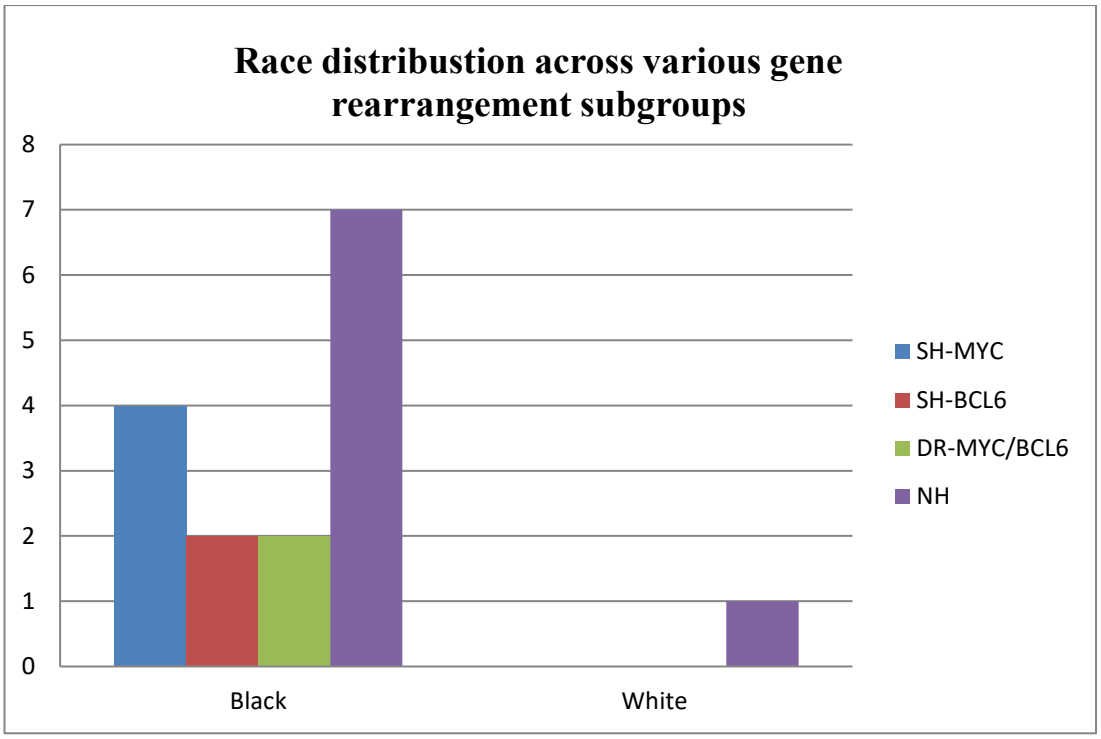

Figure 4: The distribution of race, including Black and White, across both the DLBCL, NOS Experimental groups (single-hits and dual-rearrangements) and Control group (null-hits).

3.5.2 Classification

The study cohort was divided into two molecular subgroups; ABC and GCB (refer to Figure 5). Our findings indicated that 25% of the cohort was classified as ABC DLBCL, NOS, while the remaining 75% were classified as GCB DLBCL, NOS.

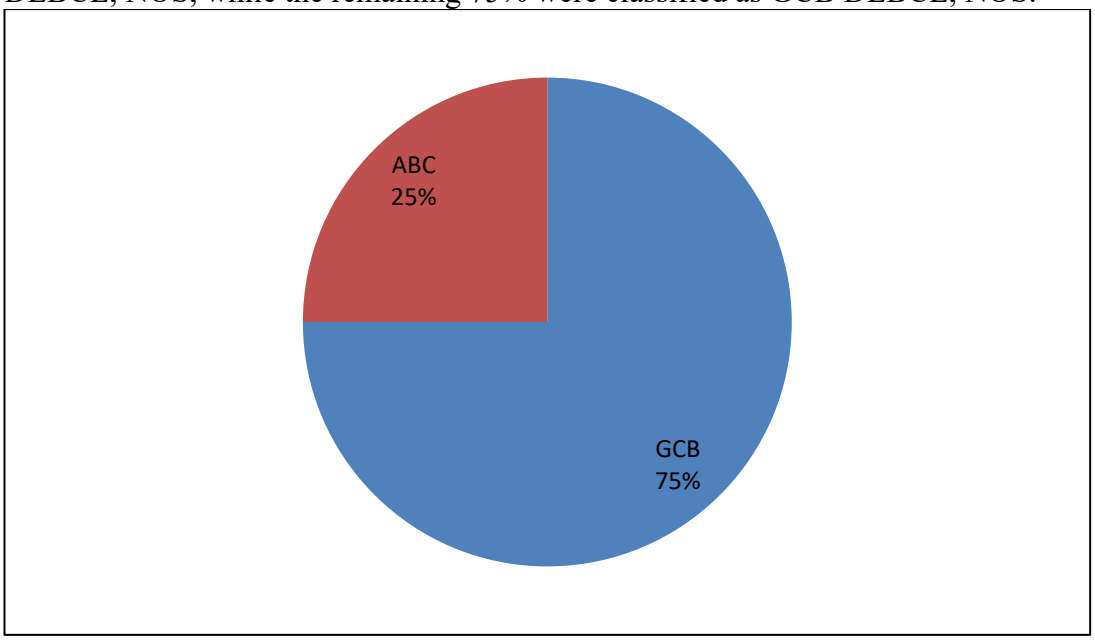

Figure 5: Pie chart showing the distribution of the DLBCL, NOS cohort across the two molecular subtypes, ABC and GCB.

3.5.3 Sample type

The tumours were sourced from various regions of the body. We assessed the frequency of occurrence and the specific locations where they were identified, Figure 6. Across the subgroups, we observed that tumours found in the liver, breast, and anal region belonged to the null-hit subgroup. Tumours located in the abdomen, skin, thorax, and stomach belonged to the single-hit (MYC^R) subgroup. Tumours in the bone marrow were from the dual-rearrangement (MYC^RBCL6^R) subgroup, while those found in the tonsils belonged to the single-hit ($BCL6^R$) subgroup. Lymph node tumours were predominantly classified under the null-hit (65%) subgroup, with 15% each in the single-hit subgroups.

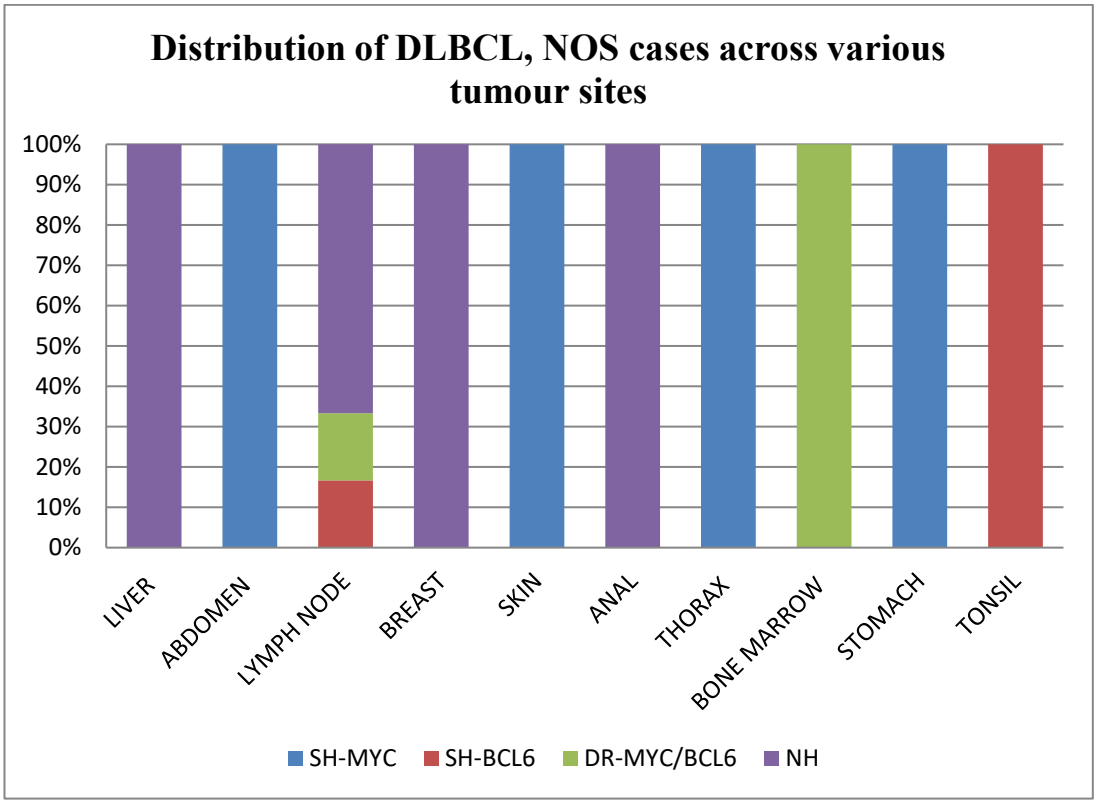

Figure 6: The frequency of the various DLBCL, NOS tumour sites across the experimental and control groups.

3.5.4 Single-hit MYC^R compared to Null-hit

When comparing the experimental group (MYC^R single-hit) with the control group (null-hit), it was observed that three out of the twenty miRNAs showed downregulation. These downregulated miRNAs include miR-17-5p (3 folds), miR-92a-3p (6 folds), and miR-155-5p (3 folds). Let-7d-5p had no change. Conversely, the remaining sixteen miRNAs exhibited up-regulation. The five most up-regulated

miRNAs were miR-18a-5p (539 folds), miR-19a-3p (204 folds), miR-144-3p (141 folds), miR-29a-3p (70 folds), and miR-222-3p (47 folds).

All the miRNAs used as diagnostic markers displayed up-regulation, except for miR-155-5p, which demonstrated downregulation. Among the seven miRNAs employed for prognostication, only miR-92a-3p exhibited downregulation, while the other six miRNAs showed up-regulation. The scatterplot of all the miRNAs examined in single-hit MYC^R group compared to null-hit (control group) is shown in Figure 7. Only the fold regulation of 20 miRNAs that were aberrantly expressed is shown on Table 3.

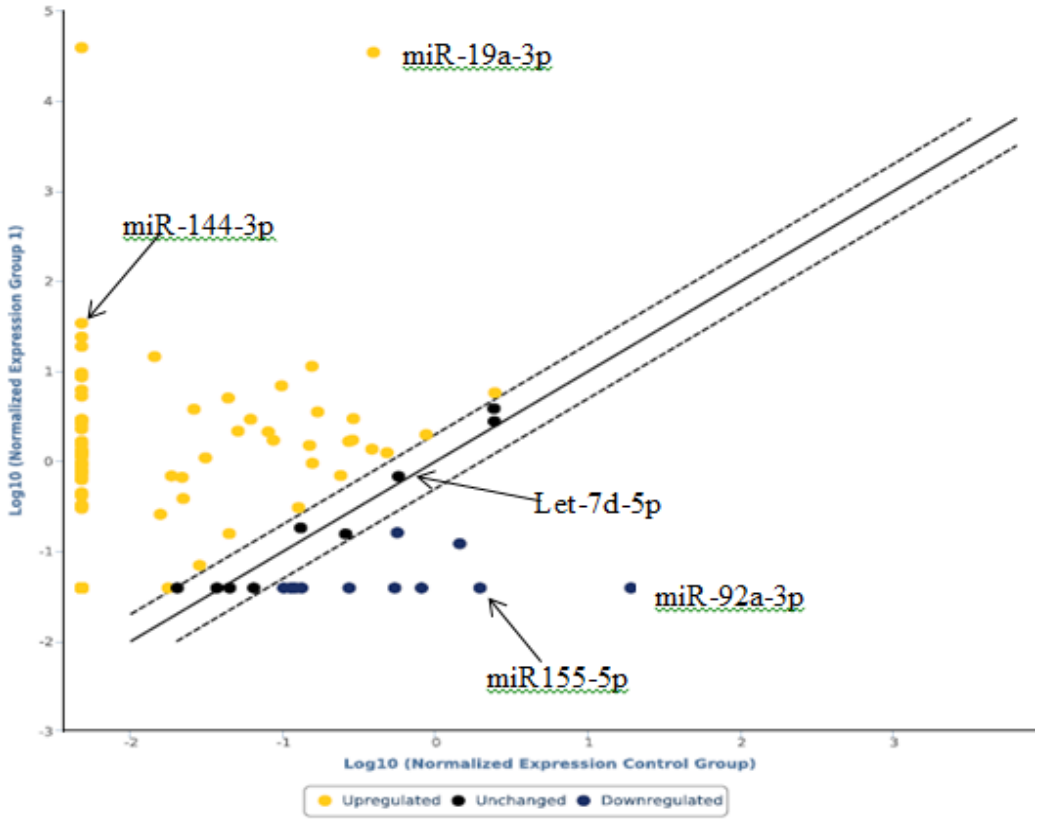

Figure 7: Scatter plot showing the up- (yellow), down- (blue) regulated miRNAs and those that remained unchanged (black) when the MYC^R single-hits are compared to the null-hits. Group 1(single-hit MYC^R) and Control group (null-hit).

Table 3: Aberrantly expressed, diagnostic, and prognostic microRNA and fold regulation in DLBCL, NOS in the single-hits MYC^R group compared to the null-hit (control group)

Aberrantly expressed microRNAs		Diagnostic		Prognostic	
MicroRNA	Fold Regulation	MicroRNA	Regulation	MicroRNA	Regulation
miR-9-5p	8,1984	miR-15a-5p	↑	miR-19a-3p	↑
miR-15a-5p	8,1984	miR-16-5p	↑	miR-21-5p	↑
miR-16-5p	3,5675	miR-21-5p	↑	miR-23b-3p	↑
miR-17-5p	-3,0559	miR-29a-3p	↑	miR-27a-3p	↑
miR-18a-5p	539,182	miR-34a-5p	↑	miR-34a-5p	↑
miR-19a-3p	204,231	miR-155-5p	↓	miR-92a-3p	↓
miR-20a-5p	2,9081			miR-127-5p	↑
miR-21-5p	2,2802				
miR-27a-3p	10,0806				
miR-23b-3p	8,1984				
miR-29a-3p	70,5067				
miR-34a-5p	3,5452				
miR-92a-3p	-6,9072				
miR-127-5p	36,9071				
miR-144-3p	141,968				
miR-150-5p	16,4181				
miR-155-5p	-3,3681				
miR-181a-5p	6,1212				
miR-222-3p	47,7367				
let-7d-5p	-0,1891				

3.5.5 Single-hit *BCL6*^{R} compared to Null-hit

When comparing the experimental group (*BCL6*^{R} single-hit) with the control group (null-hit), it was observed that fourteen out of the twenty miRNAs showed downregulation. The four most downregulated miRNAs included miR-23b-3p (545 folds), miR-127-5p (106 folds), miR-27a-3p (100 folds), and miR-144-3p (20 folds) respectively. Let-7d-5p had no change. Conversely, the remaining five miRNAs exhibited up-regulation. These up-regulated miRNAs include miR-15a-5p, miR-18a-5p, miR-19a-3p, miR-92a-3p, and miR-155-5p.

Diagnostic marker miRNAs that displayed up-regulation included miR-15a-5p and miR-155-5p. The remaining four diagnostic miRNAs were downregulated. These include miR-16-5p, miR-21-5p, miR-29a-3p, and miR-34a-5p. Only two Prognostic miRNAs were up-regulated (miR-19a-3p and miR-92a-3p). The remaining five diagnostic miRNAs were downregulated and include miR-21-5p, miR-23b-3p, miR-27a-3p, miR-34a-5p, and miR-127-5p. The scatterplot of all the miRNAs examined in single-hit *BCL6*^{R} group compared to null-hit (control group) is shown in Figure 8. Only the fold regulation of 20 miRNAs that were aberrantly expressed is shown on Table 4.

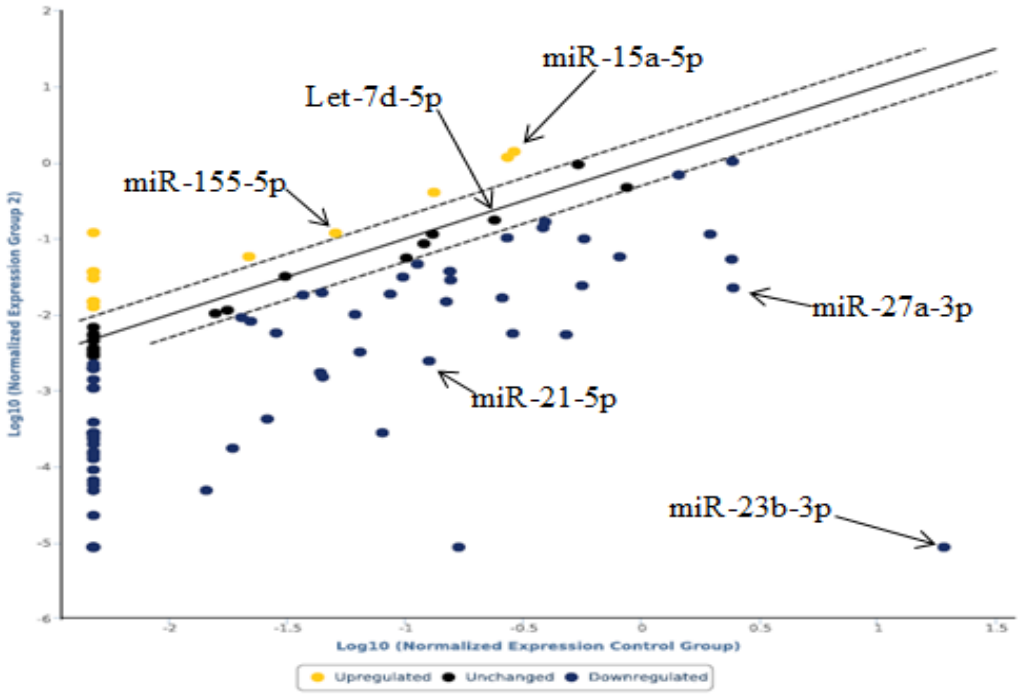

Figure 8: Scatter plot showing the up- (yellow), down- (blue) regulated miRNAs and those that remained unchanged (black) when the *BCL6*^{R} single-hit are compared to the null-hits. Group 2 (single-hits *BCL6*^{R}) and Control group (null-hits)

Table 4: Aberrantly expressed, diagnostic, and prognostic microRNA and fold regulation in DLBCL, NOS in the single-hit $BCL6^R$ group compared to the null-hit (control group)

Aberrantly expressed microRNAs		Diagnostic		Prognostic	
		MicroRNA	Regulation	MicroRNA	Regulation
miR-9-5p	-1,6618	miR-15a-5p	↑	miR-19a-3p	↑
miR-15a-5p	1,4279	miR-16-5p	↓	miR-21-5p	↓
miR-16-5p	-2,7383	miR-21-5p	↓	miR-23b-3p	↓
miR-17-5p	-1,3934	miR-29a-3p	↓	miR-27a-3p	↓
miR-18a-5p	1,1034	miR-34a-5p	↓	miR-34a-5p	↓
miR-19a-3p	3,1362	miR-155-5p	↑	miR-92a-3p	↑
miR-20a-5p	-1,3557			miR-127-5p	↓
miR-21-5p	-1,8347				
miR-23b-3p	-545,7726				
miR-27a-3p	-10,0112				
miR-29a-3p	-3,1118				
miR-34a-5p	-2,276				
miR-92a-3p	4,3525				
miR-127-5p	-106,0365				
miR-144-3p	-20,785				
miR-150-5p	-1,5092				
miR-155-5p	3,0868				
miR-181a-5p	-5,425				
miR-222-3p	-6,0713				
let-7d-5p	-0,4269				

3.5.6 Dual-rearrangement *MYC*^{R}*BCL6*^{R} compared to Null-hit

When comparing the experimental group (*MYC*^{R}*BCL6*^{R} dual-rearrangements) with the control group (null-hit), it was observed that nine out of the twenty miRNAs showed downregulation. The most downregulated miRNAs include miR-181a-5p (6 folds), miR-9-5p (3 folds), miR-15a-5p (3 folds), and miR-27a-3p (1 fold). Let-7d-5p had no change. Conversely, the remaining ten miRNAs exhibited up-regulation. The five most up-regulated miRNAs include miR-19a-3p (17 folds), miR-155-5p (8 folds), miR-150-5p (6 folds), miR-144-3p (3 folds), and miR-92a-3p (2 folds).

Diagnostic marker miRNAs that displayed up-regulation included miR-21-5p, miR-155-5p, miR-34a-5p, and miR-29a-3p. The remaining two diagnostic miRNAs were downregulated. These include miR-16-5p, and miR-15a-5p. Only two Prognostic miRNAs were downregulated, miR-23b-3p and miR-27a-3p. The remaining five diagnostic miRNAs were up-regulated and include miR-21-5p, miR-23b-3p, miR-19a-3p, miR-34a-5p, miR-92a-3p and miR-127-5p. The scatterplot of all the miRNAs examined in dual-rearrangement *MYC*^{R}*BCL6*^{R} group compared to null-hit (control group) is shown in Figure 9. Only the fold regulation of 20 miRNAs that were aberrantly expressed is shown on Table 5.

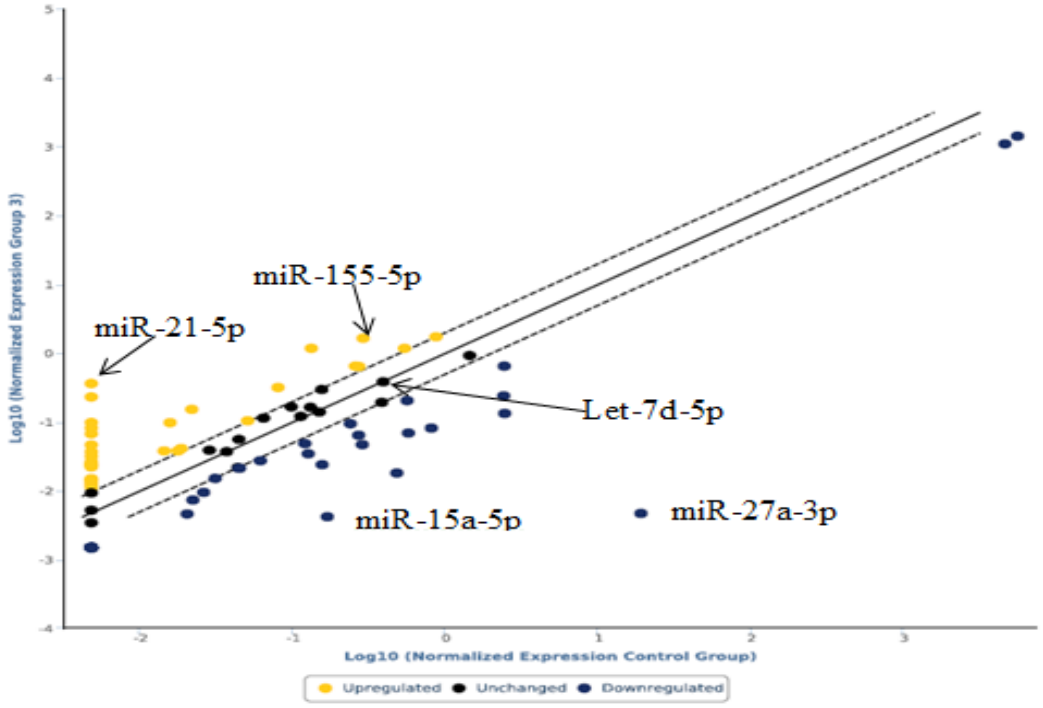

Figure 9: Scatter plot showing the up- (yellow), down- (blue) regulated miRNAs and those that remained unchanged (black) when the dual-rearrangement *MYC*^{R}*BCL6*^{R} are compared to the null-hits. Group 3 (DLBCL, NOS *MYC*^{R}*BCL6*^{R} dual-rearrangement) and Control group (DLBCL, NOS null-hit)

Table 5: Aberrantly expressed, diagnostic, and prognostic microRNA and fold regulation in DLBCL, NOS in the dual-rearrangement $MYC^{R}BCL6^{R}$ group compared to the null-hit (control group)

Aberrantly expressed microRNAs		Diagnostic		Prognostic	
		MicroRNA	Regulation	MicroRNA	Regulation
miR-9-5p	-3,1698	miR-15a-5p	↓	miR-19a-3p	↑
miR-15a-5p	-3,1698	miR-16-5p	↓	miR-21-5p	↑
miR-16-5p	-1,9659	miR-21-5p	↑	miR-23b-3p	↓
miR-17-5p	-2,4454	miR-29a-3p	↑	miR-27a-3p	↓
miR-18a-5p	5,59	miR-34a-5p	↑	miR-34a-5p	↑
miR-19a-3p	17,2055	miR-155-5p	↑	miR-92a-3p	↑
miR-20a-5p	-2,5082			miR-127-5p	↑
miR-21-5p	2,0064				
miR-23b-3p	-3,1698				
miR-27a-3p	-1,0601				
miR-29a-3p	1,7106				
miR-34a-5p	1,2656				
miR-92a-3p	2,3793				
miR-127-5p	2,233				
miR-144-3p	3,0456				
miR-150-5p	6,2737				
miR-155-5p	8,9541				
miR-181a-5p	-6,4393				
miR-222-3p	-2,2205				
let-7d-5p	-0,2048				

3.5.7 Validation of microRNA expression analysis

Validation of microRNA data by determining Let-7d:

To validate the expression of miRNA, we examined the expression of let-7d in various scenarios, such as cases with no genetic alterations, cases with a single *BCL6* translocation, cases with a single *MYC* translocation, and cases with both *MYC* and *BCL6* translocations.

The expression of let-7d was predominantly observed in single-hits with *BCL6* translocation, with a mean of 0.04678 ± 0.0062 (Figure 10, Appendix H). Null-hits (NH) exhibited the lowest means and standard deviations, with values of 5.959e-006 ± 1.050e-005. *BCL6*+ DLBCL, NOS had a mean and standard deviation of 0.04678 ± 0.0543, while *MYC*+ DLBCL, NOS had a mean and standard deviation of 0.0368 ± 0.0062. No significant differences in expression were observed between any of the groups (Figure 10, Appendix H). The p-value for let-7d in the null-hits was 0.0339 indicating significant differences in means, as the p-value was less than 0.05.

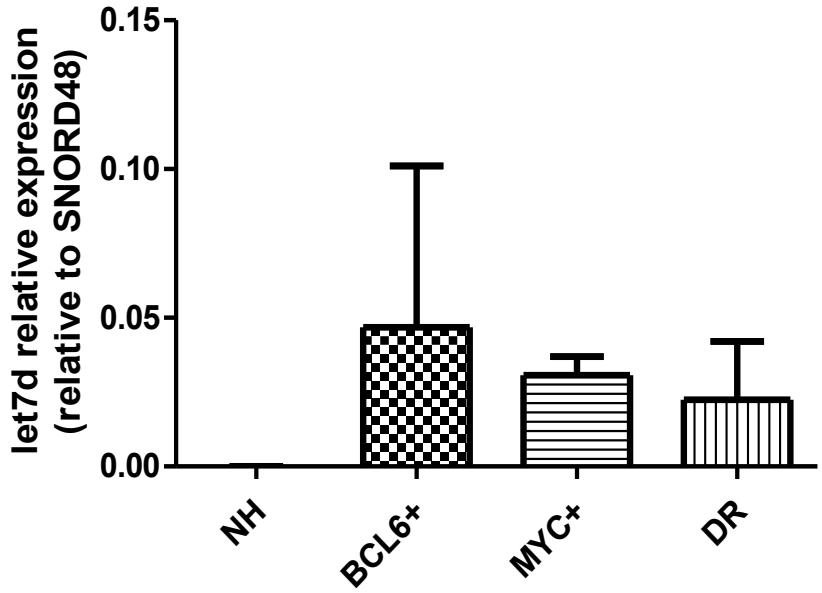

Figure 10: The expression of let-7d in genetically altered lymphoma cases including DLBCL, NOS with *MYC* and/or *BCL6* translocations (*MYC*+, *BCL6*+, and dual-rearrangement (DR)) or without translocations, null-hit (NH)

Validation of microRNA data by determining *KRAS* expression:

The expression of *KRAS* in relation to SNORD48 was evaluated using RT-qPCR in NH (null-hit), single-hits with *BCL6* translocation, single-hits with *MYC* translocation, and dual-rearrangement cases. The RT-qPCR is stipulated in the methodology chapter, refer to section 3.3.2. Expression values in Appendix I.

Figure 11 depicts the expression of *KRAS* relative to SNORD48 in the various assessed groups. The NHs group showed the lowest mean and standard deviation (SD), with values of 0.0009791 ± 0.001117. The *BCL6*+ DLBCL, NOS group displayed a mean and SD of 0.04366 ± 0.04757, while the *MYC*+ DLBCL, NOS group exhibited a mean and standard deviation of 0.4365 ± 0.04698, which was the highest among the groups. Lastly, the dual-rearrangement group demonstrated a mean and SD of 0.1948 ± 0.2629 (Figure 11, Appendix I). The KRAS expression was found to be greater in *MYC* rearranged cases followed by dr cases. The *BCL6* single hits showed the lowest KRAS expression while null-hits showed no KRAS expression.

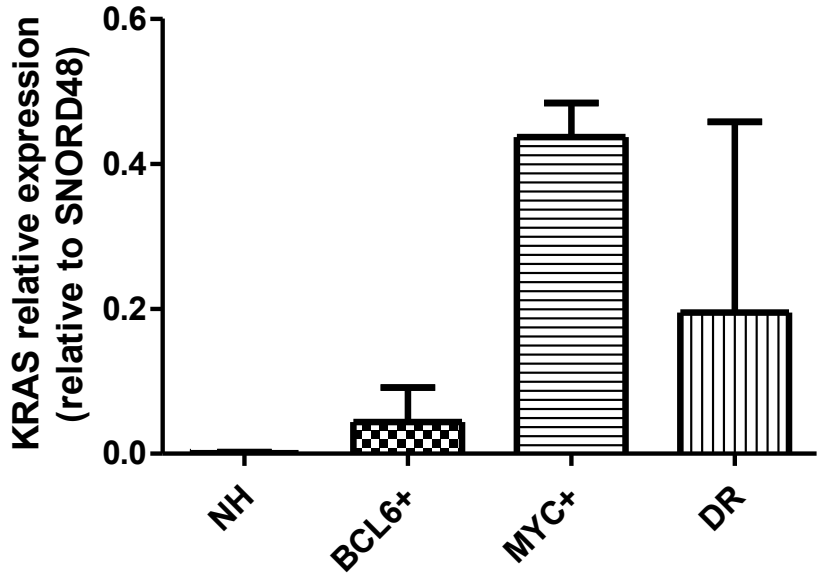

Figure 11: The expression of KRAS in genetically altered lymphoma cases including DLBCL, NOS with *MYC* and/or *BCL6* translocations (*MYC*+, *BCL6*+, and DR) or without translocations, null-hit (NH)

3.6 DISCUSSION

Lymphocytes are essential components of the immune system and play a fundamental role in defending the body against diseases. Lymphomas, which are a form of cancer, often originate from B lymphocytes that have undergone abnormal cell growth. There are various subtypes of B-cell lymphomas, each characterised by unique genetic and clinical features (Esmeray and Kucuk, 2020). The development of B-cells is a complex process that involves the interaction of transcription factors, cytokines, and miRNAs (Souza and Popi, 2022). In a study conducted by S. Koralov et al. (2008), it was discovered that the Dicer ribonuclease, responsible for processing miRNAs, plays a role in B lymphocyte development (Koralov et al., 2008). This finding suggests that a sophisticated signalling cascade is involved in regulating this biological process.

Our study characterises DLBCL, NOS with *MYC* and/or *BCL6* translocations by assessing the miRNA profile of 16 DLBCL, NOS cases. These cases were selected from a cohort of 100 DLBCL cases, based on confirmed results from IHC and FISH. The 16 DLBCL, NOS cases that met the inclusion criteria and had both IHC and FISH results were divided into experimental and control groups. The experimental group comprised DLBCL, NOS cases with genetic rearrangements in the *MYC* and/or *BCL6* genes, while the control group consisted of DLBCL, NOS cases without any genetic alterations in the *MYC* and *BCL6* genes.

From a total of 100 cases of DLBCL, we observed that 6% (n=6) were single-hits, 2% (n=2) were dual-rearrangements with concurrent *MYC* and *BCL6* rearrangements, and 8% (n=8) were null-hits. Considering the inclusion criteria, the experimental group consisted of 16 cases, which accounted for 8% of the entire cohort. This finding aligns with previous studies that reported identification rates of 5-15% for DLBCL, NOS, with at least one genetic rearrangement in the *MYC* or *BCL6* genes within their study cohorts (Swerdlow et al., 2016).

3.6.1 Aberrantly expressed miRNAs in DLBCL, NOS

Studies have demonstrated a correlation between aberrant miRNA expression and various forms of human cancer, including lymphomas (Lawrie et al, 2013). As the field of genomics has progressed, miRNAs have garnered considerable interest in the field of cancer research. Consequently, numerous techniques have been developed to detect miRNAs, with reverse transcription-quantitative polymerase chain reaction

(RT-qPCR) emerging as the most commonly utilised method due to its sensitivity and specificity (Chen et al., 2015). RT-qPCR has effectively identified multiple dysregulated miRNAs in DLBCL, NOS compared to controls. We present findings on 20 miRNAs that were selected from a panel of 80 miRNAs based on their aberrant expression.

MicroRNAs play a crucial role in the pathology of DLBCL, functioning as either oncogenes or tumour suppressors. Our study has revealed significant dysregulation of specific microRNAs in the experimental groups compared to the control group, including miR-155-5p, miR-21-5p, miR-34a-5p, and the miR-17-92 cluster. Specifically, miR-155-5p, miR-21-5p, and the miR-17-92 cluster exhibit an oncogenic role, as they alter the expression of the *MYC* gene. Conversely, miR-34a-5p acts as a tumour suppressor by modulating the expression of the *BCL6* gene.

3.6.1.1 Single-hit MYC^R compared to null-hits

When comparing the single-hit MYC^R group to the control group (null-hits), we observed that four miRNAs (miR-17-5p, miR-92a-3p, miR-155-5p, and let-7d-5p) were downregulated, while the remaining 16 miRNAs were up-regulated. Among the up-regulated miRNAs, we identified four miRNAs (miR-15a-5p, miR-16-5p, miR-21-5p, and miR-29a-3p) that were also significantly up-regulated in a study conducted by Fang et al. (2012) on DLBCL. However, two miRNAs, namely miR-34a-5p and miR-155-5p, exhibited contrasting regulation patterns in our study compared to the findings of Fang et al. (2012). This inconsistency can be attributed to a genetic rearrangement identified in the *MYC* gene. We observed an up-regulation of miR-34a-5p and a downregulation of miR-155-5p. The upregulation of miR-34a-5p and downregulation of miR-155-5p represent positive developments, as they contribute to tumour suppression. The dysregulation of these miRNAs indicates a direct association between their expression and MYC gene rearrangement.

The transcription factor *MYC* is known to downregulate members of the let-7 family, miR-29 family, miR-34a, and miR-150, and upregulate miRNAs of the miR-17-92 cluster in different models (Chang et al., 2008; O'Donnell et al., 2005). MYC-repressed miRNAs decrease the tumorigenic potential of lymphoma cells, indicating that MYC-repressed miRNAs function as tumour suppressor genes. Among the miRNAs regulated by *MYC*, the miR-17-92 cluster has oncogenic effects by promoting cell cycle progression. *MYC* can promote cell proliferation instead of apoptosis

(Mihailovich et al., 2015). *MYC* stimulates the BCR activation by upregulating the miR-17-92 cluster and suppressing inhibitors that restrict BCR (Psathas et al., 2013).

3.6.1.2 Single-hit $BCL6^R$ compared to null-hits

In the evaluation comparing single-hit $BCL6^R$ to the control group, we observed upregulation in the expression of only five miRNAs (miR-15a-5p, miR-18a-5p, miR-19a-3p, miR-92a-3p, and miR-155-5p), while the remaining fifteen miRNAs were all downregulated. A study conducted by Roehle et al. (2012), which investigated the differential expression of specific miRNAs between DLBCL and normal tissue, revealed a similar finding to our study, reporting significant upregulation of miR-155-5p. However, a contrasting result was observed with miR-17-5p, as they reported upregulation, whereas in our evaluation, we found it to be downregulated. These results can be attributed to the genetic rearrangement of *BCL6* on our cohort. This rearrangement presents a challenge by altering the *BCL6* gene's capacity to suppress tumours and potentially endowing it with oncogenic properties.

3.6.1.3 Dual-rearrangement MYC^RBCL6^R compared to null-hits

Interestingly, in the dual-rearrangement MYC^RBCL6^R group, as compared to the controls, we observed an equal distribution of aberrantly expressed miRNAs. Specifically, we found ten miRNAs that were either upregulated or downregulated. Notably, miR-21-5p and miR-155-5p exhibited significant upregulation. The elevated expression levels of these miRNAs have been characterised by Lawrie et al. (2013) as discriminatory miRNAs between the ABC and GCB subtypes. Particularly, the upregulation of both miR-21-5p and miR-155-5p is more pronounced in the ABC immunophenotype when compared to the GCB subtype.

MicroRNA-155-5p is often found to be highly active in B-cell lymphoproliferative disorders (Sandhu et al., 2011). Zhong et al (2012) reported that miR-155-5p is significantly more active in DLBCL compared to normal cells. MicroRNA-155-5p is essential for the growth of DLBCL cells, their ability to progress from the G1 to S phase of the cell cycle, and their resistance to apoptosis (Linnstaedt et al., 2010). Furthermore, miR-155-5p indirectly suppresses the expression of *BCL6* through the repression of the *BCL6* corepressor histone deacetylase 4 (Martin-Perez et al., 2012).

MicroRNA-21-5p is dysregulated in DLBCL and is believed to play a significant role in the progression of cancers. A previous study conducted by Pan et al. (2010) revealed that overexpression of miR-21-5p leads to the development of pre-B cell lymphoma, highlighting the profound impact of this miRNA in tumour formation. MicroRNA-21-5p is associated with tumour growth, invasion, and metastasis by targeting multiple tumour and metastasis suppressor genes, including programmed cell death 4 (a neoplastic transformation inhibitor), tropomyosin 1-α, and phosphatase and tensin homolog (PTEN) (Zhu et al., 2007; Fang et al., 2012).

The joint dysregulation of these major miRNAs (miR-155-5p and miR-21-5p) coupled with the rearrangements on the *BCL6*, a tumour suppressor gene, results in the continuous progression of tumour development.

3.6.2 Diagnostic and Prognostic miRNAs in DLBCL, NOS

Methods for diagnosing cancer can be burdensome, expensive, and invasive, particularly when it comes to early-stage cancer detection. Consequently, physicians require innovative approaches that can address the limitations of current methods. One promising avenue is the utilisation of miRNAs, which provide a novel means of diagnosing DLBCL and predicting patients' response to treatment. Numerous studies have demonstrated that miRNAs in human cancers become dysregulated, and their expression is specific to particular tissues, tumours, and even cell types. Through the analysis of miRNA expression profiles and specific miRNAs in patient tissue, researchers have made significant advancements in understanding prognosis and clinical outcomes for individuals with DLBCL.

3.6.3 Diagnosis

A total of six miRNAs (miR-15a-5p, miR-16-5p, miR-21-5p, miR-29a-3p, miR-34a-5p, and miR-155-5p) have been identified as diagnostic markers for DLBCL. We observed that miR-155-5p is significantly downregulated in cases with *MYC* rearrangements, but elevated in cases with *BCL6* rearrangements and cases with both *MYC* and *BCL6* rearrangements. Another important marker, miR-21-5p, is elevated in cases with *MYC* rearrangements and cases with both *MYC* and *BCL6* rearrangements but downregulated in cases with *BCL6* rearrangements. Only cases with *BCL6* rearrangements show downregulation of miR-34a-5p.

Fang et al. (2012) also identified and reported that the five miRNAs (miR-15a-5p, miR-16-5p, miR-21-5p, miR-29a-3p, and miR-155-5p) are significantly elevated in DLBCL compared to normal controls, while miR-34a is downregulated. These findings suggest that miRNA expression profiles can potentially serve as a useful tool for diagnosing DLBCL. Specifically, miR-15a-5p, miR-16-5p, miR-21-5p, miR-29a-3p, and miR-34a-5p can positively diagnose DLBCL with *MYC* rearrangements, miR-15a-5p and miR-155-5p can be used to diagnose DLBCL with *BCL6* rearrangements, and miR-29a-3p, miR-34a-5p, and miR-155-5p can diagnose DLBCL with both *MYC* and *BCL6* rearrangements.

3.6.4 Prognosis

DLBCL is a highly heterogeneous malignant tumour, and the clinical effects and prognoses vary among patients. It is crucial to provide stratified and individualised therapy for DLBCL treatment. However, the selection of the most effective treatment and clinical approach for patients remains unresolved. Therefore, an effective prognostic evaluation system is necessary to guide the stratified treatment required by DLBCL patients. One molecular method used to assist with prognostication is the analysis of microRNA expression.

Seven miRNAs (miR-19a-3p, miR-21-5p, miR-23b-3p, miR-27a-3p, miR-34a-5p, miR-92a-3p, and miR-127-5p) have been identified as potential prognostic markers. In cases with *MYC* rearrangement, only miR-92a-3p was found to be downregulated, while miR-19a-3p, miR-21-5p, miR-23b-3p, miR-27a-3p, miR-34a-5p, and miR-127-5p were upregulated. The downregulation of miR-92a-3p is quite significant as it indicative of a high relapse and poor overall survival rates post treatment, the upregulation of miR-21-5p confirms the poor prognosis status (Lawrie et al., 2008; Gilad et al., 2008; Li et al., 2014).

Cases with *BCL6* rearrangement showed upregulation of miR-19a-3p and miR-92a-3p, this is an indication that the prognosis for these patients is good (Roehle et al., 2008). Although the downregulation of miR-21-5p corroborates a good prognosis status, the downregulation of miR-23b-3p, miR-27a-3p, miR-34a-5p, and miR-127-5p suggests poor overall survival rate (Roehle et al., 2008; Li et al., 2014).

Cases with both *MYC* and *BCL6* rearrangement exhibited downregulation of miR-23b-3p and miR-27a-3p and upregulation of miR21-5p indicating poor overall survival rate

of these patients (Roehle et al., 2008; Lawre et al., 2008; Li et al., 2014). However, miR-19a-3p, miR-34a-5p, miR-92a-3p, and miR-127-5p were found to be upregulated which is a good indication as this translates to event free survival, good overall survival rate, and low relapse rate (Lawrie et al., 2008; Gilad et al., 2008; Roehle et al., 2008). In such cases, Roehle et al (2008) mention that miRNAs that are significantly upregulated or downregulated dictate the ultimate prognosis for the patient.

Lawrie et al. (2013) reported that increased expression of miR-21-5p in DLBCL is associated with a better prognosis. The authors subsequently conducted RT-qPCR tests and obtained similar results, demonstrating that high levels of miR-21-5p in DLBCL patients are linked to improved relapse-free survival time, however, the overall survival rate remained poor (Lawrie et al., 2013). Chen et al. (2014) also reported similar findings. We observed upregulation of miR-21-5p in cases with *MYC* rearrangement and in cases where both *MYC* and *BCL6* were rearranged concurrently. However, Li et al. (2014) contradicted these previous studies by demonstrating that patients with DLBCL have high levels of miR-21-5p, and overexpression of miR-21-5p is associated with a poor prognosis. In cases where only *BCL6* was rearranged, downregulation of miR-21-5p was also observed, suggesting that *BCL6* rearrangement may affect the expression of this particular miRNA. The discrepancy in results may also stem from the identification of miRNAs in the early stages of the disease, and further research is needed to clarify this.

Roehle et al (2008) found that patients with downregulated expression of miR-21-5p, miR-23b-3p, miR-27a-3p, and miR-34a-5p had poor overall survival (OS) time. Additionally, those with low expression of miR-19a-3p had a shorter event-free survival (EFS). Patients with downregulation in these miRNAs in our evaluation were cases with rearranged *BCL6*. This is suggestive of the fact that DLBCL with *BCL6* rearrangement have a poor prognosis. Cases with both *MYC* and *BCL6* only exhibited downregulation of miR-23b-3p and miR-27a-3p, by virtue of these molecular indicators we can infer a poor prognosis for them as well. None of the experimental groups exhibited downregulation of miR-19a-3p. It is tempting to infer that the genetic rearrangement contributes to improved event-free survival outcomes in patients.

We discovered that miR127-5p is only downregulated in cases with *BCL6* rearrangements, while it is upregulated in the other two experimental groups. In a study conducted by Saito et al. (2006), it was observed that miR-127-5p and *BCL6* exhibited

contrasting expression patterns in DLBCL, suggesting that *BCL6* may directly or indirectly suppress miR-127-5p in this type of lymphoma. *BCL6* is a recognised proto-oncogene that encodes a transcriptional repressor and is expressed in NHL originating from GC cells. Interestingly, a high level of *BCL6* expression is associated with a favourable prognosis in DLBCL patients, regardless of their IPI score. Conversely, miR-127-5p functions as a tumour suppressor and has the potential to serve as a prognostic indicator for DLBCL.

Patients with $MYC^{R}BCL6^{R}$ DLBCL, NOS exhibited no significant differences in disease conditions compared to those with single-hit MYC^{R} or $BCL6^{R}$ DLBCL, NOS, indicating a potentially poor prognosis. Previous studies have also suggested that *BCL6* expression is associated with favourable survival in DLBCL patients (Horn et al., 2013). *BCL6* represses *MYC* (Basso and Dalla-Favera, 2010; Nahar et al., 2011). We have demonstrated that *MYC* expression levels significantly impact the prognosis of MYC^{R} rearranged DLBCL, NOS (Xu-Monette et al., 2015). Since *BCL6* expression is correlated with better survival, the adverse prognostic effect of *MYC* may be mitigated by high *BCL6* expression.

3.6.5 Validation of the microRNA data

Expression of the miRNAs identified by RT-qPCR from the sixteen samples that formed the population of our study was validated by statistical analysis where let-7d and *KRAS* expression were evaluated.

Let-7d was found to be expressed in the single-hit (MYC^{R} and $BCL6^{R}$) and in dual-rearrangements ($MYC^{R}BCL6^{R}$). According to the Gaussian Approximation and Dunn's Multiple Comparison Test, the expression of let-7d assessed across the DLBCLs showed no statistically significant difference. This finding validated the miRNA data as it indicated that there's no significant change in the expression of let-7d across all comparison groups in the study sample.

In comparison to the DLBCL evaluated cases, we observed a high expression of *KRAS* relative to SNORD48 in DLBCL with *MYC* translocation. Let-7d and miR-155 both have a common target gene which they regulate, the *KRAS* gene. In our evaluation, let-7d was found to have been similarly expressed in all experimental groups but miR-155 was found to have been upregulated in dual-rearrangements and $BCL6^{R}$ single-hits,

however, downregulated in MYC^R single-hits. The expression of *KRAS* in dual-rearrangements is elevated compared to single-hits. What this means is that the miR-155 in dual-rearrangements is dysregulated because essentially there exists an inverse relationship between the miRNA and the expression of a gene it regulates. In this instance we were expecting to see reduced expression of the *KRAS* gene in the dual-rearrangements given that the miR-155 was upregulated, however, the opposite was observed. This can be attributed to the genetic rearrangements. This validates the observed aberrantly miRNAs resulting from *MYC* and *BCL6* translocation. With let-7d, there was no significant change in the *KRAS* gene which was in keeping with our expectations since miR-Let-7d was not similarly expressed in all the experimental groups.

3.7 CONCLUSION

MicroRNAs play a crucial role in regulating and controlling target genes. However, when these genes undergo rearrangement such as translocations, it disrupts the normal functioning of miRNAs, leading to their dysregulation. The identification of miRNA has created a novel opportunity to increase the understanding of the diagnosis, prognosis, and treatment methods. There has been great success concerning the role of miRNA in DLBCL, NOS. The dysregulation of miRNAs in this cancer suggests that miRNAs are important in the development of DLBCL, NOS. This dysregulation and aberrant expression are particularly observed for the miR-155-5p, miR-21-5p, miR-29a-3p, miR-34a-5p and the miR-17-92 cluster.

We conclude that miR-15a-5p, miR-16-5p, miR-21-5p, miR-29a-3p, miR-34a-5p, and miR-155-5p are potent diagnostic biomarkers for DLBCL, NOS with genetic rearrangements on the *MYC* and/or *BCL6* genes. Furthermore, miR-19a-3p, miR-21-5p, miR-23b-3p, miR-27a-3p, miR-34a-5p, miR-92a-3p, and miR-127-5p have been found to be important prognostic biomarker for DLBCL, NOS with *MYC* and/or *BCL6* alterations as they have implications in the treatment sensitivity, overall survival rate, event free survival and disease relapse.

DLBCL, NOS with *MYC* rearrangements exhibit poor prognosis, high relapse and poor survival rate when miR-92a-3p is significantly downregulated and miR-21-5p is significantly upregulated. DLBCL, NOS with *BCL6* rearrangements exhibit poor prognosis, high relapse and poor overall survival rates when miR-23b-3p, miR-27a-3p, miR-34a-5p, and miR-127-5p are downregulated. DLBCL, NOS with concurrent *MYC* and *BCL6* rearrangements exhibit poor prognosis when miR-21-5p is upregulated, miR-23b-3p and miR-27-5p are downregulated. However, exhibits good overall survival rate, high event free survival, and low relapse rate when miR-19a-3p, miR-34a-5p, miR-93a-3p, and miR-127-5p are upregulated. In summary, miRNAs are potential biomarkers for the diagnosis and prognosis of DLBCL, NOS and may be potential targets for gene therapy in this disease.

Chapter 4: The Proteomic profile of DLBCL, NOS with rearrangements in *MYC* and *BCL6*

4.1 OVERVIEW

The primary emphasis of this chapter is to report the proteomic data of the study. Section 4.2 will delve into the existing literature regarding DLBCL, NOS with genetic rearrangements on specific genes, namely *MYC* and *BCL6*. Section 4.3 discusses the research design and methodology for processing specimens to obtain results which are subsequently analysed and reported in section 4.4. For a comprehensive understanding of the findings, sections 4.5 and 4.6 serve as platforms to thoroughly examine and deliberate upon the obtained results before drawing an encompassing conclusion from them.

4.2 LITERATURE REVIEW

Proteomics involve the identification and characterisation of all proteins synthesised by a cell (Chandramouli and Qian, 2009). Proteins play a crucial role in cellular processes as they determine cell structure and function (Chandramouli and Qian, 2009). Proteins can undergo changes in structure and function during cellular processes, disease conditions, cellular stress, or in response to medication. The human genome sequence has enabled the discovery and characterisation of proteins with diagnostic and prognostic value (Tuma and Pratt, 1982).

In cancer research, proteomics aim to identify protein markers for the early detection of specific cancers. Prostate-specific antigen is considered a reliable biomarker for prostate cancer (Hixson et al., 2017). However, despite the discovery of numerous biomarkers for various cancers through proteomic technology, these biomarkers are not yet utilised in clinical settings due to their low sensitivity and specificity (Paulo et al., 2012).

Proteomic methods are labour-intensive and involve sample preparation, protein digestion, and identification (Yu et al., 2010). The complexity of biological samples poses challenges in proteomic analysis studies (Chandramouli and Qian, 2009). Various fractionation methods have been developed to reduce sample complexity and increase the yield of extracted proteins in FFPE tissue specimens (Chandramouli and Qian, 2009; Wisniewski, 2013).

The most commonly used fractionation methods are liquid chromatography (LC) and gel electrophoresis (Chandramouli and Qian, 2009; Yu et al., 2010; Paulo et al., 2012). The LC approach simplifies protein separation and identification by enzymatically digesting proteins into peptides before mass-spec analysis (Fouad and Aanei, 2017). The peptides are then sequenced using tandem mass spectrometry (MS/MS) (Zhang and Ge, 2011; Hixson et al., 2017).

The advantage of the LC approach is that it enables faster and simpler separation and identification of proteins compared to 2DE electrophoresis. In quantitative proteomic studies, 2DE gel electrophoresis is commonly used to separate proteins based on molecular weight or isoelectric point using a polyacrylamide gel (Chandramouli and Qian, 2009). The separated protein fragments are then visualised on the gel using fluorescent dyes and extracted for mass-spec analysis (Chandramouli and Qian, 2009).

The advantage of using a 2DE gel-based proteomic approach is its ability to identify intact and hydrophilic proteins (Chandramouli and Qian, 2009; Gundry et al., 2009).

4.2.1 Mass spectrometry

Mass spectrometry is an analytical technique that is widely utilised for the quantification and identification of compounds in each sample, regardless of whether they are known or unknown (Alexandrov, 2012). During this process, proteins are converted into gaseous ions through an ion source within the mass spectrometer. These ions are then separated and detected based on their mass-to-charge ratio, commonly referred to as m/z (Tuma and Pratt, 1982).

Various types of mass spectrometry technologies exist, which primarily differ in terms of the ion source and mass analyser employed. The two most commonly utilised ion sources are matrix-assisted laser desorption/ionisation (MALDI) and electrospray ionisation (ESI) (Paulo et al., 2012; Alexandrov, 2012). There are four main types of mass analysers: time-of-flight (TOF), ion trap, quadrupole, and Fourier transform ion cyclotron resonance (FTICR) (Franck et al., 2009).

MALDI is a gentle ionisation technique that is often coupled with TOF analysers, while ESI is typically combined with ion trap analysers (Aburaya et al., 2017). In MALDI experiments, a matrix solution is applied to tissue sections, and it crystallises along with the analyte before being ionised through laser beams. The time taken by an ion molecule to reach the ion detector determines the mass spectrum, with smaller ions reaching the detector first and larger ions reaching it last (Alexandrov, 2012, Balluff et al., 2011).

4.2.2 Matrix-assisted laser desorption/ionisation (MALDI)

Mass spectrometry imaging (MSI) is a technique used where molecules are ionised and desorbed from a sample by use of a thin layer of matrix deposited on the sample, A laser then shoots across the sectioned tissue recording the mass-to-charge ratio and relative density (biomolecular profile) of each of the acquired position (Barre et al., 2018). Histological information at a biomolecular level can be obtained using matrix-assisted desorption ionisation imaging mass spectrometry (MALDI IMS), which has an exceptionally high spatial resolution of up to 5 micrometres and an acquisition speed of 50 pixels per second (Caprioli et al., 1997).

In the histopathology laboratory, the tissue is received already preserved in formalin, and protein-protein and nucleic acid-protein crosslinking are produced as a result of this fixation (Sompuram et al., 2004). However, not all is lost as these types of tissue come to the laboratory with clinical data, the tissue samples have proven beneficial in the identification of biomarkers. To access the proteins housed within the tissue the crosslinking process must be reversed. The techniques to reverse cross-linking in MALDI IMS include the use of an antigen retrieval step with a suitable buffer (Casadonate and Caprioli, 2011; Gustafsson et al., 2010) or an in situ trypsin digestion step (Lemaire et al., 2007).

4.2.3 DLBCL, NOS protein biomarker

Histones:

The specific distribution of histones and their variations throughout the genome, which is controlled by specialised deposition machinery, provide chromatin with its distinctive features (Ray-Gallet and Almouzni, 2022). The histone variations have crucial functions in chromosome segregation, cell differentiation and early development (Filipescu, Muller, and Almouzni, 2014). Recent developments have further clarified how these variations in mutations and transcriptional dysregulation contribute to tumourigenesis (Ray-Gallet and Almouzni, 2022).

A component of the epigenetic regulator polycomb repressive complex 2 (PRC2) called enhancer zest homolog 2 (EZH2) catalyses the trimethylation of histone H3 on lysine 27, repressing target genes associated with cell control, cell differentiation, cell senescence, and malignant transformation (Varambally et al., 2002). Apparent cancer-related aberrant gain-of-function mutations in the EZH2 gene overexpression of EZH2 in a variety of haematological tumours, such as DLBCL and follicular lymphoma, are substantial alterations of EZH2 (Kim and Roberts, 2016).

Ribosomal proteins (RL15):

Involved in protein synthesis and participate in other extra-ribosomal processes such as DNA repair, transcription, RNA processing, and apoptosis (Aseev and Boni, 2011; Warner and Mclntosh, 2009). Ribosomal protein L15 (RPL15), a member of the 60S ribosomal subunit, was found in earlier research to control the processing of pre-rRNA in addition to taking part in ribosomal assembly (Klein, Moore, and Steitz, 2004). It has been discovered that RPL15 is dysregulated in a variety of diseases, upregulation of RPL15 is linked to colon cancer and the downregulation of PRL15 is associated

with pancreatic ductal adenocarcinoma and cutaneous squamous cell carcinoma (Yan et al., 2016).

Actin:

A highly conserved group of proteins that is central to the operation of the actin cytoskeleton, which participates in natural processes including cellular division, adhesion, migration, and contraction (Merino et al., 2020). These processes take place throughout various stages of cancer progression.

Keratin:

Fibrous protein is involved in the development of intermediate filaments as well as other crucial cellular processes. Keratins also function as epithelial cell markers, which makes them key components in cancer diagnosis, cancer progression, and treatment (Werner, Keller, and Pantel, 2020). Several transformed cells, including cells that have undergone oxidative stress and malignant cells, show elevated levels of cell surface keratin expression (Hinbest et al., 2020).

Pyruvate kinase:

Pyruvate kinase is an enzyme that plays a critical role in the regulation of cellular metabolism. Its function involves the conversion of phosphoenolpyruvate and adenosine diphosphate into pyruvate and adenosine triphosphate during the process of glycolysis (Eigenbrodt and Glossmann, 1980). There exist four distinct isoforms of this enzyme, with each isoform demonstrating a unique pattern of tissue expression and regulatory characteristics (Lunt et al, 2015). One of these isoforms is responsible for promoting anabolic metabolism and is present in both normal and neoplastic cells (Maurek, 2011).

Ras:

The survival, differentiation, and proliferation of tumour cells depend on the Ras protein signalling pathway. Lymphomas have been found to contain gain-of-function mutations in the Ras isoforms (H-Ras, K-Ras, and N-Ras) that directly stimulate Ras signalling (Samatar and Poulikakos, 2014; Vaque et al., 2014). Ras cascade also promotes the development of cancer by interfering with immune-suppressive elements present in the tumour microenvironment, including AS macrophages, Th17 cells, regulatory T cells, and myeloid-derived suppressor cells (MDSC) (Dias et al., 2018). Insulin-like growth factor 1 (IGF1) and JUN N-terminal kinases (JNK) are two important conserved pathways involved in the transmission of Ras protein signalling that is overexpressed in DLBCL (Blonska et al., 2015).

4.3 AIM AND OBJECTIVES

4.3.1 Aim

The study aimed to profile the proteins associated with DLBCL, NOS with *MYC* and/or *BCL6* rearrangements.

4.3.2 Objective

Determine and evaluate the protein expression profile of DLBCL, NOS with *MYC* and/or *BCL6* rearrangements in comparison to DLBCL, NOS without genetic rearrangement, in order to assess proteins associated with *MYC* and/or *BCL6* translocations.

4.4 METHODOLOGY AND RESEARCH DESIGN

4.4.1 Study design

Refer to chapter 3 section 3.4.1

4.4.1.1 Ethical considerations

Refer to chapter 3 section 3.4.1.1

4.4.1.2 Study site

This study was conducted at the University of Cape Town, The Hair and Skin Research Lab, Department of Medicine.

4.4.1.3 Study population

Refer to chapter 3 section 3.4.1.3

4.4.1.4 Sample collection

Refer to chapter 3 section 3.3.1.5

4.4.2 Methodology

Preparation of tissue slides:

Tissue blocks were chilled on ice before sectioning. Using Microtome RM 2255 (Leica, United States), the tissue blocks were sectioned at 8µm onto ITO-coated slides (Bruker, Germany). After sectioning, they were left to dry at 37ºC overnight, the temperature was increased in the morning to 60ºC for half an hour to initiate deparaffinisation. Sections were then dewaxed using 100% xylene (Sigma-Aldrich, United States) and graduated grades of ethanol (Sigma-Aldrich, United States) (absolute, 96%, and 70%) and then brought to water. Antigen retrieval was followed, by incubating the slides in Tris, EDTA pH 9 at 60ºC for 2 hours. Following this, 5 ng/l of trypsin (Promega, United States) was prepared in 50mM of Ammonium bicarbonate (Sigma-Aldrich, United States). A syringe pump was used to spray trypsin onto tissue sections. The flow rate was then set to 0.2 ml/min and the temperature was set at 30ºC. After spraying the slides, they were incubated at 37ºC for 4 hours, in a humid chamber, before them being sprayed with alpha-cyano-4-hydroxycinnamic mix (HCCA) matrix.

Matrix preparation was the next step where 0.35mg/ml of HCCA was prepared in 60% Acetonitrile (Sigma-Aldrich, United States) with 0.1% Trifluoroacetic acid. After preparation, it was sonicated for 15 minutes. The matrix was sprayed using the HTX

MX sprayer (HTX Technologies, United States) at a set temperature of 75ºC and nitrogen set at 12 bar. Slides were then allowed to air-dry at room temperature.

Matrix-assisted laser desorption ionisation imaging mass spectrometry (MALDI IMS) analysis:

Before the analysis, slides were scanned using a Tissue scanner. Teaching points were drawn around the tissue using Tippex. The RapiFlex Tissue typer (Bruker, Daltonics) instrument was first calibrated using a peptide calibration standard II (Bruker, Germany) and HCCA (Sigma-Aldrich, United States) (7g/l in 60% acetonitrile, 0.2% trifluoroacetic acid) was deposited on to tissue sections. The mass spectrometer was operated with positive polarity in reflectron mode and spectra were acquired in the range of m/z 700 – 5000. Image acquisition of the spotted array was carried out using the Flex Imaging 2.0 (Bruker, Daltonics) software package. A total of 1600 spectra was acquired at each spot position in a customised spiral raster pattern in 200-shot increments at a laser frequency of 200 Hz. The customised raster pattern was used to sample the entire spot area. Ion images were assembled using the Flex Imaging 2.0 software package. Statistical analysis of the generated data was done using Scils Lab software.

Peptide (m/z ions) identification:

The m/z ions identified in this study were identified by using an in-house database which came from previously published MALDI IMS and MALDI-LC MS analysis on DLBCL and carcinoma of the breast (Magangane et al., 2016). The MSi database was also consulted to assist in m/z ion identification (https://ms-imaging.org/wp/msi-mass-list/)

Validation of proteomic data:

The proteomics data was validated through immunohistochemical evaluation of anti-Histone H3 expression

IHC conditions for Histone antibodies:

FFPE tissue blocks were sectioned at 5 µm with Microtome RM 2255 (Leica, USA) onto superfrost-OT plus microscope slide (Bruker, Germany) and stained with Invitrogen anti-Histone H3 (EPR 17785) monoclonal antibody (ThermoFisher, United States). For optimal staining conditions see Appendix O Antigen retrieval buffer with pH 9 and linker were used for the antibodies (Appendix O). The control tissue used for IHC staining was the kidney for histone H3. The Dako Envision FLEX antibody

(Agilent, United States) was used to detect the primary antibody. Staining of all IHC specimens was performed with Dako Autostainer Link 48 (Agilent, United States).

Scoring system:

The assessment of the staining patterns on the sections was done by a single pathologist. The extent or intensity of the stains was evaluated using the Geisinger method (Lin and Chen, 2014): Where a negative result was 0 (greater than 5% of targeted cells stained), positive results was 1+ (between 5% and 25% of targeted cells stained), 2+ (between 26% and 50% of targeted cells stained), 3+ (between 27% and 75% of targeted cells stained), 4+ (greater than 76% of targeted cells stained). The staining signal was recorded as Weak (can be observed at high magnification), Intermediate (can be observed between low and high magnification), Strong (can be observed at low magnification).

4.4.3 Data analysis

Proteomics data analysis:

Statistical analysis of the generated data was done using Scils Lab software (Bruker, Germany). ROC curve analysis and the 'peak finding' pipeline were used to determine the most discriminatory m/z ions between the two groups. Normalisation was done using the total ion count (TIC) method, working with the mean spectra per group.

4.5 RESULTS

The study consisted of three experimental groups including single-hits with *BCL6* translocation (n=2), *MYC* translocation (n=4), dual-rearrangement with *BCL6* and *MYC* concurrent translocations (n=2), and a control group called null-hit with no translocation in the *MYC* or *BCL6* genes (n=8). Initially, we compared the expression of the total peptide using MALDI IMS (Table 6). Appendix P is the MALDI IMS spectrum where all the molecular ion peaks represent the peptides (m/z ions).

Table 6: Peptides (m/z ions) that were differentially expressed in the various comparison groups.

$MYC^{R}BCL6^{R}$ vs. Null-hit	$BCL6^{R}$ vs. Null-hit	MYC^{R} vs. Null-hit
655,025	841,73	655,48
780,338 (Histone H3)	1246,381(keratin type 1 cytoskeletal)	671,295
841,73	1268,35 (Histone H2A type 1)	1268,35 (Histone H2A type 1)
1268,352 (Histone H2A type 1)	1353,46 (Ribosomal Protein L15)	2256,79
1353,46 (Ribosomal Protein L15)	2254,79 (pyruvate kinase)	2299,74 (Actin, cytoplasmic 1)
	2299,74 (Actin, cytoplasmic 1)	

Using MALDI IMS and LC-MS/MS we identified a total of 10 proteins (Table 6) that were differentially expressed between dual-rearrangements ($MYC^{R}BCL6^{R}$), single-hits (MYC^{R} or $BCL6^{R}$), and null-hits (*MYC*- and *BCL6*-) using the peak finder pipeline. These proteins belonged to the cytoskeletal family of proteins including keratin, actin, histones and pyruvate kinase (Table 7). We then sought to identify peptides that could discriminate the various groups using the ROC pipeline. All the identified proteins could differentiate between two groups with at least an area under the curve (AUC) of 0.8 (Figure 12-14).

Table 7: Identification of peptides (m/z ions) from MSi Mass list and Nano-scale Liquid Chromatography (nLC) database.

m/z from MALDI IMS	**Probable Identity**
655,02	
671,295	
780,338	Histone H3
841,73	
1246,38	keratin type 1 cytoskeletal
1268,352	Histone H2A type 1
1353,46	Ribosomal Protein L15
2254,791	pyruvate kinase
2256,79	
2299,74	Actin, cytoplasmic 1

4.5.1 Dual-rearrangements (*MYC^{R}BCL6^R*) compared to Null-hits

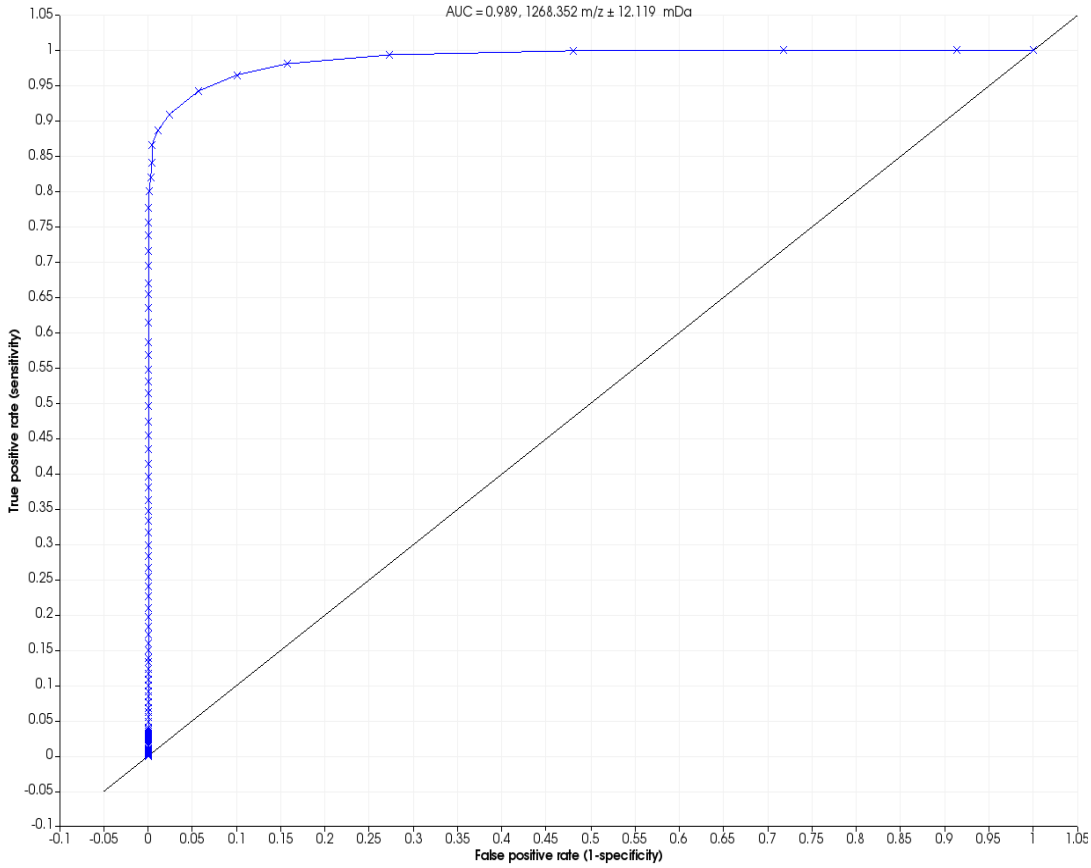

Figure 12: ROC analysis of m/z 1268.352 (Histone H2A) in DLBCL, NOS dual-rearrangements (*MYC^{R}BLC6^R*) vs. DLBCL, NOS null-hits (*BCL6- and MYC-*) cases

From this comparison, five proteins were identified when the dual-rearrangement (*MYC^{R}BLC6^R*) and null-hit (*BCL6- and MYC-*) groups were compared including histone H3 (m/z 780.338), histone H2A type 1 (m/z 1268.352), ribosomal protein LI5 (m/z 1353.46), and two unknowns (m/z 655.25 and m/z 841.73) (Table 6). The histone HA2 type 1 peptide m/z 1268.352 showed the highest AUC of 0.989 (Figure 12, Appendix J).

4.5.2 Single-hits (*BCL6*^{R}) compared to Null-hits

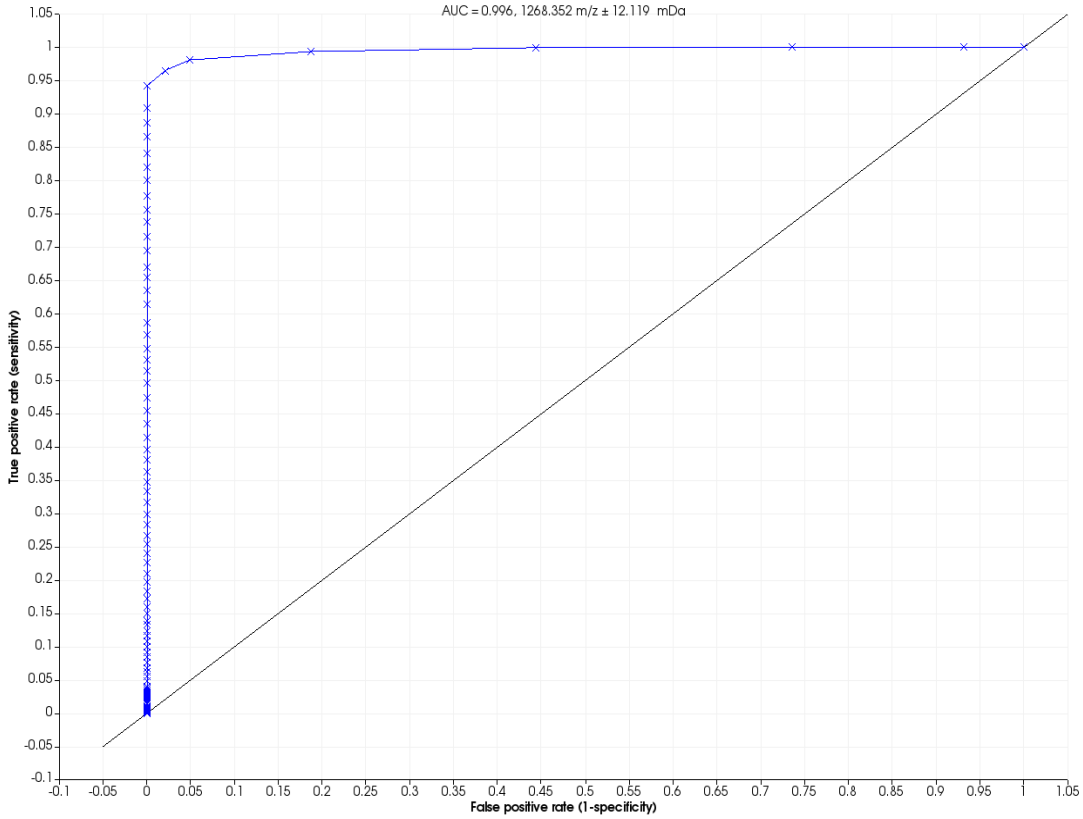

Figure 13: ROC analysis of m/z 1268.352 in DLBCL, NOS single-hits (*BLC6*^{R}) vs. DLBCL, NOS null-hits (*BCL6- and MYC-*) cases

Six proteins that were differentially expressed were identified when the triple-negative (*BCL6- and MYC-*) and single-hit (*BCL6*^{R}) groups were compared, they include keratine type 1 cytoskeletal (m/z 1246.381), histone H2A type 1 (m/z 1268.352), ribosomal protein LIS (m/z 1353.46), pyruvate kinase (m/z 2254.79), actin cytoplasmic 1 (m/z 2299.74), and an unknown (m/z 841.73) (Table 6). The histone HA2 type 1 peptide m/z 1268.352 showed the highest AUC of 0.996 (Figure 13, Appendix K).

4.5.3 Single-hits (*MYC*^{R}) compared to Null-hits

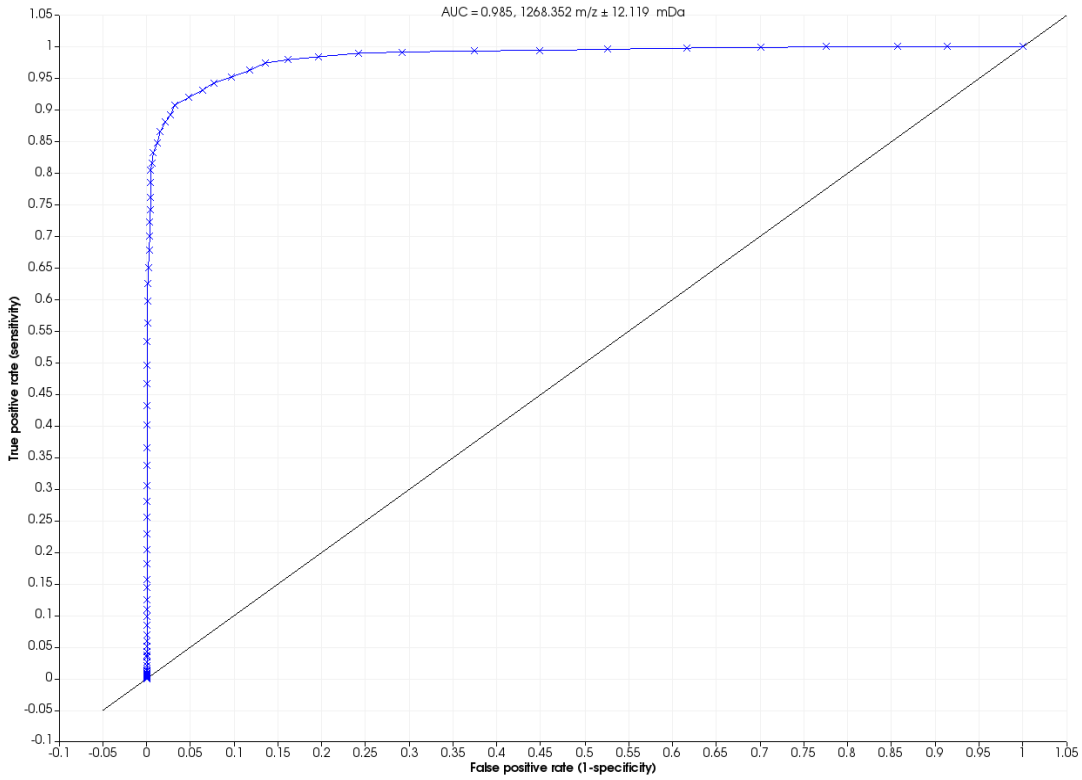

Figure 14: ROC analysis of m/z 1268.352 in DLBCL, NOS single-hits (*MYC*^{R}) vs. DLBCL, NOS null-hit (*BCL6- and MYC*-) cases

Five proteins were identified when single-hit (*MYC*^{R}) and null-hit (*BCL6*- and *MYC*-) groups were compared, proteins include histone H2A type 1 (m/z 1268.352), actin cytoplasmic 1 (m/z 2299.738), and three unknowns (m/z 655.48, m/z 671,295, and m/z 2256.79) (Table 6). The histone H2A type 1 peptide m/z 1246.381 showed the highest AUC of 0.985 (Figure 14, Appendix L).

4.5.4 Validation of proteomic data with determining IHC expression of Histone protein

The expression of proteins detected from the MALDI IMS data was validated by IHC with the anti-Histone H3 antibody, in a sample of n=18 cases. (Table 8, Appendix M). Figure 15 below, histone ROC.

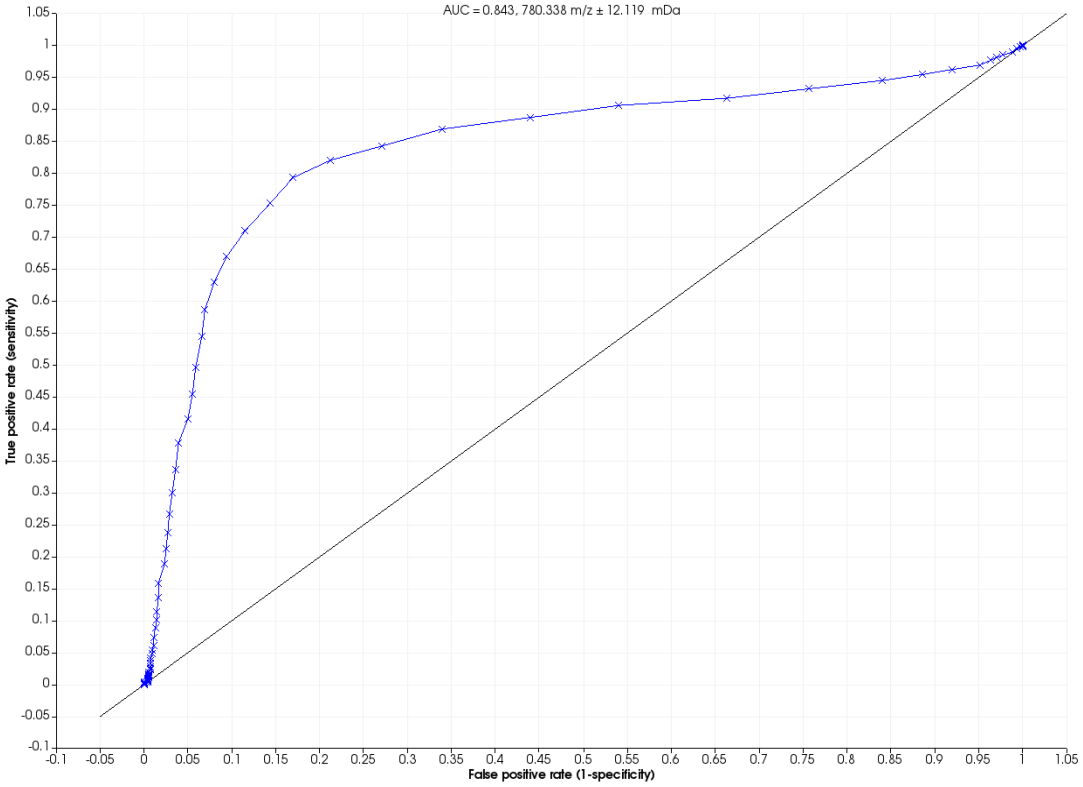

Figure 15: ROC analysis of m/z 780.338, Histone H3 protein, differentiated with an area under the curve (AUC) of 0.843.

Table 8: IHC results for anti-histone H3 antibody stained for proteomics validation of the samples

Antibody (anti-Histone H3) stain		DLBCL, Null-hit (n=2)	BL (*MYC*^{R}) (n=10)	*MYC*^{R} DLBCL (n=2)	*MYC*^{R}*BCL6*^{R} DLBCL (n=2)	*BCL6*^{R} DLBCL (n=2)
Signal	Extent (%)	N %	n %	n %	n %	n %
0	<5					
1+	6-25					
2+	26 - 50					
3+	51 - 75		3 (30)	1 (50)		2 (100)
4+	>75	2 (100)	7 (70)	1 (50)	2 (100)	

We conducted an evaluation on 10 cases of Burkitt's lymphoma (BL), in which a *MYC* translocation was identified in 55.6% of the population. Among the BL cases, three (30%, n=3) exhibited a signal strength of 3+ and an extent of staining ranging from 51% to 75%. The remaining seven cases (70%, n=7) displayed a signal strength of at least 4+ and an extent of staining greater than 75%. We also observed two cases of DLBCL with *MYC* translocations, representing 11.1% of the population. In one of these cases (50%, n=1), the staining showed a signal strength of 3+ and an extent ranging from 51% to 75%, while the other case (50%, n=1) exhibited a signal strength of 4+ and an extent of staining greater than 75%, Table 8, Figures 16 and 17.

Furthermore, there were two cases of *BCL6* rearranged DLBCL, accounting for 11.1% of the population. Both cases exhibited staining with signal strength of 3+ and an extent ranging from 51% to 75%., Figure 16. We further evaluated two dual-rearrangement cases, which had *MYC* and *BCL6* translocations, representing 11.1% of the population. Both cases, the staining displayed a signal strength of 4+ and an extent of staining greater than 75%, Figure 17. Lastly, there were two cases of DLBCL with unknown characteristics, which accounted for 11% of the population. Both of these cases exhibited staining with a signal strength of 4+ and an extent of staining greater than 75%, Table 8, Figures 16 and 17.

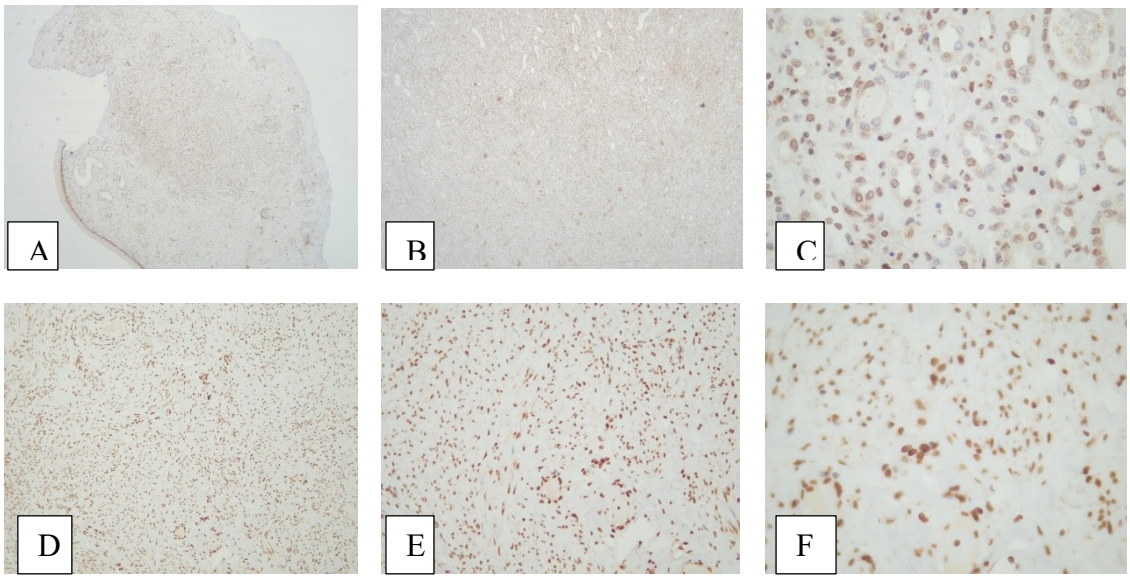

Figure 16: Immunohistochemistry photomicrograph of tissue stained with the H3 antibody showing representative stain signal of 3+ (positivity). Where A, B, and C represent the control tissue at 10x, 20x, and 40x magnification respectively. D, E, and F show the test tissue at 10x, 20x, and 40x magnification respectively.

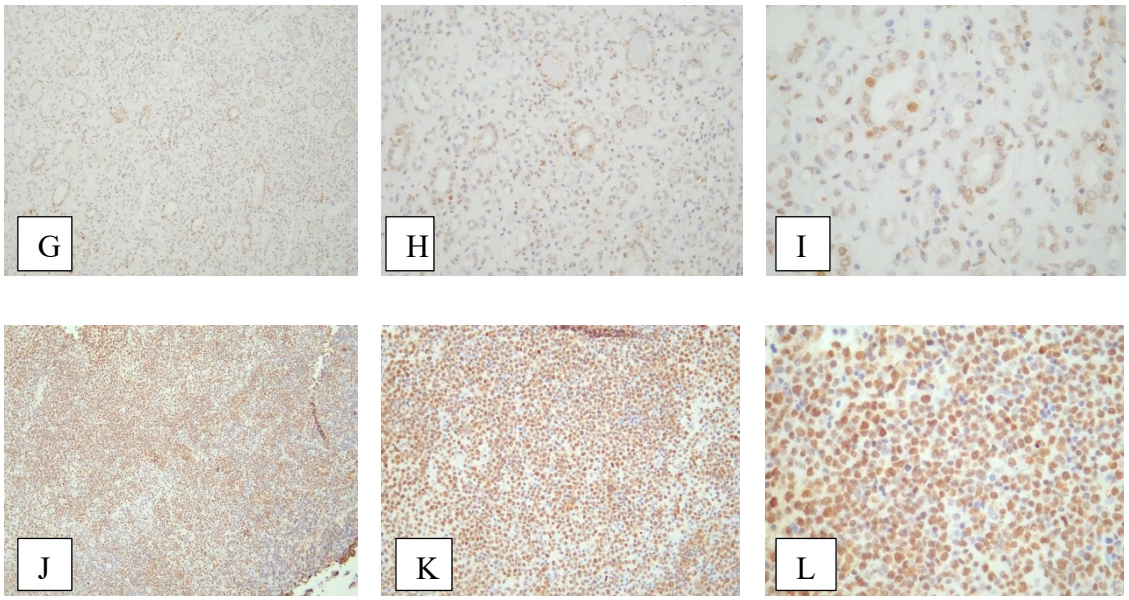

Figure 17: Immunohistochemistry photomicrograph of tissue stained with the H3 antibody showing representative stain signal of 4+ (positivity). Where G, H, and I represent the control tissue at 10x, 20x, and 40x magnification respectively. J, K, and L show the test tissue at 10x, 20x, and 40x magnification respectively.

.

4.6 DISCUSSION

In this study, the FFPE tumour tissue was analysed using a proteomic approach. The findings revealed protein overexpression mostly in Histone and Ribosomal proteins respectively. The most expressed protein was Histone H2A type1 seen in the following compared groups: dual-rearrangement vs. Null-hit, $BCL6^R$ vs. Null-hit, and MYC^R vs. Null-hit.

The histone proteins H1, H2A, H2B, H3, and H4 are wrapped around the DNA, which contains our genetic code, in the nucleus forming structures known as chromatin. Chromatin structure is controlled by complexes that remodel nucleosomes in an ATP-dependent manner and those that covalently change histone tails, both work in concert to dynamically regulate chromatin shape, and as a result, they play crucial roles in the regulation of gene expression, DNA repair, cell division, and apoptosis (Liu et al., 2016). Variations, mutations and transcriptional dysregulation of histones contribute to tumourigenesis as histones are responsible for crucial functions in chromosome segregation, cell differentiation and early development (Ray-Gallet and Almouzni, 2022). Chromosomal and somatic mutations are the two events that affect *BCL6* in B-cell tumours.

Evaluation of the dual-rearrangement with concurrent *BCL6* and *MYC* rearrangements ($BCL6^RMYC^R$), equally divided into GBC and ABC COO Subtypes. Genetic alterations leading to ABC and GCB subtypes are common and have been identified in $BCL6^RMYC^R$ (Zhang et al., 2020). The primary reasons for drug resistance, refractory disease or early relapse in DLBCL include the downregulation of intrinsic apoptotic pathways, enhancement of multidrug export machinery and activation of alternative survival pathways, this was observed by Camicia et al. (2015). In contrast to GCB-type, ABC-type exhibits persistent BCR signalling along with constantly activated NF-kB which may cause a poor chemotherapy response due to its numerous downstream anti-apoptotic effectors as noted by Godwin et al. (2013).

Immune evasion, Notch signalling, and the ubiquitin-proteasome degradation mechanism are all affected by genetic alterations in $BCL6^RMYC^R$ (Schmitz et al., 2018). This subtype also exhibits pro-proliferative characteristics such as cell cycle gene alterations, activation of the BCR and NF-kB pathways, and inhibition of the p53 pathway (Schmitz et al., 2018; Write et al., 2020). Dual-rearrangements have more pronounced BCR and NF-kB pathway gene mutations, which upregulate BCR

signalling. Refaeli et al. (2008) found that BCR signalling can cooperate with *MYC* oncogene to accelerate lymphogenesis (Refaeli et al., 2008).

A change in UBE2A (ubiquitin-conjugating enzyme E2A) could affect the ubiquitination of histone H2A, which would then affect the transcriptome related to myeloid development (Magistroni et al., 2019; de Oliveira et al., 2019). Through controlling the stability of proteins like PARP1, CDKN2A, RNF168, USP7, and p53, ubiquitin E3 ligase TRIP12 engages in bioprocesses like cell proliferation, DNA repair, and chromatin remodelling (de Oliveira et al., 2019). TRIP12 (ubiquitin E3 ligase) is mutated and to be expressed more frequently in $BCL6^{R}MYC^{R}$ (de Oliveira et al., 2019; Brunet et al., 2020).

Since several significant proteins, including IkB (inhibitory switch of NF-kB), p53 (a tumour suppressor), and other ubiquitin-conjugating enzymes found to be mutated in the $BCL6^{R}MYC^{R}$, are associated with the ubiquitin-proteasome system, ubiquitin-proteasome-dependent degradation has been considered as a potential strategy (Karmali and Gordon, 2017).

4.6.1 Protein expressed in DLBCL, NOS with a *MYC* rearrangement

A common protein was found to be differentially expressed, Histone H2A type 1 (m/z 1268.352) in this evaluation. Given the fact that the common chromosomal rearrangement in each group was on *MYC*, it is tempting to infer that there is an association that exists between *MYC* translocations and the expression of this protein. *MYC* is most affine to locations with higher amounts of the histone methylation mark H3K4me3 (tri-methylate histone 3 at position 27), and proper target recognition depends on its connection with BPTF and WDR5 (Richard et al., 2016; Thomas et al., 2015). Overexpression of enhancer of zest homolog2 (EZH2) and its gain of function has been reported in a couple of studies to be an oncogenic driver in DLBCL as it silences tumour suppressors and promotes tri-methylation of H3K27 (Yan et al., 2013; Marchesi and Bangella, 2016).

4.6.2 Protein expressed in DLBCL, NOS with a *BCL6* rearrangement

The evaluation showed a common protein Pyruvate kinase (m/z 2254.791), that was differentially expressed. Pyruvate kinase is an enzyme that controls cell metabolism in glycolysis (Eigenbrodt and Glossmann, 1980). The *PKM* gene undergoes alternative splicing to produce two variations: Pyruvate kinase M 1 and -2 (PKM1 and PKM2)

(Zahra et al., 2020). PKM1 is present in fully developed tissues like the brain and muscle, whereas PKM2 is found in rapidly dividing tissue cells as well as tumour cells (Zahra et al., 2020). The transformation of PKM1 to PKM2 plays a vital role in redirecting glucose metabolism towards aerobic glycolysis (Zhra et al., 2020). Moreover, PKM2 acts as an accomplice for transcription factors that play a part in activating different signalling pathways such as STAT3, β-catenin, HIF-1α, OCT-4 and ERα, this association greatly aids the proliferation and metastasis of cancer cells in DLBCL (Zahra et al., 2020; Lee et al., 2021).

4.6.3 Proteins expressed in DLBCL, NOS with *MYC* and *BCL6* rearrangements

Two differentially expressed proteins, histone H2A type 1 and ribosomal protein LI5, were found to be common DLBCL, NOS that contained *MYC* and *BCL6* rearrangements. We also observed the overexpression of keratin type 1 cytoskeletal.

Ribosomal protein L15 is involved in protein synthesis and participates in other extra-ribosomal processes such as DNA repair, transcription, RNA processing, and apoptosis (Aseev and Boni, 2011; Warner and Mclntosh, 2009). Ribosomal protein L15 (RPL15) is dysregulated in a variety of diseases, upregulation of RPL15 is linked to colon cancer and the downregulation of PRL15 is associated with pancreatic ductal adenocarcinoma and cutaneous squamous cell carcinoma (Yan et al., 2016). The expression of RPL15 in our study suggests that there can be a link between the progression of DLBCL and the upregulation of PRL15.

Keratins are key components in cancer diagnosis, cancer progression, and treatment (Werner, Keller, and Pantel, 2020). Several transformed cells, including cells that have undergone oxidative stress and malignant cells, show elevated levels of cell surface keratin expression (Hinbest et al., 2020). Our study corroborates this finding as we also observed the overexpression of the keratin protein, it is therefore evident that the pathways that favour the production of keratin are favoured or triggered indefinitely by DLBCL.

4.6.4 Validation of the proteomic data

Expression of the 10 proteins identified by MALDI IMS from the 14 samples that formed the validation population was confirmed by running an IHC stain test to check for the presence of the histone family of proteins, which was found to be differentially expressed across all comparisons. Due to its exceptional sensitivity and speed, mass

spectrometry is now a crucial tool for recognizing posttranslational modifications. Nonetheless, when peptide fragmentation is ambiguous, there may be false positive identifications or incorrectly assigned protein modification sites. Moreover, in cases of non-restrictive protein sequence alignment with large databases and highly homologous candidate sequences, the risk of error increases further. It is for this reason that it is important that the data generated from MALDI IMS be validated with another test method, IHC in our case. An anti-histone H3 antibody was used for this validation test on a control kidney sample. A positive stain is an indication of the presence of the target protein, in our case histone.

Although the staining extent and signal varied across all the comparison groups, none of the samples stained below a signal of 3+ (extent of at least 51%). This translates to a positive result for the presence of the histone protein. The proteomic data generated by MALDI IMS, more especially the identification histone peptides, is therefore validated.

4.7 CONCLUSION

In conclusion, the proteomic analysis of the DLBCL, NOS tissue with genetic rearrangements on the *MYC* and/or *BCL6* identified important protein biomarkers that are overexpressed, histones, ribosomal proteins and keratin. These proteins have been shown to play a role in cancer development, progression and aggressiveness. Upregulation in histones, is a consequence of genetic alterations such as mutations, along with the dysregulation of transcription processes contribute to tumorigenesis. This is due to histones playing significant roles in critical cellular functions like cell differentiation, chromosome segregation and early developmental stages. DLBCL, NOS exhibits dysregulation of Ribosomal protein and its upregulation is associated with dysregulated protein synthesis and processes such as DNA repair, transcription, RNA processing, and apoptosis. The role of keratins in cancer progression and treatment is crucial. Upregulation of cell surface keratin expression has been observed in various transformed cells, including those that have undergone oxidative stress and malignant cells. Evidently, DLBCL, NOS trigger pathways leading to continuous production of keratins.

Dual-rearrangements carrying concurrent translocations of *MYC* and *BCL6* display pro-proliferative traits including changes in cell cycle genes, and activation of the BCR and NF-kB pathways while inhibiting the p53 pathway. There are heightened gene mutations within the BCR and NF-kB pathways for these dual-rearrangements which increase signalling through upregulation. The upregulation of BCR and NF-kB pathways proves to be indicators of severe disease, possible poor patient prognosis and treatment response. Noteworthy is that concurrent genetic rearrangements are suggestive of adverse disease conditions compared to only a single translocation.

Chapter 5: General Conclusion

As we continue to accumulate knowledge about the intricate genetic makeup of DLBCL, NOS our ultimate aim is to conduct a thorough assessment of gene expression and mutation patterns in tumour cells. This can potentially lead to early diagnosis and more accurate prognoses and personalised treatment options for patients with the disease. Our study sought to achieve this using identifying possible diagnostic and prognostic biomarkers and the associated dysregulated pathways. Profiling microRNA and proteomics of DLBCL, NOS seemed like a reasonable starting point.

We found that DLBCL, NOS with *MYC* and/or *BCL6* translocations are associated with dysregulated miR-155-5p, miR-21-5p, miR-29a-3p, miR-34a-5p, the miR-17-92 cluster, histones, Keratin, and ribosomal proteins. These proteins are associated with pathways including the NF-kB and BCR, and developments of poor response or resistance to treatment. Decreased patient overall survival rate and increased poor prognosis can be attributed to concurrent rearrangements with the two genes, *MYC* and *BCL6*.

Understanding and analysing proteomics and various miRNAs and their expression levels could prove to be a valuable tool for the diagnosis, and differentiation of different subtypes of NHL, particularly in treating DLBCL, NOS. It would greatly benefit the field if more investigations were focused on transgenic models that carry human genes to better grasp the therapeutic roles played by miRNAs and proteomics in DLBCL, NOS. Conventional treatment combined with specific miRNA combinations may have the potential as a preferred treatment for DLBCL, NOS.

Chapter 6: Study Limitations

This study was limited by the small sample size which then meant that we could not do a thorough epidemiology evaluation on the population. Consequently, this limited us in drawing certain conclusions especially those related to the effects of "race-related" genetics. The absence of samples with genetic translocation on the *BCL2* gene was also a great limitation because we could not expand our evaluation to extremes of comparing the effects of *MYC*, *BCL6* and *BCL2* against each other and report on their role in DLBCL, NOS. We could not evaluate single-hits (MYC^R or $BCL6^R$ or $BCL2^R$) against dual-rearrangements (MYC^RBCL6^R or MYC^RBCL2^R or $BCL6^RBCL2^R$) and triple-hit ($MYC^RBCL6^RBCL2^R$), this would have added great value to the already existing body of knowledge on DLBCL, NOS.

Bibliography

1. Abbas, A.K. and Lichtman, A.H. (2012). “Immune responses against tumors and transplants”, *Basic Immunology*, 1(2), pp. 189–204.
2. Alaggio, R., Amador, C., Anagnostopoulos, I. *et al*. (2022) “The 5th Edition of the World Health Organization Classification of Haematolymphoid Tumours: Lymphoid Neoplasms,” *Leukemia*, 36(7), pp. 1720–1748.
3. Anders, S., Pyl, P. T., and Huber, W. (2015). “Htseq--a Python framework to work with high-throughput sequencing data,” *Bioinformatics*, 31 (2), pp.166–169.
4. Anderson, M.A., Huang, D. and Roberts, A. (2014). “Targeting BCL2 for the treatment of lymphoid malignancies”, *Seminars in Hematology*, 51(3), pp.219–227.
5. Aseev, L.V. and Boni, I.V. (2011). “Extraribosomal functions of bacterial ribosomal proteins,” *Molecular Biology*, 45(5), pp. 739–750.
6. Aukema, S.M., Siebert, R., Schuuring,E, *et al*. (2011). “Dual-hit B-cell lymphomas”, *Blood*, 117 (11), pp. 2319-2331.
7. Bai, H., Wang, J., Deng, C. *et al*. (2012). “MicroRNA-21 regulates the sensitivity of diffuse large B-cell lymphoma cells to the CHOP chemotherapy regimen”, *International Journal of Hematology*, 97(2), pp.223–231.
8. Barrans, S., Crouch, S., Smith, A. *et al*. (2010). “Rearrangement of MYC is associated with poor prognosis in patients with diffuse large B-cell lymphoma treated in the era of rituximab”, *Journal of Clinical Oncology*, 28 (1), pp. 3360-3365.
9. Barré, F., Rocha, B., Dewez, F. *et al*. (2019). “Faster raster matrix-assisted laser desorption/ionization mass spectrometry imaging of lipids at high lateral resolution”, *International Journal of Mass Spectrometry*, 437(3), pp.38–48.
10. Barrington, S.F., Mikhaeel, N.G., Kostakoglu, L. *et al*. (2014). “Role of Imaging in the Staging and Response Assessment of Lymphoma: Consensus of the International Conference on Malignant Lymphomas Imaging Working Group”, *Journal of Clinical Oncology*, 32(27), pp.3048–3058.
11. Bartel, D.P. (2009). “MicroRNAs: Target Recognition and Regulatory Functions”, *Cell*, 136(2), pp.215–233.
12. Basso, K. and Dalla-Favera, R. (2012) “Roles of BCL6 in normal and transformed germinal center B Cells”, *Immunological Reviews*, 247(1), pp. 172–183.
13. Basso, K. and Dalla-Favera, R. (2015) “Germinal centres and B cell lymphomagenesis”, *Nature Reviews Immunology*, 15(3), pp. 172–184.
14. Basso, K., Schneider, C., Shen, Q. *et al*. (2012). “BCL6 positively regulates AID and germinal center gene expression via repression of miR-155”, *Journal of Experimental Medicine*, 209(13), pp.2455–2465.
15. Beguelin, W., Popovic, R., Teater, M., *et al*. (2013). “Ezh2 is required for germinal center formation and somatic Ezh2 mutations promote lymphoid transformation,” *Cancer Cell*, 23 (5), pp.677–692.
16. Bertrand, P., Maingonnat, C., Penther, D. *et al*. (2013). “The costimulatory molecule CD70 is regulated by distinct molecular mechanisms and is associated with overall survival in diffuse large B-cell lymphoma”, *Genes Chromosomes Cancer*, 52(8), pp.764–774.

17. Blonska, M., Zhu, Y., Chuang, H.H. *et al.* (2015). "Jun-regulated genes promote interaction of diffuse large B-cell lymphoma with the microenvironment", *Blood*, 125(6), pp.981–991.
18. Bolisetty, M. T., Dy, G., Tam, W. et al. (2009). "Reticuloendotheliosis virus strain T induces miR-155, which targets JARID2 and promotes cell survival," *J Virol*, 83, pp.12009-12017.
19. Braun, T.P., Eide, C.A. and Druker, B.J. (2020). 'Response and resistance to BCR-ABL1-targeted therapies', *Cancer Cell*, 37(4), pp. 530–542.
20. Broyde, A., Boycov, O., Strenov, Y. *et al.* (2009). "Role and prognosis significance of the ki-67 index in non-hodgkin's lymphomas," *American Journal of Hematology*, 84(6), pp. 319–391.
21. Brudno, J., Tadmor, T., Pittaluga, S. *et al.* (2016). "Discordant bone marrow involvement in non-Hodgkin Lymphoma," *Blood*, 127(8), pp. 965–970.
22. Brunet, M., Vargas, C., Larrieu, D. *et al*. (2020). "E3 Ubiquitin Ligase TRIP12: Regulation, Structure, and Physiopathological Functions", *International Journal of Molecular Sciences*, 21(22).
23. Cai, Q., Medeiros, L.J., Xu, X. *et al*. (2015). "MYC-driven aggressive B-cell lymphomas: Biology, Entity, Differential Diagnosis and Clinical Management", *Oncotarget*. 6(3), pp.38591–616.
24. Caganova, M., Carrisi, C., Varano, G., *et al*. (2013). "Germinal center dysregulation by histone methyltransferase Ezh2 promotes lymphomagenesis..," *J. Clin. Investig*, 123(12), pp.5009–5022.
25. Calado, D.P., Sasaki, Y., Godinho, S.A. *et al.* (2012). "The cell-cycle regulator c-Myc is essential for the formation and maintenance of germinal centers", *Nature Immunology*, 13(11), pp.1092–1100.
26. Caprioli, R.M., Farmer, T.B. and Gile, J. (1997). "Molecular Imaging of Biological Samples: Localization of Peptides and Proteins Using MALDI-TOF MS", *Analytical Chemistry*, 69(23), pp.4751–4760.
27. Camicia, R., Winkler, H.C. and Hassa, P.O. (2015). "Novel drug targets for personalized precision medicine in relapsed/refractory diffuse large B-cell lymphoma: a comprehensive review", *Molecular Cancer*, 14(1), pp.188-196.
28. Campo, E., Jaffe, E. S., Cook, J. R., et al. (2022). "The international Consensus classification of mature lymphoid Neoplasms: A report from the clinical advisory committee," *Blood*, 140(11), pp.1229–1253.
29. Campo, E., Swerdlow, S.H., Harris, N.L. *et al*. (2011). "The 2008 WHO classification of lymphoid neoplasms and beyond: evolving concepts and practical applications", *Blood*, 117(19), pp.5019–5032.
30. Cao,Y., Zhu, T.,Zhang, P. *et al*. (2016). "Mutations or copy number losses of Cd58 and Tp53 genes in diffuse large B cell lymphoma are independent unfavourable prognostic factors," *Oncotarget*, 7(50), pp.83294–83307.
31. Casadonte, R. and Caprioli, R.M. (2011). "Proteomic analysis of formalin-fixed paraffin-embedded tissue by MALDI imaging mass spectrometry", *Nature Protocols*, 6(11), pp.1695–1709.
32. Chang, T.C., Yu, D., Lee, Y.S. *et al*. (2008). "Widespread microRNA repression by Myc contributes to tumorigenesis", *Nature Genetics*, 40(1), pp.43–50.
33. Chapuy, B., Roemer, M. G., Stewart, C., *et al*. (2016). "Targetable genetic features of primary testicular and primary central nervous system lymphomas," *Blood*, 127(7), pp.869–881.

34. Chapuy, B., Stewart, C., Dunford, A.J. *et al* (2018). "Molecular subtypes of diffuse large B cell lymphoma are associated with distinct pathogenic mechanisms and outcomes", *Nature Medicine*, 24(5), pp.679–690.
35. Chen, C., Ridzon, D. A., Broomer, A. J. *et al*. (2005). "Real-time quantification of microRNAs by stem-loop RT-PCR," *Nucleic Acids Res*, 33, pp.e179.
36. Chen, W., Wang, H., Chen, H. et al. (2014) "Clinical significance and detection of microRNA-21 in serum of patients with diffuse large B-cell lymphoma in Chinese population," *Eur J Haematol*, 92, pp.407-412.
37. Chendrimada, T.P., Gregory, R.I., Kumaraswamy, E. *et al.* (2005). "TRBP recruits the Dicer complex to Ago2 for microRNA processing and gene silencing", *Nature*, 436(7051), pp.740–744.
38. Chihara, D., Nastoupil, L.J., Williams, J.N. *et al*. (2015). "New insights into the epidemiology of non-Hodgkin lymphoma and implications for therapy", *Expert review of anticancer therapy*, 15(5), pp.531–544.
39. Chang, C.J., Hsu, C.C., Chang, C.H. *et al*. (2011). "Let-7d functions as novel regulator of epithelial-mesenchymal transition and chemoresistant property in oral cancer", *Oncology Reports*, 26(2).
40. Coiffier, B. and Sarkozy, C. (2016). "Diffuse large B-cell lymphoma: R-Chop failure-what to do?," *Hematol. Am. Soc Hematol. Educ. Program*, 2016(1), pp.366–378.
41. Cook, G. (2000). 'Immunobiology: The immune system in health and disease', *Immunology Today*, 21(4), pp. 201.
42. Copie-Bergman, C., Cuilliere-Dartigues, P., Baia, M. et al. (2015). "MYC-IG rearrangements are negative predictors of survival in DLBCL patients treated with immunochemotherapy: a GELA/LYSA study", *Blood*, 126(2), pp. 2466-2474.
43. Compagno, M., Lim, W.K., Grunn, A. *et al*. (2009). "Mutations of multiple genes cause deregulation of NF-κB in diffuse large B-cell lymphoma", *Nature*, 459(7247), pp.717–721.
44. Costinean, S., Sandhu, S.K., Pedersen, I.M. *et al.* (2009). "Src homology 2 domain-containing inositol-5-phosphatase and CCAAT enhancer-binding protein beta are targeted by miR-155 in B cells of Emicro-MiR-155 transgenic mice", *Blood*, 114(7), pp.1374–1382.
45. Craig, V.J., Tzankov, A., Flori, M. *et al*. (2012). "Systemic microRNA-34a delivery induces apoptosis and abrogates growth of diffuse large B-cell lymphoma in vivo", *Leukemia*, 26(11), pp.2421–2424.
46. Cucco, F., Barrans, S., Sha, C. *et al*. (2019). "Distinct genetic changes reveal evolutionary history and heterogeneous molecular grade of DLBCL with MYC/BCL2 Dual-hit", *Leukemia*, 34(5), pp.1329–1341.
47. Dalla-Favera, R., Bregni, M., Erikson, J. *et al*. (1982). "Human c-myc onc gene is located on the region of chromosome 8 that is translocated in Burkitt lymphoma cells", *Proceedings of the National Academy of Sciences*, 79(24), pp.7824–7827.
48. Dang, C. V. (2012). "Myc on the path to cancer," *Cell*, 149(1), pp.22–35.
49. Dang, C.V., O'Donnell, K.A., Zeller, K.I. *et al*. (2006). "The c-Myc target gene network", *Seminars in Cancer Biology*, 16(4), pp.253–264.
50. De, S., Shaknovich, R., Riester, M., *et al*. (2013). "Aberration in DNA methylation in B-cell lymphomas has a complex origin and increases with disease severity," *PLoS Genet*, 9(1), pp.e1003137
51. Denli, A.M., Tops, B.B.J., Plasterk, R.H.A. *et al.* (2004). "Processing of primary microRNAs by the Microprocessor complex", *Nature*, 432(7014), pp.231–235.

52. de Oliveira, J.F., do Prado, P.F.V., da Costa, S.S. *et al*. (2018). "Mechanistic insights revealed by a UBE2A mutation linked to intellectual disability", *Nature Chemical Biology*, 15(1), pp.62–70.
53. De Santis, C. and Götte, M. (2021). "The Role of microRNA Let-7d in Female Malignancies and Diseases of the Female Reproductive Tract", *International Journal of Molecular Science*, 22(14), pp.7359-7360.
54. Deutsch, A. J., Aigelsreiter, A., Staber, P. B., *et al*. (2007). "Malt lymphoma and extranodal diffuse large B-cell lymphoma are targeted by aberrant somatic hypermutation," *Blood*, 109(8), pp.3500–3504
55. Dias, A., Correia, A., Pereira, M.S. *et al*. (2018). "Metabolic control of T cell immune response through glycans in inflammatory bowel disease", *Proceedings of the National Academy of Sciences of the United States of America*, 115(20), pp.92-93.
56. Di Lisio, L., Sánchez-Beato, M., Gómez-López, G. *et al*. (2012). "MicroRNA signatures in B-cell lymphomas", *Blood Cancer Journal*, 2(2), pp.57–58.
57. Dorsett, Y., McBride, K.M., Jankovic, M. *et al.* (2008). "MicroRNA-155 Suppresses Activation-Induced Cytidine Deaminase-Mediated Myc-Igh Translocation", *Immunity*, 28(5), pp.630–638.
58. Dymond, J.S. (2013). "Explanatory Chapter: quantitative PCR", *Methods in Enzymology*, 529, pp.279–289.
59. Eigenbrodt, E. and Glossman, E. (1980). "Glycolysis—one of the keys to cancer?", *Trends in Pharmacological Sciences*, 1(2), pp. 240–245.
60. Einerson, R.R., Kurtin, P.J., Dayharsh, G.A. *et al*. (2005). "Fish is superior to PCR in detecting t(14;18)(q32;q21)–igh/bcl-2 in follicular lymphoma using paraffin-embedded tissue samples," *American Journal of Clinical Pathology*, 124(3), pp. 421–429.
61. Ennishi, D., Mottok, A., Ben-Neriah, S., *et al*. (2017). "Genetic profiling of myc and Bcl2 in diffuse large B-cell lymphoma determines cell-of-originspecific clinical impact," *Blood*, 129(20), pp.2760–2770.
62. Esmeray, E. and Kucuk, C. (2020). "Genetic alterations in B cell lymphoma subtypes as potential biomarkers for noninvasive diagnosis, prognosis, therapy, and disease monitoring," *Turk. J. Biol*, 44(1), pp.1-14.
63. Fabian, M.R., Sonenberg, N. and Filipowicz, W. (2010). "Regulation of mRNA Translation and Stability by microRNAs", *Annual Review of Biochemistry*, 79(1), pp.351–379.
64. Fang, C., Zhu, D. X., Dong, H. J. *et al*. (2012). "Serum microRNAs are promising novel biomarkers for diffuse large B cell lymphoma," *Ann Hematol*, 9, pp.553-559.
65. Feugier, P., Van Hoof, A., Sebban, C., *et al*. (2005). "Long-term results of the R-chop study in the treatment of elderly patients with diffuse large B-cell lymphoma: A study by the groupe D'etude des lymphomes de L'adulte," *J. Clin. Oncol*, 23(18), pp.4117–4126.
66. Filipits, M., Jaeger, U. and Pohl, G. (2002). "Cyclin D3 is a predictive and prognostic factor in diffuse large B-cell lymphoma". *Clinical Cancer Research*, 8(3), pp.729–33.
67. Filipescu, D., Müller, S. and Almouzni, G. (2014). "Histone H3 variants and their chaperones during development and disease: Contributing to epigenetic control," *Annual Review of Cell and Developmental Biology*, 30(1), pp. 615–646.
68. Fn, Q., Meng, X., Liang, H. *et al*. (2016). "miR-10a inhibits cell proliferation and promotes cell apoptosis by targeting BCL6 in diffuse large B-cell lymphoma", *Protein & Cell*, 7(12), pp.899–912.

69. Franco, F., Gonzalez-Rincon, J., Lavernia, J., *et al.* (2017). "Mutational profile of primary breast diffuse large B-cell lymphoma," *Oncotarget*, 8(61), pp.102888–102897.
70. Friedberg, J. W. (2011). "Relapsed/refractory diffuse large B-cell lymphoma," *Hematol. Am. Soc. Hematol. Educ. Program*, 2011(11), pp.498–505.
71. Fulci, V., Chiaretti, S., Goldoni, M. *et al*. (2007). "Quantitative technologies establish a novel microRNA profile of chronic lymphocytic leukemia," *Blood*, 109(11), pp.4944–4951.
72. Garg, M., Takyar, J., Dhawan, A. *et al*. (2022). "Diffuse Large B-Cell Lymphoma (DLBCL): A Structured Literature Review of the Epidemiology, Treatment Guidelines, and Real-World Treatment Patterns.," *Blood*, 140(s1), pp.12106–12107.
73. Gisselbrecht, C., Glass, B., Mounier, N., *et al*. (2010). "Salvage regimens with autologous transplantation for relapsed large B-cell lymphoma in the rituximab era," *J. Clin. Oncol*, 28(27), pp.4184–4190.
74. Goodwin, J.F., Schiewer, M.J., Dean, J.L. *et al*. (2013). "A hormone-DNA repair circuit governs the response to genotoxic insult", *Cancer Discovery*, 3(11), pp.1254–1271.
75. Green, J. A., Suzuki, K., Cho, B., *et al*. (2011). "The sphingosine 1-phosphate receptor $S1P_2$ maintains the homeostasis of germinal center B cells and promotes niche confinement," *Nat. Immunol*, 12(7), pp.672–680.
76. Gustafsson, O.J.R., Arentz, G. and Hoffmann, P. (2015) "Proteomic developments in the analysis of formalin-fixed tissue", *Biochimica et Biophysica Acta (BBA) - Proteins and Proteomics*, 1854(6), pp. 559–580.
77. Hans, C.P. (2004). "Confirmation of the molecular classification of diffuse large B-cell lymphoma by immunohistochemistry using a tissue microarray", *Blood*, 103(1), pp.275–282.
78. Harris, C.C. (1996). "Structure and function of the p53 tumor suppressor gene: Clues for rational cancer therapeutic strategies," *Journal of the National Cancer Institute*, 88(20), pp. 1442–1455.
79. Hashwah, H., Schmid, C. A., Kasser, S., *et al*. (2017). "Inactivation of crebbp expands the germinal center B cell compartment, downregulates mhcii expression and promotes dlbcl growth," *Proc. Natl. Acad. Sci. U. S. A.*, 114(36), pp.9701–9706.
80. Hatzi, K., Jiang, Y., Huang, C., *et al*. (2013). "A hybrid mechanism of action for Bcl6 in B cells defined by formation of functionally distinct complexes at enhancers and promoters," *Cell. Rep*, 4(3), pp.578–588.
81. Hawkins, P.G. and Morris, K.V. (2008). "RNA and transcriptional modulation of gene expression", *Cell Cycle*, 7(5), pp.602–607.
82. He, B., Qiao, X., Klasse, P.J. *et al.* (2006). "HIV-1 envelope triggers polyclonal IG class switch recombination through a CD40-independent mechanism involving BAFF and C-type lectin receptors," *The Journal of Immunology*, 176(7), pp. 3931–3941.
83. Hermeking, H. (2009). "The miR-34 family in cancer and apoptosis", *Cell Death & Differentiation*, 17(2), pp.193–199.
84. Hinbest, A.J., Eldirany, S., Ho, M. *et al.* (2020). "Molecular modeling of pathogenic mutations in the keratin 1B domain," *International Journal of Molecular Sciences*, 21(18), pp. 6641–6643.
85. Honda, R., Tanaka, H. and Yasuda, H. (1997). "Oncoprotein MDM2 is a ubiquitin ligase E3 for tumor suppressor p53," *FEBS Letters*, 420(1), pp. 25–27.
86. Horn, H., Ziepert, M., Becher, C. *et al*. (2013). "MYC status in concert with BCL2 and BCL6 expression predicts outcome in diffuse large B-cell lymphoma", *Blood*, 121(12), pp.2253–2263.

87. Hu, S., Xu-Monette, Z., Balasubramanyam, A. *et al*. (2013). "CD30 expression defines a novel subgroup of diffuse large B-cell lymphoma with favorable prognosis and distinct gene expression signature: A report from the International DLBCL RITUXIMAB-CHOP consortium program study," *Blood*, 121(14), pp. 2715–2724.
88. Huang, X., Shen, Y., Liu, M. *et al*. (2012). "Quantitative Proteomics Reveals that miR-155 Regulates the PI3K-AKT Pathway in Diffuse Large B-Cell Lymphoma", *American Journal of Pathology*, 181(1), pp.26–33.
89. Jabłońska, E., Górniak, P., Szydłowski, M. *et al*. (2017). "MiR-17-92 represses PTPROt and PP2A phosphatases and amplifies tonic BCR signaling in DLBCL cells", *Experimental Hematology*, 46(4), pp.56-61.
90. Jethwa, A., Slabicki, M., Hüllein, J. *et al*. (2018). "TRRAP is essential for regulating the accumulation of mutant and wild-type p53 in lymphoma", *Blood*, 131(25), pp.2789–2802.
91. Jiang, Y. and Melnick, A. (2015). "The epigenetic basis of diffuse large B-cell lymphoma" *Semin. Hematol*, 52(2), pp.86–96.
92. Johnson, N.A., Savage, K.J., Ludkovski, O. *et al*. (2009). "Lymphomas with concurrent BCL2 and MYC translocations: the critical factors associated with survival", *Blood*, 114(2), pp. 2273-2279.
93. Joy, K.A., Ndindjock, R., Coyle, K.B. *et al*. (2013). "The Burden Of Illness and Prevalence In Diffuse Large B-Cell (DLBCL) and Follicular (FL) Lymphomas", *Blood*, 122(21), pp.5619–5619.
94. Karmali, R., Gordon, L.I., Chukkapalli, V. et al (2017). "GSK-3β inhibitor, 9-ING-41, reduces cell viability and halts proliferation of B-cell lymphoma cell lines as a single agent and in combination with novel agents", *Oncotarget*, 8(70), pp.114924–114934.
95. Karube, K. and Campo, E. (2015). "Myc alterations in diffuse large B-cell lymphomas," *Semin. Hematol*, 52(2), pp.97–106.
96. Kanagal-Shamanna, R., Medeiros, L.J., Lu, G. *et al*. (2012). "High-grade B cell lymphoma, unclassifiable, with blastoid features: an unusual morphological subgroup associated frequently with BCL2 and/or MYC gene rearrangements and a poor prognosis", *Histopathology*, 61 (2), pp. 945-954.
97. Khare, D., Goldschmidt, N. and Aya Bardugo (2017). "Plasma microRNA profiling: Exploring better biomarkers for lymphoma surveillance", *PLOS ONE*, 12(11), pp.e0187722–e0187722.
98. Kim, S.H, Ramasamy, K., Bouamar, H. *et al*. (2012). "MicroRNAs miR-125a and miR-125b constitutively activate the NF-κB pathway by targeting the tumor necrosis factor alpha-induced protein 3 (TNFAIP3, A20)", *Proceedings of the National Academy of Sciences of the United States of America*, 109(20), pp.7865–7870.
99. Kim, K.H. and Roberts, C.W. (2016). "Targeting EZH2 in cancer," *Nature Medicine*, 22(2), pp. 128–134.
100. Klein, D.J., Moore, P.B. and Steitz, T.A. (2004). "The roles of ribosomal proteins in the structure assembly, and evolution of the large ribosomal subunit," *Journal of Molecular Biology*, 340(1), pp. 141–177.
101. Kloosterman, W.P. and Plasterk, R.H.A. (2006). "The Diverse Functions of MicroRNAs in Animal Development and Disease", *Developmental Cell*, 11(4), pp.441–450.
102. Koralov, S. B., Mulijo, S. A., Galler, G. R., et al. (2008). "Dicer ablation affects antibody diversity and cell survival in the B lymphocyte lineage," *Cell*, 132(5), pp.860-874.

103. Korkolopoulou, P., Vassilakopoulos, T., Milionis, V. *et al*. (2016). "Recent advances in aggressive large B-cell lymphomas: A comprehensive review," *Advances in Anatomic Pathology*, 23(4), pp. 202–243.
104. Lacy, S.E., Barrans, S., Beer, P.A., Hodson, D.J. *et al* (2020). "Targeted sequencing in DLBCL, molecular subtypes, and outcomes: a Haematological Malignancy Research Network report", *Blood*, 135(20), pp.1759–1771.
105. Lai, C., Roschewski, M., Melani, C., *et al*. (2018). "Myc gene rearrangement in diffuse large B-cell lymphoma does not confer a worse prognosis following dose-adjusted epoch-R," *Leuk. Lymphoma*, 59(2), pp.505–508.
106. Landsburg, D.J., Nasta, S.D., Svoboda, J. *et al*. (2014). "Dual-hit' cytogenetic status may not be predicted by baseline clinicopathological characteristics and is highly associated with overall survival in B cell lymphoma patients", *British Journal of Haematology*, 166(3), pp.369–374.
107. Landsburg, D.J., Petrich, A.M., Abramson, J.S. *et al*. (2016). "Impact of oncogene rearrangement patterns on outcomes in patients with Dual-hit non-Hodgkin Lymphoma", *Cancer*, 122(4), pp. 559–564.
108. Lawrie,C. H., Chi, J., Taylor, S., *et al*. (2009). "Expression of microRNAs in diffuse large B cell lymphoma is associated with immunophenotype, survival and transformation from follicular lymphoma," *Journal of Cellular and Molecular Medicine*, 13(7), pp.1248-1260.
109. Lawrie, C. H., Gal, S., Dunlop, H.M. *et al*. (2008). "Detection of elevated levels of tumour-associated microRNAs in serum of patients with diffuse large B-cell lymphoma," *Br J Haematol*, 141, pp.672-675.
110. Lawrie, C.H., Soneji, S., Marafioti, T. *et al*. (2007). "Microrna expression distinguishes between germinal center B cell-like and activated B cell-like subtypes of diffuse large B cell lymphoma", *International Journal of Cancer*, 121(5), pp.1156–1161.
111. Lee, Y., Hur, I., Park, S.Y. *et al.* (2006). "The role of PACT in the RNA silencing pathway", *The EMBO journal*, 25(3), pp.522–532.
112. Lemaire, R., Desmons, A., Tabet, J.C. *et al*. (2007). "Direct Analysis and MALDI Imaging of Formalin-Fixed, Paraffin-Embedded Tissue Sections", *Journal of Proteome Research*, 6(4), pp.1295–1305.
113. Lenz, G. and Staudt, L.M. (2010). "Aggressive Lymphomas", *New England Journal of Medicine*, 362(15), pp.1417–1429.
114. Lenz, G., Wright, G.W., Emre, N.C.T. *et al*. (2008). "Molecular subtypes of diffuse large B-cell lymphoma arise by distinct genetic pathways", *Proceedings of the National Academy of Sciences*, 105(36), pp.13520–13525.
115. Leonard, J.P., Kolibaba, K.S., Reeves, J.A. *et al*. (2017). "Randomized Phase II Study of R-CHOP With or Without Bortezomib in Previously Untreated Patients With Non–Germinal Center B-Cell–Like Diffuse Large B-Cell Lymphoma", *Journal of Clinical Oncology*, 35(31), pp.3538–3546.
116. Letai, A.G. (2008). "Diagnosing and exploiting cancer's addiction to blocks in apoptosis", *Nature Reviews Cancer*, 8(2), pp.121–132.
117. Li, C. H., Fu, R., Wang, Y.H. *et al*. (2014). "Expression and clinical significance of miR-21 in diffuse large B cell lymphoma," *Zhongguo Shi Yan Xue Ye Xue Za Zhi*, 22, pp.339-343.
118. Li, J., Wan, Y., Ji, Q. *et al.* (2013). "The role of microRNAs in B-cell development and function", *Cellular & Molecular Immunology*, 10(2), pp.107–112.

119. Li, S., Lin, P., Fayad, L.E. *et al*. (2012). "B-cell lymphomas with MYC/8q24 rearrangements and IGH@BCL2/t(14;18)(q32;q21): An aggressive disease with heterogeneous histology, germinal center B-cell immunophenotype and poor outcome", *Modern Pathology*, 25(1), pp. 145–156.
120. Li, S., Saksena, A., Desai, P. *et al*. (2016). "Prognostic impact of history of follicular lymphoma, induction regimen and stem cell transplant in patients with MYC/BCL2 double hit lymphoma", *Oncotarget*, 7 (1), pp. 38122-38132.
121. Li, S., Desai, P., Lin, P. *et al*. (2016). "MYC/BCL6 Dual-hit lymphoma (DHL): a tumour associated with an aggressive clinical course and poor prognosis", *Histopathology*, 68 (2), pp. 1090-1098.
122. Lin, F. and Chen, Z. (2014). "Standardization of diagnostic immunohistochemistry: Literature review and geisinger experience," *Archives of Pathology & Laboratory Medicine*, 138(12), pp. 1564–1577.
123. Linnstaedt, S. D., Gottwein, E., Skalsky, R.L. *et al*. (2010). "Virally induced cellular MicroRNA miR-155 plays a key role in B-Cell immortalization by Epstein-Barr virus," *J Virol*, 84, pp,11670-11678.
124. Liu, Y., Gonzalez, Y. and Amengual, J.E. (2019). "Chromatin-remodeled state in lymphoma," *Current Hematologic Malignancy Reports*, 14(5), pp. 439–450.
125. Lohr, J. G., Stojanov, P., Lawrence, M. S. *et al*. (2012). "Discovery and prioritization of somatic mutations in diffuse large B-cell lymphoma (dlbcl) by whole-exome sequencing," *Proc. Natl. Acad. Sci. U. S. A*., 109(10), pp.3879–3884.
126. Lossos, I.S. and Morgensztern, D. (2006). "Prognostic Biomarkers in Diffuse Large B-Cell Lymphoma", *Journal of Clinical Oncology*, 24(6), pp.995–1007.
127. Lunt, S.Y., Muralidhar, V., Hosios, A.M. *et al.* (2015). "Pyruvate kinase isoform expression alters nucleotide synthesis to impact cell proliferation," *Molecular Cell*, 57(1), pp. 95–107.
128. Ma, A. and Malynn, B. A. (2020). "A20: Linking a complex regulator of ubiquitylation to immunity and human disease," *Nat. Rev. Immunol*, 12(11), pp.774–785.
129. Ma, X., Becker Buscaglia, L.E., Barker, J.R. *et al.* (2011) "MicroRNAs in NF- B signalling", *Journal of Molecular Cell Biology*, 3(3), pp. 159–166.
130. Mackay, I.M., Arden, K.E., Nitsche, A. *et al*. (2002). "Real-time PCR in virology", Nucleic Acids Research, 30(6), pp,1292-1305.
131. Magistroni, V., Mauri, M., D'Aliberti, D. *et al*. (2019). "De novo UBE2A mutations are recurrently acquired during chronic myeloid leukemia progression and interfere with myeloid differentiation pathways", *Haematologica*, 104(9), pp.1789–1797.
132. Mandelbaum, J., Bhagat, G., Tang, H. *et al*. (2010). "Blimp1 is a tumor suppressor gene frequently disrupted in activated B cell-like diffuse large B cell lymphoma," *Cancer Cell*, 18(6), pp.568–579.
133. Mansouri, L., Thorvaldsdottir, B., Laidou, S., *et al*. (2022). "Precision diagnostics in lymphomas - recent developments and future directions," *Semin. Cancer Biol*, 84, pp.170–183.
134. Martín-Pérez, D., Vargiu, P., Montes-Moreno, S. *et al*. (2012) "Epstein-Barr virus microRNAs repress BCL6 expression in diffuse large B-cell lymphoma," Leukemia 26, pp.180-183.
135. Mazurek, S. (2011). "Pyruvate kinase type M2: A key regulator of the metabolic budget system in tumor cells," *The International Journal of Biochemistry & Cell Biology*, 43(7), pp. 969–980.

136. Medina, P.P., Nolde, M. and Slack, F.J. (2010). "OncomiR addiction in an in vivo model of microRNA-21-induced pre-B-cell lymphoma", *Nature*, 467(7311), pp.86–90.
137. Metzler, M., Wilda, M., Busch, K. *et al*. (2004). "High expression of precursor microRNA-155/BIC RNA in children with Burkitt lymphoma," *Genes Chromosomes Cancer*, 39, pp.167-169.
138. Merino, F., Pospich, S. and Raunser, S. (2020). "Towards a structural understanding of the remodeling of the actin cytoskeleton," *Seminars in Cell & Developmental Biology*, 102, pp.51–64.
139. Miao, Y., Medeiros, L.J., Li, Y. *et al*. (2019). "Genetic alterations and their clinical implications in DLBCL", *Nature Reviews Clinical Oncology*, 16(10), pp.634–652.
140. Mihailovich, M., Bremang, M., Spadotto, V. *et al*. (2015). "miR-17-92 fine-tunes MYC expression and function to ensure optimal B cell lymphoma growth", *Nature Communications*, 6(1), pp.8725.
141. Mitchell, P. S., Parkin, R.K., Kroh, E.M. *et al*. (2008) "Circulating microRNAs as stable blood-based markers for cancer detection," *Proc Natl Acad Sci USA*, 105, pp.10513-10518.
142. Moore, N.M., Aggarwal, N., Surti, U. *et al*. (2017). "Further exploration of the complexities of large B-cell lymphomas with MYC abnormalities and the importance of a blastoid morphology", *American Journal of Surgical Pathology*, 41(2), pp. 1155-1166.
143. Morin, R.D., Assouline, S., Alcaide, M. *et al*. (2016). "Genetic Landscapes of Relapsed and Refractory Diffuse Large B-Cell Lymphomas", *Clinical Cancer Research*, 22(9), pp.2290–2300.
144. Morin, R. D., Mendez-Lago, M., Mungall, A. J., *et al*. (2011). "Frequent mutation of histone-modifying genes in non-hodgkin lymphoma," *Nature*, 476(7360), pp.298–303.
145. Muppidi, J. R., Schmitz, R., Green, J. A., *et al*. (2014). "Loss of signalling via Gα13 in germinal centre B-cell-derived lymphoma," *Nature*, 516(7530), pp.254–258.
146. Musilova, K. and Mraz, M. (2014). "MicroRNAs in B-cell lymphomas: how a complex biology gets more complex", *Leukemia*, 29(5), pp.1004–1017.
147. Nahar, R., Ramezani-Rad, P., Mossner, M. *et al*. (2011). "Pre-B Cell Receptor-Mediated Activation of BCL6 Induces Pre-B Cell Quiescence Through Transcriptional Repression of MYC", *Blood*, 118(21), pp.1406–1406.
148. Niitsu, N., Okamoto, M., Miura, I. *et al*. (2009). "Clinical features and prognosis of de novo diffuse large B-cell lymphoma with t(14;18) and 8q24/c-MYC translocations", *Leukemia*, 23 (9), pp. 777-783.
149. Ngo, V. N., Young, R. M., Schmitz, R., *et al*. (2011). "Oncogenically active Myd88 mutations in human lymphoma," *Nature*, 470(7332), pp.115–119.
150. Nuovo, G.J., Garofalo, M., Valeri, N. *et al*. (2012). "Reovirus-associated reduction of microRNA-let-7d is related to the increased apoptotic death of cancer cells in clinical samples", *Modern Pathology*, 25(10), pp.1333–1344.
151. Obermann, E.C., Csato, M., Dirnhofer, S. *et al*. (2009). "Aberrations of the MYC gene in unselected cases of diffuse large B-cell lymphoma are rare and unpredictable by morphological or immunohistochemical assessment", *Journal of Clinical Pathology*, 62(8), pp.754–756.
152. O'Donnell, K.A., Wentzel, E.A., Zeller, K.I. *et al.* (2005). "c-Myc-regulated microRNAs modulate E2F1 expression", *Nature*, 435(7043), pp.839–843.

153. Ok, C.Y., Medeiros, L.J., Thakral, B. *et al*. (2019). "High-grade B-cell lymphomas with TdT expression: a diagnostic and classification dilemma", *Modern Pathology*, 32(1), pp. 48-58.
154. Oki, Y., Noorani, M., Lin, P. *et al*. (2014). "Double hit lymphoma: The MD Anderson Cancer Center Clinical experience", *British Journal of Haematology*, 166(6), pp. 891–901.
155. Pan, X., Wang, Z. X., and Wang, R. (2010). "MicroRNA-21: A novel therapeutic target in human cancer," *Cancer Biol Ther*, 10, pp.1224-1232.
156. Pasqualucci, L., Trifonov, V., Fabbri, G., *et al*. (2011). "Analysis of the coding genome of diffuse large B-cell lymphoma," *Nat. Genet*, 43(9), pp.830–837.
157. Pedersen, M.O., Gang, A.O., Poulsen, T.S. *et al*. (2012). "Dual-hit BCL2/MYC translocations in a consecutive cohort of patients with large B-cell lymphoma – a single centre's experience", *European Journal of Haematology*, 89 (2), pp. 63-71.
158. Perry, A.M., Diebold, J., Nathwani, B.N. *et al*. (2016). "Non-Hodgkin lymphoma in the developing world: review of 4539 cases from the International Non-Hodgkin Lymphoma Classification Project", *Haematologica*, 101(10), pp.1244–1250..
159. Petrich, A.M., Gandhi, M., Jovanovic, B. *et al*. (2014) "Impact of induction regimen and stem cell transplantation on outcomes in Dual-hit lymphoma: a multicenter retrospective analysis", *Blood*, 124 (4), pp. 2354-236.
160. Pfreundschuh, M., Schubert, J., Ziepert, M., *et al*. (2008). "Six versus eight cycles of Bi-weekly chop-14 with or without rituximab in elderly patients with aggressive Cd20+ B-cell lymphomas: A randomised controlled trial (Ricover-60)," *Lancet Oncol*, 9(2), pp.105–116.
161. Pillai, R.K., Sathanoori, M., Van Oss, S.B. et al. (2013). "Dual-hit B-cell lymphomas with BCL6 and MYC translocations are aggressive, frequently extranodal lymphomas distinct from BCL2 Dual-hit B-cell lymphomas", *American Journal of Surgical Pathology*, 37(2), pp. 323-332.
162. Phan, R.T. and Dalla-Favera, R. (2004). "The BCL6 proto-oncogene suppresses p53 expression in germinal-centre B cells", *Nature*, 432(7017), pp.635–639.
163. Phelan, J. D., Young, R. M., Webster, D. E., Roulland, S., Wright, G. W., Kasbekar, M., *et al*. (2018). "A multiprotein supercomplex controlling oncogenic signalling in lymphoma," *Nature*, 560(7718), pp.387–39.
164. Psathas, J.N., Doonan, P.J., Raman, P. *et al*. (2013). "The Myc-miR-17-92 axis amplifies B-cell receptor signaling via inhibition of ITIM proteins: a novel lymphomagenic feed-forward loop", *Blood*, 122(26), pp.4220–4229.
165. Quesada, A.E., Medeiros, L.J., Desai, P.A. *et al*. (2017). "Increased MYC copy number is an independent prognostic factor in patients with diffuse large B-cell lymphoma", *Modern Pathology*, 30(1), pp. 1688-1697.
166. Rai, D., Kim, S.W., McKeller, M. R. *et al*. (20110). "Targeting of SMAD5 links microRNA-155 to the TGF-beta pathway and lymphomagenesis," *Proc Natl Acad Sci USA*, 107, pp.3111-3116.
167. Ramesh, R., Munshi, A., Panda, S.K. *et al*. (1992). "Polymerase chain reaction", *National Medical Journal of India*, 5(3), pp.115-119.
168. Rawlings,D. J.,Metzler,G.,Wray-Dutra,M., *et al*. (2017). "Altered Bcell signalling in autoimmunity," *Nat. Rev. Immunol*, 17(7), pp.421–436.
169. Ray-Gallet, D. and Almouzni, G. (2020). "The histone H3 family and its deposition pathways," *Histone Mutations and Cancer*, pp. 17–42.

170. Rao, D.S., O'Connell, R.M., Chaudhuri, A.A. *et al*. (2010). "MicroRNA-34a Perturbs B Lymphocyte Development by Repressing the Forkhead Box Transcription Factor Foxp1", *Immunity*, 33(1), pp.48–59.
171. Richards, E.J. and Elgin, S.C.R. (2002). "Epigenetic Codes for Heterochromatin Formation and Silencing", *Cell*, 108(4), pp.489–500.
172. Robb, G.B. and Rana, T.M. (2007). "RNA Helicase A Interacts with RISC in Human Cells and Functions in RISC Loading", *Molecular Cell*, 26(4), pp.523–537.
173. Robertus, J.-L., Harms, G., Reijmers, R.M. *et al*. (2010). "MiRNA profiling in B non-Hodgkin lymphoma: a MYC-related miRNA profile characterizes Burkitt lymphoma", *British Journal of Haematology*, 149(6), pp.896–899.
174. Rodriguez, A., Vigorito, E., Clare, S. *et al*. (2007). "Requirement of bic/microRNA-155 for Normal Immune Function", *Science*, 316(5824), pp.608–611.
175. Roehle, A., Hoefig, K.P., Repsilber, D. et al. (2008). "MicroRNA signatures characterize diffuse large B-cell lymphomas and follicular lymphomas", *British Journal of Haematology,* 142(5), pp.732–744.
176. Rosenquist, R., Bea, S., Du, M. Q., *et al*. (2017). "Genetic Landscape and deregulated pathways in B-cell lymphoid malignancies," *J. Intern Med*, 282(5), pp.371–394.
177. Rosenquist, R., Rosenwald, A., Du, M. Q., *et al*. (2016). "Clinical impact of recurrently mutated genes on lymphoma diagnostics: State-of-the-Art and beyond," *Haematologica*, 101(9), pp.1002–1009.
178. Rosenwald, A., Wright, G., Chan, W.C. *et al*. (2002). "The Use of Molecular Profiling to Predict Survival after Chemotherapy for Diffuse Large-B-Cell Lymphoma", *New England Journal of Medicine*, 346(25), pp.1937–1947.
179. Saito, T., Chiba, S., Ichikawa, M. *et al*. (2003). Notch2 Is Preferentially Expressed in Mature B Cells and Indispensable for Marginal Zone B Lineage Development. Immunity, 18(5), pp.675–685.
180. Saito, Y., Liang, G., Egger, G. *et al*. (2006). "Specific activation of microRNA-127 with downregulation of the proto-oncogene BCL6 by chromatin-modifying drugs in human cancer cells," *Cancer Cell*, 9, pp.435-443.
181. Sandhu, S. K., Croce, C. M., and Garzon, R. (2011). "Micro-RNA expression and function in lymphomas," *Adv Hematol*, 2011, pp.1-12.
182. Samatar, A.A. and Poulikakos, P.I. (2014). "Targeting RAS–ERK signalling in cancer: promises and challenges", *Nature Reviews Drug Discovery*, 13(12), pp.928–942.
183. Schmitt, C.A. and Lowe, S.W. (2001). "Bcl-2 Mediates Chemoresistance in Matched Pairs of Primary Eμ-myc Lymphomas in Vivo", *Blood Cells Molecules and Diseases*, 27(1), pp.206–216.
184. Schmitz, R., Young, R.M., Ceribelli, M. *et al*. (2012). "Burkitt lymphoma pathogenesis and therapeutic targets from structural and functional genomics", *Nature*, 490(7418), pp.116–120.
185. Schmitz, R., Wright, G.W., Huang, D.W. *et al.* (2018). "Genetics and Pathogenesis of Diffuse Large B-Cell Lymphoma", *New England Journal of Medicine*, 378(15), pp.1396–1407.
186. Schuetz, J.M., Johnson, N.A., Morin, R.D. *et al*. (2012). "BCL2 mutations in diffuse large B-cell lymphoma", *Leukemia*, 26(6), pp.1383–1390.
187. Sebestyen, E., Nagy, A., Marosvari, D., et al. (2022). "Distinct miRNA expression signatures of primary and secondary central nervous system lymphoma,"*J. Mol. Diagn.*, 24(3), pp.224-240.

188. Sehn, L.H., Donaldson, J., Chhanabhai, M. *et al*. (2005). "Introduction of Combined CHOP Plus Rituximab Therapy Dramatically Improved Outcome of Diffuse Large B-Cell Lymphoma in British Columbia", *Journal of Clinical Oncology*, 23(22), pp.5027–5033.
189. Skalt, D., Schmidt, C., Schoel, W. *et al*. (2022). "Budget Impact Analysis of CAR T-cell Therapy for Adult Patients With Relapsed or Refractory Diffuse Large B-cell Lymphoma in Germany," *HemaSphere*, 6(7), pp.e736–e736.
190. Sompuram, S.R., Vani, K., Messana, E. *et al.* (2004). "A Molecular Mechanism of Formalin Fixation and Antigen Retrieval", *American Journal of Clinical Pathology*, 121(2), pp.190–199.
191. Souza, O. F. and Papi, A. F. (2022) "Role of microRNAs in B-cell compartments: development, proliferation and haematological diseases," *Bomedicines*, 10(8), pp.2004.
192. Sesques, P. and Johnson, N.A. (2016). "Approach to the diagnosis and treatment of high-grade B-cell lymphomas withMYCandBCL2and/orBCL6rearrangements", *Blood*, 129(3), pp.280–288.
193. Sterfancikova, L., Smardova, J., Zainudden, N. *et al.* (2011). "Prognostic impact of p53 aberrations for R-chop-treated patients with diffuse large B-cell lymphoma," *International Journal of Oncology*. Available at: https://doi.org/10.3892/ijo.2011.1170.
194. Swerdlow, S.H. (2008). "WHO Classification of Tumours of Haematopoietic and Lymphoid Tissues", *Critical Values*, 2(2), pp.30–32.
195. Swerdlow, S.H. (2014). "Diagnosis of 'double hit' diffuse large B-cell lymphoma and B-cell lymphoma, unclassifiable, with features intermediate between DLBCL and Burkitt lymphoma: when and how, FISH versus IHC", *Hematology*, 2014(1), pp.90–99.
196. Swerdlow, S.H., Campo, E., Pileri, S. *et al.* (2016). "The 2016 revision of the World Health Organization classification of lymphoid neoplasms," *Blood*, 127(20), pp. 2375–2390.
197. Syrykh, C., Chaouat, C., Poullot, E. *et al*.(2022). "Lymph node excisions provide more precise lymphoma diagnoses than core biopsies: a French Lymphopath network survey", *Blood*, 140(24), pp.2573–2583.
198. Thomas, L.R., Wang, Q., Grieb, B.C. *et al*. (2015). "Interaction with WDR5 Promotes Target Gene Recognition and Tumorigenesis by MYC", *Molecular Cell*, 58(3), pp.440–452
199. Turakhia, S.K., Hill, B.T., Dufresne, S.D. *et al*. (2014). "Aggressive B-cell lymphomas with translocations involving BCL6 and MYC have distinct clinical-pathologic characteristics", *American Journal of Clinical Pathology*, 142 (2), pp. 339-346.
200. Velichutina, I., Shaknovich, R., Geng, H., *et al*. (2010). "Ezh2-Mediated epigenetic silencing in germinal center B cells contributes to proliferation and lymphomagenesis," *Blood*, 116(24), pp.5247–5255.
201. Vaque, J.P., Martinez, N., Batlle-Lopez, A. *et al*. (2014). "B-cell lymphoma mutations: improving diagnostics and enabling targeted therapies", *Haematologica*, 99(2), pp.222–231.
202. Varambally, S., Dhanasekaran, S.M., Zhou, M. *et al.* (2002). "The Polycomb group protein EZH2 is involved in progression of prostate cancer," *Nature*, 419(6907), pp. 624–629.

203. Vousden, K.H. and Lu, X. (2002). “Live or let die: The cell's response to p53,” *Nature Reviews Cancer*, 2(8), pp. 594–604.
204. Wang, X.J., Medeiros, L.J., Lin, P. *et al*. (2015). “MYC Cytogenetic Status Correlates With Expression and Has Prognostic Significance in Patients With MYC/BCL2 Protein Double-positive Diffuse Large B-cell Lymphoma”, *The American Journal of Surgical Pathology*, 39(9), pp.1250–1258.
205. Wang, H., Wang, A., Hu, Z. *et al*. (2016). “A Critical Role of miR-144 in Diffuse Large B-cell Lymphoma Proliferation and Invasion”, *Cancer immunology research*, 4(4), pp.337–344.
206. Warner, J.R. and McIntosh, K.B. (2009). “How common are extraribosomal functions of ribosomal proteins?”, *Molecular Cell*, 34(1), pp. 3–11.
207. Werner, S., Keller, L. and Pantel, K. (2020). “Epithelial keratins: Biology and implications as diagnostic markers for liquid biopsies,” Molecular Aspects of Medicine, 72(1), pp. 817–819.
208. Wilson, W.H., Young, R.M., Schmitz, R. *et al.* (2015). “Targeting B cell receptor signaling with ibrutinib in diffuse large B cell lymphoma”, *Nature medicine*, 21(8), pp.922–6.
209. Wright, G.W., Huang, D.W., Phelan, J.D. *et al*. (2020). “A Probabilistic Classification Tool for Genetic Subtypes of Diffuse Large B Cell Lymphoma with Therapeutic Implications”, *Cancer Cell*, 37(4), pp.551-568.e14.
210. Wu, P., Zhang, X.D., Zhu, J. *et al*. (2014). “Low expression of microRNA-146b-5p and microRNA-320d predicts poor outcome of large B-cell lymphoma treated with cyclophosphamide, doxorubicin, vincristine, and prednisone”, *Human Pathology*, 45(8), pp.1664–1673.
211. Xie, K., Minkenberg, B. and Yang, Y. (2015). “Boosting CRISPR/Cas9 multiplex editing capability with the endogenous tRNA-processing system*”, Proceedings of the National Academy of Sciences*, 112(11), pp.3570–3575.
212. Xu-Monette, Z.Y., Dabaja, B.S., Wang, X. *et al*. (2015). “Clinical features, tumor biology, and prognosis associated with MYC rearrangement and Myc overexpression in diffuse large B-cell lymphoma patients treated with rituximab-CHOP”, *Modern Pathology*, 28(12), pp.1555–1573.
213. Xu-Monette, Z.Y., Deng, Q.,Manyam,G. C., *et al*. (2016).”Clinical and biologic significance of myc genetic mutations in de novo diffuse large B-cell lymphoma,” *Clin. Cancer Res*, 22(14), pp.3593–3605.
214. Xu-Monette, Z.Y., Wu, L., Visco, C. *et al.* (2012). “Mutational profile and prognostic significance of TP53 in diffuse large B-cell lymphoma patients treated with R-CHOP: Report from an international DLBCL RITUXIMAB-CHOP Consortium program study,” *Blood*, 120(19), pp. 3986–3996.
215. Yan, T.T., Fu, X.L., Li, J. *et al.* (2015). “Downregulation of RPL15 may predict poor survival and associate with tumor progression in pancreatic ductal adenocarcinoma,” *Oncotarget*, 6(35), pp. 37028–37042.
216. Ye, Q., Xu-Monette, Z.Y., Tzankov, A. *et al*. (2015). “Prognostic impact of concurrent MYC and BCL6 rearrangements and expression in de novo diffuse large B-cell lymphoma”, *Oncotarget*, 7(3), pp.2401–2416.
217. Yosef Refaeli, Young, R.M., Turner, B.C. *et al*. (2008). “The B Cell Antigen Receptor and Overexpression of MYC Can Cooperate in the Genesis of B Cell Lymphomas”, *PLOS Biology*, 6(6), pp.152–152.

218. Zahra, K., Dey, T., Mishra, S.P. *et al*. (2020). "Pyruvate Kinase M2 and Cancer: The Role of PKM2 in Promoting Tumorigenesis", *Frontiers in Oncology*, 10(5), pp.144–155.
219. Zainuddin, N., Burglund, M., Wanders, A. et al. (2009). "TP53 mutations predict for poor survival in de novo diffuse large B-cell lymphoma of Germinal Center subtype," Leukemia Research, 33(1), pp. 60–66.
220. Zhang, M., Xu, P., Wang, L. *et al*. (2021). "Genetic subtype guided rituximab-based immunochemotherapy improves outcome in newly diagnosed diffuse large b-cell lymphoma: first report of a randomized phase 2 study". *Hematological Oncology*, 39(S2), pp.1705–1716.
221. Zhao, C., Wang, G., Zhu, Y. *et al*. (2015). "Aberrant regulation of miR-15b in human malignant tumors and its effects on the hallmarks of cancer", *Tumor Biology*, 37(1), pp.177–183.
222. Zhong, H., Xu, L., Zhong, J.H. et al. (2012). "Clinical and prognostic significance of miR-155 and miR-146a expression levels in formalin-fixed/paraffin-embedded tissue of patients with diffuse large B-cell lymphoma", Experimental and Therapeutic Medicine, 3(5), pp.763–770.
223. Zhou, X., Ren, Y., Moore, L. *et al*. (2010). "Downregulation of miR-21 inhibits EGFR pathway and suppresses the growth of human glioblastoma cells independent of PTEN status", *Laboratory Investigation*, 90(2), pp.144–155.
224. Zhu, S., Si, M. L., Wu, H. et al. (2007). "MicroRNA-21 targets the tumor suppressor gene tropomyosin 1 (TPM1)," *J Biol Chem*, 282, pp.14328-14336.

Appendices

Appendix A: Ethics clearance certificate

UNIVERSITY OF THE WITWATERSRAND, JOHANNESBURG

R14/49 Mr SZ Radebe

HUMAN RESEARCH ETHICS COMMITTEE (MEDICAL)
CLEARANCE CERTIFICATE NO. M200434

NAME: (Principal Investigator)	Mr SZ Radebe
DEPARTMENT:	School of Pathology Department of Anatomical Pathology Medical School University
PROJECT TITLE:	Characterisation of double and triple hit high-grade B-cell lymphomas with rearrangement in MYC and BCL2 and/or BCL6
DATE CONSIDERED:	2020/04/24
DECISION:	Approved unconditionally
CONDITIONS:	
SUPERVISOR:	Dr P Magangane
APPROVED BY:	Dr CB Penny, Chairperson, HREC (Medical)
DATE OF APPROVAL:	2020/09/10

This clearance certificate is valid for 5 years from the date of approval. Extension may be applied for.

DECLARATION OF INVESTIGATORS

To be completed in duplicate and **ONE COPY** returned to the Research Office Secretary on the 3rd Floor, Phillip Tobias Building, Parktown, University of the Witwatersrand, Johannesburg.
I/we fully understand the conditions under which I am/we are authorized to carry out the above-mentioned research and I/we undertake to ensure compliance with these conditions. Should any departure be contemplated, from the research protocol as approved, I/we undertake to submit details to the Committee. **I agree to submit a yearly progress report**. When a funder requires annual re-certification, the application date will be one year after the date when the study was initially reviewed. In this case, the study was initially reviewed in **April** and will therefore reports and re-certification will be due early in the month of **April** each year. Unreported changes to the application may invalidate the clearance given by the HREC (Medical).

Principal Investigator Signature _____ Date _____

Appendix B: Study population

Research number	Race	Sex	Age	Tissue	Diagnosis	IHC-BCL6	FISH-MYC	FISH-BCL6	Subtype	Rearrangement status
1	B	M	37	LIVER	DLBCL,NOS	NEG	NEG	NEG	ABC	NH
2	B	M	29	LIVER	DLBCL,NOS	NEG	NEG	NEG	ABC	NH
3	B	F	28	ABDOMINAL	DLBCL,NOS	POS	POS	NEG	GCB	SH-MYC
4	B	M	30	CERVICAL LYMPH NODE	DLBCL,NOS	POS	NEG	NEG	ABC	NH
5	B	F	53	LEFT BREAST	DLBCL,NOS	POS	NEG	NEG	GCB	NH
6	B	M	40	CERVICAL LYMPH NODE	DLBCL,NOS	POS	POS	POS	GCB	DH-MYC/BCL6
7	B	F	23	AXILLARY LYMPH NODE	DLBCL,NOS	POS	NEG	NEG	GCB	NH
8	B	F	40	SUBMANDIBULAR LYMPH NODE	DLBCL,NOS	POS	NEG	POS	GCB	SH-BCL6
9	B	F	37	SKIN	DLBCL,NOS	POS	POS	NEG	GCB	SH-MYC
10	B	M	35	ANAL MASS	DLBCL,NOS	POS	NEG	NEG	GCB	NH
11	B	M	47	LYMPH NODE	DLBCL,NOS	NEG	NEG	POS	GCB	SH-BCL6
12	W	M	34	TONSILLAR MASS	DLBCL,NOS	POS	NEG	NEG	GCB	NH
13	B	F	45	AXILLARY LYMPH NODE	DLBCL,NOS	POS	NEG	NEG	ABC	NH
14	B	F	32	CHEST WALL MASS	DLBCL,NOS	POS	POS	NEG	GCB	SH-MYC
15	B	M	40	BONE MARROW TREPHINE	DLBCL,NOS	NEG	POS	POS	GCB	DH-MYC/BCL6
16	B	F	50	GASTRIC	DLBCL,NOS	POS	POS	NEG	GCB	SH-MYC

Appendix C: Data collection sheet

Assigned Research Number: _____

Age	Sex		Morphology	IHC tests	FISH results		Tests	
	Male	Female			*MYC*	*BCL6*	Proteomic (MALDI, LC-MS/MS)	MicrRNA (PCR)

Appendix D: Cytogenetics Fluorescence *in situ* Hybridisation Testing

FISH testing

The *MYC* rearrangement on chromosome 8q24 was detected by using a dual colour break-apart probe kit, Vysis LSI-MYC (Abbott Laboratories, USA), containing LSI-MYC SpectrumOrange probe and LSI-MYC SpectrumGreen probe. A positive for *MYC* (8q24) rearrangement was conferred using a cut-off value of ≥23% of total rearranged nuclei (Wiktor et al., 2006). Detection of *BCL6* rearrangement on chromosome 3q27.3 was achieved by the use of an IGH-BCL6 Fusion/Translocation FISH probe kit (CytoTest, USA) containing LSP-BCL6 CytoOrange FISH probe. A positive *BCL6* (3q27.3) rearrangement was conferred using a cut-off value of > 9 ± 2.76% of total rearranged nuclei (Ueda et al., 1997). The detection of *BCL2* rearrangement on chromosome 18q21.33 was performed with an IGH-BCL2 dual Fusion/Translocation FISH probe kit (CytoTest, USA) containing LSP-BCL2 CytoOrange FISH probe. Positive for *BCL2* (18q21.33) rearrangement cut-off value was ≥2.5% of total rearranged nuclei (Einerson et al., 2005).

Appendix E: MicroRNA – cDNA Concentrations and Purity Data

Group	Sample Name	Concentration (ng/ul)	260/280	260/230
BCL6^R **(single hit)**	B1	296.5	1.93	2.18
	B2	188	1.96	2.14
BCL6^{R}MYC^R **(dual-rearrangements)**	D1	2722.2	1.95	2.17
	D2	116.5	1.95	1.82
MYC^R **(single hit)**	M1	554	1.94	1.97
	M2	6.6	1.89	1.2
	M3	704.6	1.97	2.04
	M4	941.9	1.98	1.91
Null-hits	N1	1236.8	1.96	2.03
	N2	1156.9	1.98	1.98
	N3	1530.4	2.01	2.09
	N4	158.1	1.98	1.97
	N5	709.7	1.94	1.99
	N6	105.0	1.85	1.18
	N7	195.3	1.88	1.67
	N8	1147.5	1.88	2.04

Appendix F: MicroRNA fold regulation in all the experimental groups (single-hits and dual-rearrangements) against the control group (null-hit)

		Fold Regulation		
		MYC^R	***BCL6^R***	***MYC^{R}BCL6^R***
		88923,3424	-2,341	-1,0099
Position	**Mature ID**	8168958,847	-98,1197	-3,1698
A01	hsa-let-7a-5p	-485,3426	-2171650,281	-4018,8311
A02	hsa-miR-133b	68,9946	7,662	76,2393
A03	hsa-miR-122-5p	1008,142	-293,5155	2,6627
A04	hsa-miR-20b-5p	7134,8817	-17,2425	2,7422
A05	hsa-miR-335-5p	73,3934	-4,1513	1,931
A06	hsa-miR-196a-5p	244,3067	3,108	4,6656
A07	hsa-miR-125a-5p	3940,929	-19,1859	-3,1698
A08	hsa-miR-142-5p	47,7367	-6,0713	-2,2205
A09	hsa-miR-96-5p	-1,1389	-29,4019	-2,0912
A10	hsa-miR-222-3p	-6,9072	4,3525	2,3793
A11	hsa-miR-148b-3p	181,6543	-545,7726	-3,1698
A12	hsa-miR-92a-3p	21,0074	-19185,6239	-39,7313
B01	hsa-miR-184	8,1984	1,4279	-3,1698
B02	hsa-miR-214-3p	19,8089	-4,614	-1,3017
B03	hsa-miR-15a-5p	-49,7255	-16,9985	-3,4414
B04	hsa-miR-378a-3p	8,1984	-1,3746	2,6382
B05	hsa-let-7b-5p	6,1212	-5,425	-6,4393
B06	hsa-miR-205-5p	115,5398	-25,205	-1,9895
B07	hsa-miR-181a-5p	26,5146	-285,3314	4,004
B08	hsa-miR-130a-3p	2,9081	-1,3557	-2,5082
B09	hsa-miR-140-5p	35,221	1,031	-2,0321
B10	hsa-miR-20a-5p	350,0297	-2,3928	2,3429
B11	hsa-miR-146b-5p	2,2205	-1,54	2,1685
B12	hsa-miR-132-3p	1294,516	-4,4183	-3,1698
C01	hsa-miR-193b-3p	8,1984	-72,3679	7,7863
C02	hsa-miR-183-5p	1,0645	-2,0275	1,0132
C03	hsa-miR-34c-5p	6,0285	-50,3039	-6,023
C04	hsa-miR-30c-5p	8,1984	-12,4413	-3,1698
C05	hsa-miR-148a-3p	-2,5732	-1,8108	-1,2119
C06	hsa-miR-134-5p	476,1262	-1,0483	-3,1698
C07	hsa-let-7g-5p	194,6895	-24,223	5,0391
C08	hsa-miR-138-5p	2,3639	-108,067	-18,1704
C09	hsa-miR-373-3p	1,601	-44,7735	-9,9489

C10	hsa-let-7c-5p	1994,7861	-17,2563	-3,1698
C11	hsa-let-7e-5p	2,4619	-4,9368	1,3781
C12	hsa-miR-218-5p	42,7812	2,3469	2,0695
D01	hsa-miR-29b-3p	8,1984	-208,6506	1,0983
D02	hsa-miR-146a-5p	601,8589	-16,9894	5,1819
D03	hsa-miR-135b-5p	145,132	-61,1613	-2,7226
D04	hsa-miR-206	2,2802	-1,8347	2,0064
D05	hsa-miR-124-3p	17,4147	-2,7021	-2,9928
D06	hsa-miR-21-5p	269,2675	-52,3132	-3,1698
D07	hsa-miR-181d-5p	8,1984	-2,1338	20,6647
D08	hsa-miR-301a-3p	2,5968	-87,5989	-26,249
D09	hsa-miR-200c-3p	130,33	-1,4837	-3,1698
D10	hsa-miR-100-5p	-3,3681	3,0868	8,9541
D11	hsa-miR-10b-5p	609,0453	-545,7726	-3,1698
D12	hsa-miR-155-5p	16,4181	-1,5092	6,2737
E01	hsa-miR-1-3p	30,4025	2,6693	7,0733
E02	hsa-miR-150-5p	2,4284	-51,1562	-3,6314
E03	hsa-let-7i-5p	86,3296	-1,3153	2,9702
E04	hsa-miR-27b-3p	36,9071	-106,0365	2,233
E05	hsa-miR-7-5p	70,5067	-3,1118	1,7106
E06	hsa-miR-127-5p	1,3958	-1,1349	1,264
E07	hsa-miR-29a-3p	-20,5749	-13,9589	-9,8505
E08	hsa-miR-191-5p	8,1984	-1,6618	-3,1698
E09	hsa-let-7d-5p	-0,1891	-0,4269	-0,2048
E10	hsa-miR-9-5p	263,0876	-2,4499	3,1634
E11	hsa-let-7f-5p	-2,8684	-2,4309	1,0796
E12	hsa-miR-10a-5p	1104,0914	7,6853	14,1932
F01	hsa-miR-181b-5p	3,5675	-2,7383	-1,9659
F02	hsa-miR-15b-5p	1,9336	-2,2099	-4,3643
F03	hsa-miR-16-5p	-3,0559	-1,3934	-2,4454
F04	hsa-miR-210-3p	236,2602	-3,4059	-3,1698
F05	hsa-miR-17-5p	3,5452	-2,276	1,2656
F06	hsa-miR-98-5p	6,1733	-2,624	-4,1775
F07	hsa-miR-34a-5p	141,9681	-20,785	3,0456
F08	hsa-miR-25-3p	161,9039	-1,5823	-3,1698
F09	hsa-miR-144-3p	-1,6379	-19,8122	1,7882
F10	hsa-miR-128-3p	275,6647	-545,7726	-3,1698
F11	hsa-miR-143-3p	204,2305	3,1362	17,2055
F12	hsa-miR-215-5p	93,547	1,1632	2,5793
G01	hsa-miR-19a-3p	539,1819	1,1034	5,59
G02	hsa-miR-193a-5p	-1,6488	-15,4349	2,5326
G03	hsa-miR-18a-5p	-3,4748	-23,1978	-2,7186
G04	hsa-miR-125b-5p	10,0806	-10,0112	-1,0601
G05	hsa-miR-126-3p	8,1984	-82,3786	-3,1698
G06	hsa-miR-27a-3p	1806,1811	-30,4404	-3,1698

G07	hsa-miR-372-3p	8,1984	-545,7726	-3,1698
G08	hsa-miR-149-5p	316,8099	-33,1333	-3,1698
G09	hsa-miR-23b-3p	8,1984	-4,3926	-1,3825
G10	hsa-miR-203a-3p	8,1984	2,653	-3,1698
G11	hsa-miR-32-5p	5012,4265	-545,7726	-3,1698
G12	hsa-miR-181c-5p	62,5484	-37,5024	1,9599
H01	cel-miR-39-3p	66,2764	25,1658	48,6531
H02	cel-miR-39-3p	-13,7322	1,7612	2,1979
H03	SNORD61	157,7062	6,3121	6,6815
H04	SNORD68	1,1451	-2,3361	-3,7216
H05	SNORD72	-11,8127	-2,0775	-1,5467
H06	SNORD95	10,3154	4,8532	5,7562
H07	SNORD96A	132,6665	7,2435	4,9564
H08	RNU6-6P	8,1984	10,263	9,7754
H09	miRTC	-142041,9845	-516,9177	-3,8904
H10	miRTC	-63,4208	-617,7823	-4,169
H11	PPC			
H12	PPC			

Appendix G: Melt ad amplification curves

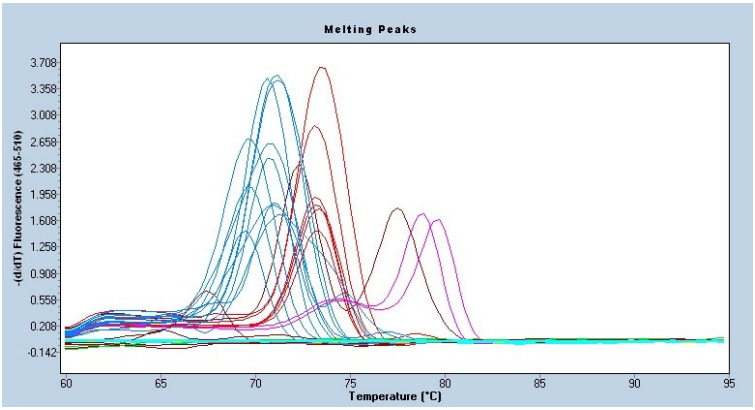

Figure 18: A representative Melt curve analysis for all the miRNAs in experimental groups

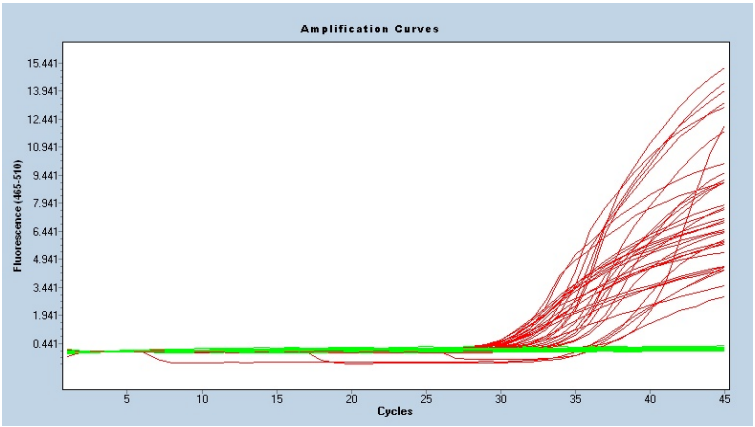

Figure 19: KRas amplification curve

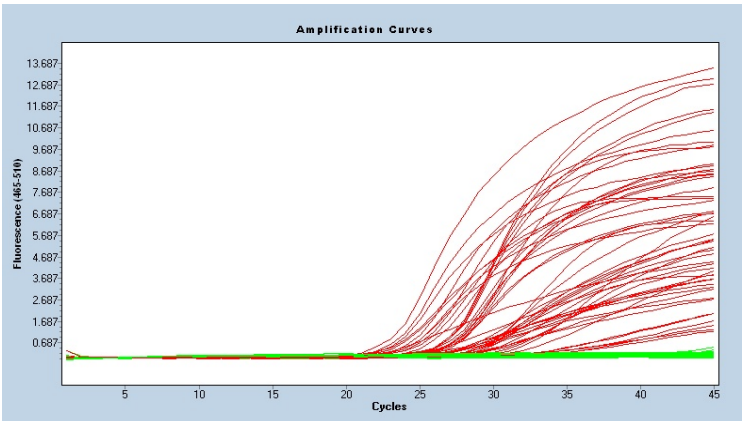

Figure 20:let-7d amplification curve

Appendix H: MicroRNA – Let-7d Statistical Data

Null-hit	*BCL6*^{R}	*MYC*^{R}	*MYC*^{R}*BCL6*^{R}
0,0000316669	0,08518048	0,02627801	0,008460743
1,103100e-006	0,00837323	0,03507694	0,03631392
4,621100e-006			
3,141750e-006			
3,282740e-006			
3,149020e-006			
4,605940e-007			
2,255580e-007			

	Null-hit	*BCL6*^{R}	*MYC*^{R}	*MYC*^{R}*BCL6*^{R}
Number of values	8	2	2	2
Minimum	2.256e-007	0.008373	0.02628	0.008461
25% Percentile	6.212e-007	0.008373	0.02628	0.008461
Median	3.145e-006	0.04678	0.03068	0.02239
75% Percentile	4.287e-006	0.08518	0.03508	0.03631
Maximum	3.167e-005	0.08518	0.03508	0.03631
Mean	5.956e-006	0.04678	0.03068	0.02239
Std. Deviation	1.050e-005	0.05431	0.006222	0.01970
Std. Error	3.714e-006	0.03840	0.004399	0.01393
Lower 95% CI	-2.825e-006	-0.4412	-0.02522	-0.1546
Upper 95% CI	1.474e-005	0.5347	0.08658	0.1993

P value	0.0339		
Exact or approximate P value?	Gaussian Approximation		
P value summary	*		
Do the medians vary significantly? (P < 0.05)	Yes		
Number of groups	6		
Kruskal-Wallis statistic	12.07		
Dunn's Multiple Comparison Test	Difference in rank sum	Significant? P < 0.05?	Summary
Null-hit vs. *BCL6*^{R}	-8.875	No	ns
Null-hit vs *MYC*^{R}	-9.375	No	ns
Null-hit vs *MYC*^{R}*BCL6*^{R}	-8.875	No	ns

Appendix I: MicroRNA – kRas Statistical Data

Null-hit	***BCL6^R***	***MYC^R***	***MYC^{R}BCL6^R***
0.001793094	0.01002677	0.4033209	0.00883023
0.000194672	0.07730292	0.4697614	0.3806842
0.000290334			
0.003158233			
0.000648772			
0.001631031			
0.0000810965			
0.0000355448			

	Null-hit	***BCL6^R***	***MYC^R***	***MYC^{R}BCL6^R***
Number of values	8	2	2	2
Minimum	3.554e-005	0.01003	0.4033	0.008830
25% Percentile	0.0001095	0.01003	0.4033	0.008830
Median	0.0004696	0.04366	0.4365	0.1948
75% Percentile	0.001753	0.07730	0.4698	0.3807
Maximum	0.003158	0.07730	0.4698	0.3807
Mean	0.0009791	0.04366	0.4365	0.1948
Std. Deviation	0.001117	0.04757	0.04698	0.2629
Std. Error	0.0003949	0.03364	0.03322	0.1859
Lower 95% CI	4.536e-005	-0.3837	0.01444	-2.168
Upper 95% CI	0.001913	0.4711	0.8586	2.557

P value	0.0119		
Exact or approximate P value?	Gaussian Approximation		
P value summary	*		
Do the medians vary significantly? (P < 0.05)	Yes		
Number of groups	6		
Kruskal-Wallis statistic	14.66		
Dunn's Multiple Comparison Test	Difference in rank sum	Significant? P < 0.05?	Summary
Null-hit vs. *BCL6^R*	-7.250	No	ns
Null-hit vs. *MYC^R*	-10.25	No	ns
Null-hit vs. *MYC^{R}BCL6^R*	-7.250	No	ns

Appendix J: Proteomics – Dual-rearrangement (*MYC*^{R}*BCL6*^{R}) vs. Null-hit (*MYC*- and *BCL6*-)

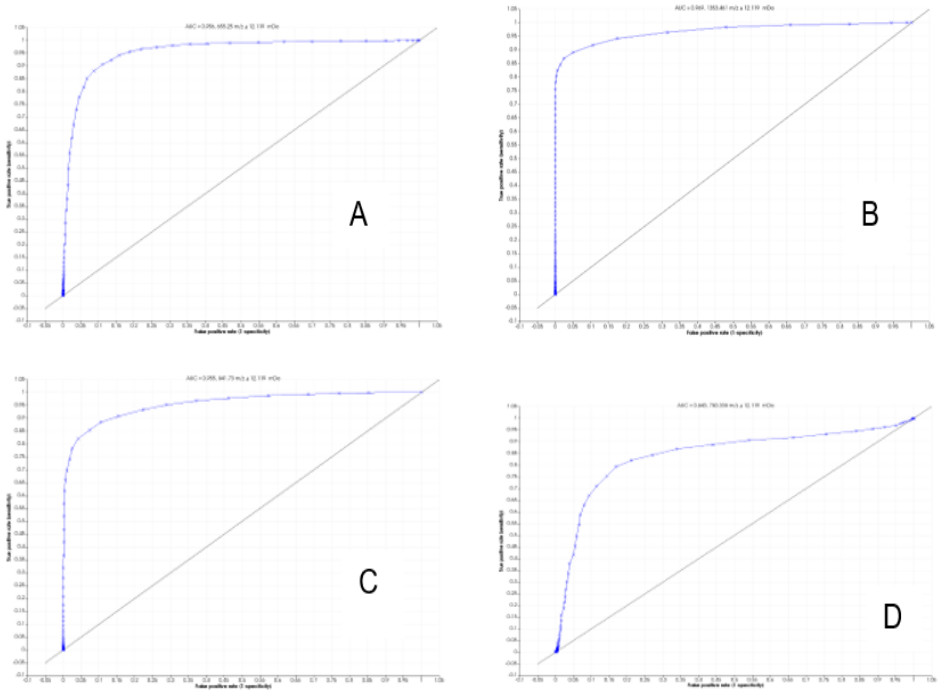

Peptides that were identified excluding the one with the highest AUC:

Label	Peptide	m/z ion	AUC
A	Unknown	655.25	0.956
B	Ribosomal protein L15	1353.46	0.969
C	Unknown	841.73	0.955
D	Histone H3	780.338	0.843

Appendix K: Proteomics – Single-hit (*BCL6*^{R}) vs. Null-hit (*MYC*- and *BCL6*-)

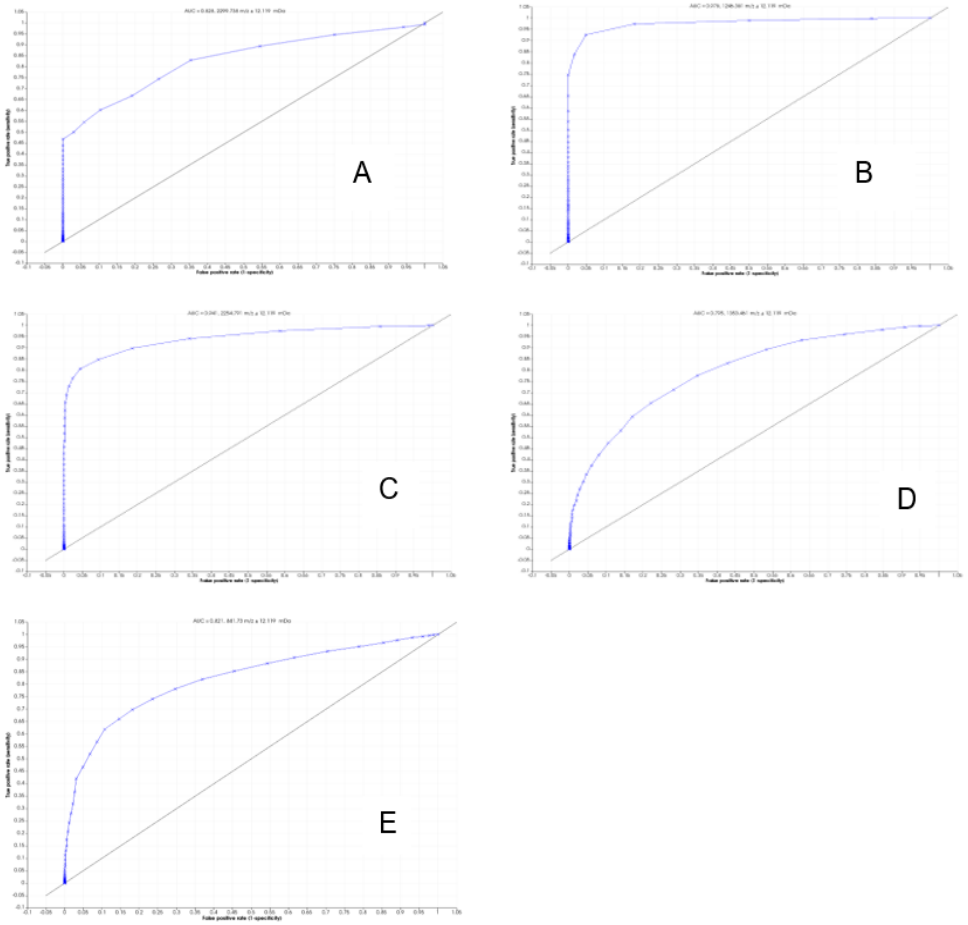

Peptides that were identified excluding the one with the highest AUC:

Label	Peptide	m/z ion	AUC
A	Actin cytoplasmic 1	2299.74	0.828
B	Keratin type 1 cytoskeletal	1246.381	0.978
C	Pyruvate kinase	2254.79	0.941
D	Ribosomal protein L15	1353.46	0.795
E	Unknown	841.73	0.821

Appendix L: Proteomics – Single-hit (*MYC*^{R}) vs. Null-hit (*MYC*- and *BCL6*-)

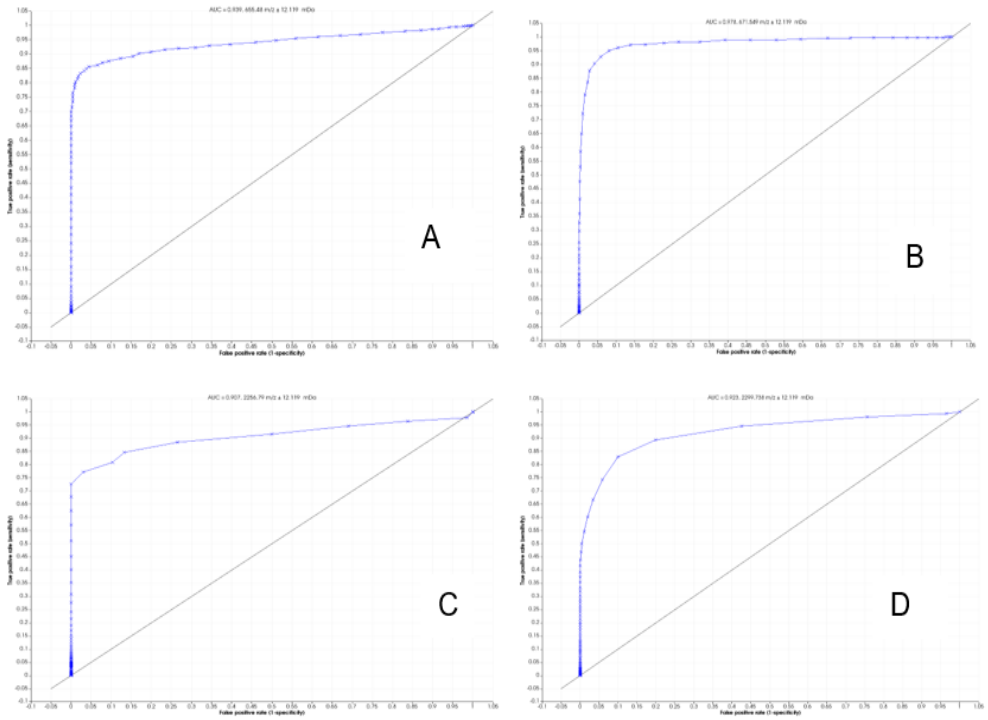

Peptides that were identified excluding the one with the highest AUC:

Label	Peptide	m/z ion	AUC
A	Unknown	655.48	0.939
B	Unknown	671.295	0.978
C	Unknown	2256.79	0.907
D	Actin cytoplasmic 1	2299.735	0.923

Appendix M: Population – Validation Samples

Research Number	H3 Ab		Diagnosis
1	3+	51% - 75%	DLBCL (SH-*BCL6*^{R})
2	3+	51% - 75%	DLBCL (SH-*BCL6*^{R})
3	3+	51% - 75%	DLBCL (SH-*MYC*^{R})
4	4+	>75%	DLBCL (SH-*MYC*^{R})
5	4+	>75%	HGBCL (DR-*MYC*^{R}*BCL6*^{R})
6	4+	>75%	HGBCL (DR- *MYC*^{R}*BCL6*^{R})
7	3+	51% - 75%	BL (SH-*MYC*^{R})
8	3+	51% - 75%	BL (SH-*MYC*^{R})
9	3+	51% - 75%	BL (SH-*MYC*^{R})
10	4+	>75%	BL (SH-*MYC*^{R})
11	4+	>75%	BL (SH-*MYC*^{R})
12	4+	>75%	BL (SH-*MYC*^{R})
13	4+	>75%	BL (SH-*MYC*^{R})
14	4+	>75%	BL (SH-*MYC*^{R})
15	4+	>75%	BL (SH-*MYC*^{R})
16	4+	>75%	BL (SH-*MYC*^{R})
17	4+	>75%	DLBCL (Null-hit)
18	4+	>75%	DLBCL (Null-hit)

Appendix N: Proteomics – Histone (m/z 801.194) ROC curve

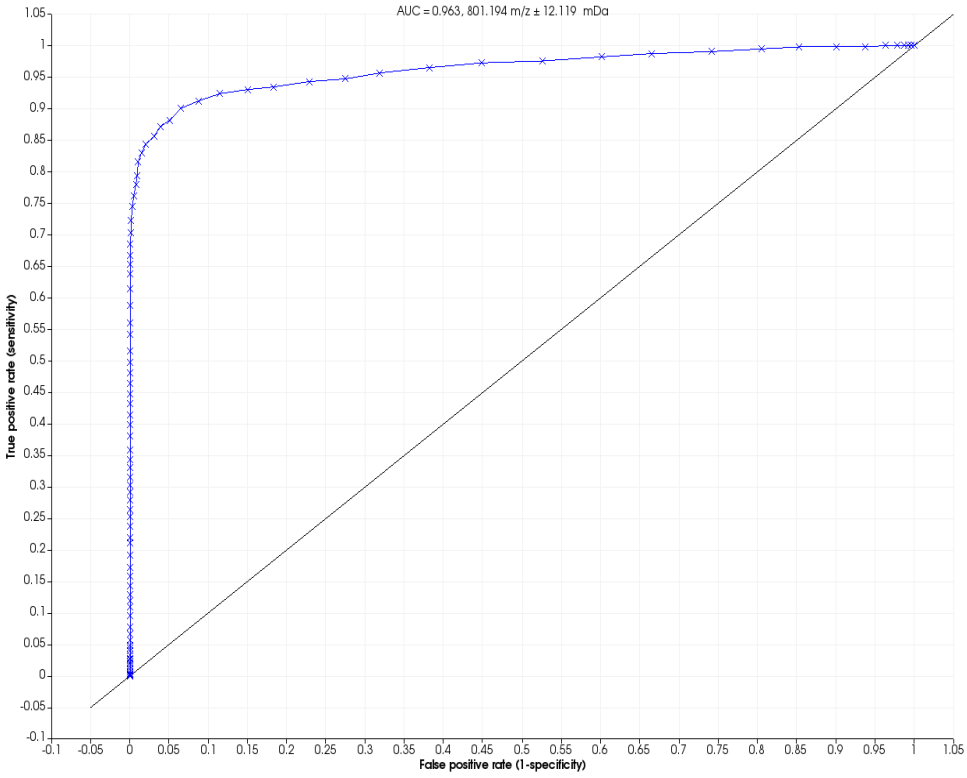

Appendix O: IHC staining optimised conditions information

Antigen retrieval buffer	Antigen	clone	Antibody dilution	Control tissue
1Mm Tris and 1mM EDTA, pH9	Histone H3	EPR 17785 (mono)	1:100 overnight	Kidney

Appendix P: MALDI IMS spectrum

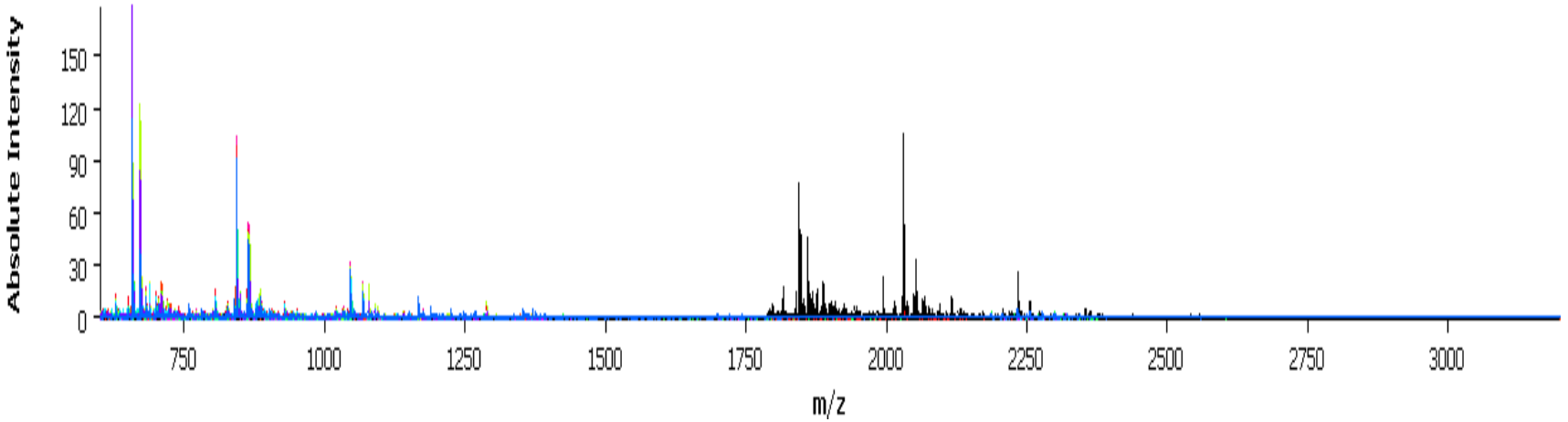

Appendix Q: Turnitin Report

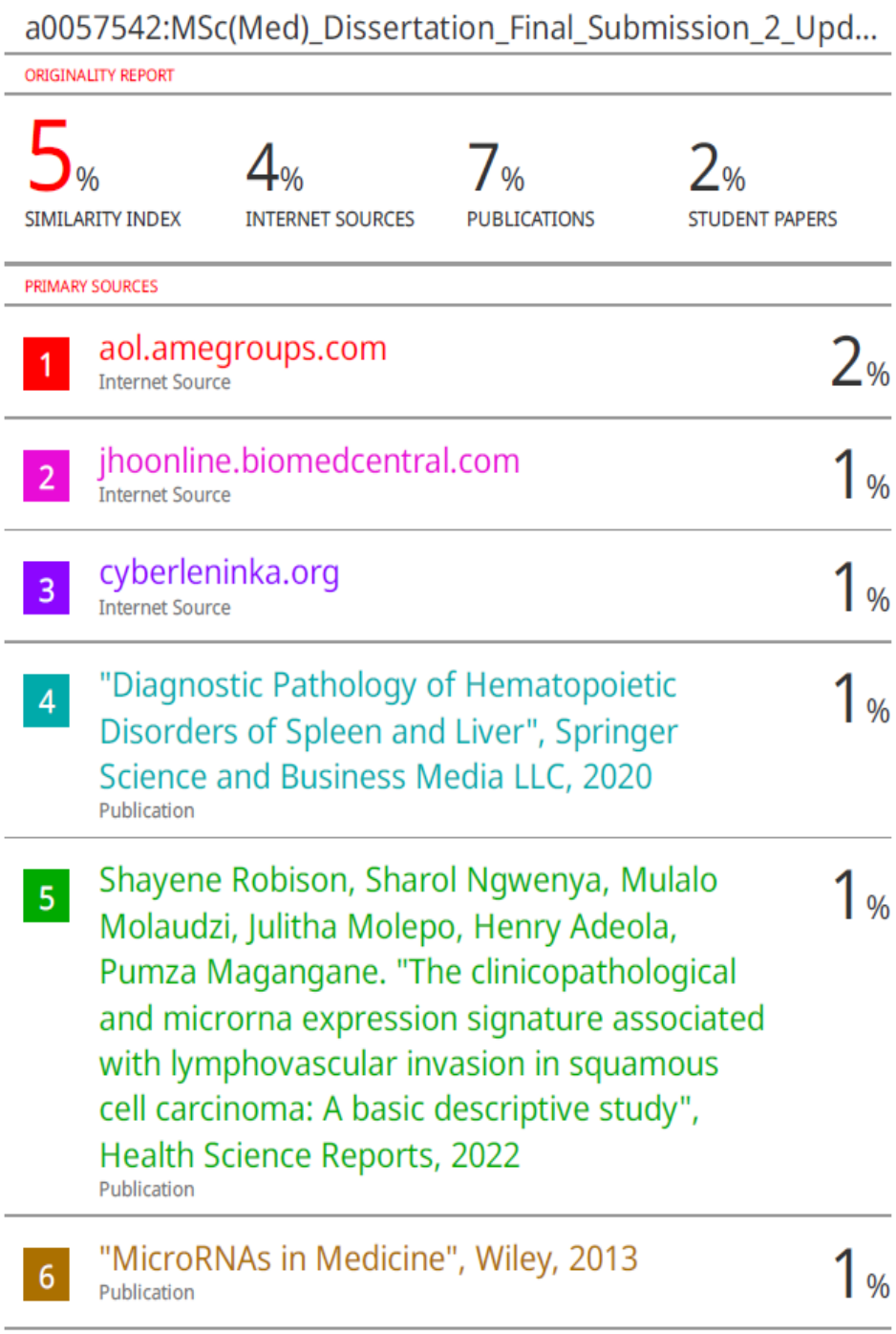

a0057542:MSc(Med)_Dissertation_Final_Submission_2_Upd...

ORIGINALITY REPORT

5%	4%	7%	2%
SIMILARITY INDEX	INTERNET SOURCES	PUBLICATIONS	STUDENT PAPERS

PRIMARY SOURCES

1	aol.amegroups.com Internet Source	2%
2	jhoonline.biomedcentral.com Internet Source	1%
3	cyberleninka.org Internet Source	1%
4	"Diagnostic Pathology of Hematopoietic Disorders of Spleen and Liver", Springer Science and Business Media LLC, 2020 Publication	1%
5	Shayene Robison, Sharol Ngwenya, Mulalo Molaudzi, Julitha Molepo, Henry Adeola, Pumza Magangane. "The clinicopathological and microrna expression signature associated with lymphovascular invasion in squamous cell carcinoma: A basic descriptive study", Health Science Reports, 2022 Publication	1%
6	"MicroRNAs in Medicine", Wiley, 2013 Publication	1%